Compositions and mobility of major, δD, δ¹⁸O, trace, and REEs patterns in water sources at Benue River Basin-Cameroon: Implications for recharge mechanisms, geo-environmental controls and public health

Wilson Y. Fantong[1], Therese L.L. Jokam Nenkam[2], Pierre Nbendah[2], Sharon B. Kimbi[3], Ernest Chi Fru[4], Brice T. Kamtchueng[1], Alain F. Takoundjou[1], Alex R. Tejiobou[5], Gabriel Ngueutchoua[6], Robert Kringel[2,7]

[1] Institute of Geological and Mining Research (IRGM), Hydrological Research Centre, Box 4110 Yaoundé, Cameroon

[2] PRESS NO & SW, P.O. Box 169 Yaoundé, Cameroon

[3] Hiroshima University 1-4-1 Kagamiyama, Higashi-hiroshima, Hiroshima-Japan, 739-8527

[4] School of Earth and Ocean Sciences, Institute of Geochemistry and Geobiology, Cardiff University, Cardiff, Park Place, Wales, United Kingdom

[5] Department of Geography, University of Yaoundé 1, P.O. Box 812, Yaoundé, Cameroon

[6] Department of Earth Sciences, University of Yaoundé 1, P.O. Box 812, Yaoundé, Cameroon

[7] Federal Institute of Geoscience and Natural Resources (BGR), Hanover-Germany

Corresponding author: fyetoh@yahoo.com; fantongy@gmail.com

Compositions and mobility of major, δD, δ¹⁸O, trace, and REEs patterns in water sources at Benue River Basin-Cameroon: Implications for recharge mechanisms, geo-environmental controls and public health

Hydrogeochemical data are required for understanding of water quality, provenance and chemical composition for the 2117700 km^2 Niger River Basin. This study presents hydrogeochemical analysis of the Benue River Basin, a major tributary of the Niger River. The distribution of, major ions, Si, δD and $\delta^{18}O$, Trace and Rare Earth Elements (TE and REEs, respectively) composition in 86 random water samples, revealed mixing of, groundwater with surface water to recharge shallow aquifers by July and September rains. Equilibration of groundwater with kaolinite, and montmorillonites by, incongruent dissolution imprints hydrochemical signatures that vary from $Ca+Mg-NO_3$ in shallow wells to $Na+K-HCO_3$ in boreholes and surface waters, with undesirable concentrations of fluoride identified as major source of fluorosis in the local population. Our results further indicate non-isochemical dissolution of local rocks by water, with springs, wells and borehole waters exhibiting surface water-gaining, weakest water-rock interaction, and strongest water-rock interaction processes, respectively. Poorly mobile elements (Al, Th and Fe) are preferentially retained in the solid residue of incongruent dissolution, while alkalis, alkaline earth and oxo-anion-forming elements (U, Mo, Na, K, Rb, Ca, Li, Sr, Ba, Zn, Pb) are more mobile and enriched in the aqueous phase, whereas transition metals display an intermediate behaviour. Trace elements vary in the order of Ba > Sr > Zn > Li > V > Cu > Ni > Co > As > Cr > Sc > Ti > Be > Pb > Cd, with Potentially Harmful Elements such as Cd, As, and Pb mobilized in acidic media attaining near undesirable levels in populated localities. With the exception of Y, REEs distribution in groundwater in the order of Eu > Sm > Ce >Nd > La > Gd > Pr > Dy > Er > Yb > Ho > Tb > Tm, differ slightly with surface water composition. Post-Archean Average Australian Shale normalized REEs patterns ranging from 1.08-199, point to the dissolution of silicates as key sources of trace elements to groundwater, coupled to deposition by eolian dust.

Keywords: *Recharge periods; Relative mobility of elements; Water-rock interaction; Public health; REEs; Benue River Basin.*

1   **Compositions and mobility of major, δD, δ^{18}O, trace, and REEs patterns in water sources at Benue River**

2   **Basin-Cameroon: Implications for recharge mechanisms, geo-environmental controls and public health**

3

4   Wilson Y. Fantong[1], Therese L.L. Jokam Nenkam[2], Pierre Nbendah[2], Sharon B. Kimbi[3], Ernest Chi Fru[4], Brice

5   T. Kamtchueng[1], Alain F. Takoundjou[1], Alex R. Tejiobou[5], Gabriel Ngueutchoua[6], Robert Kringel[2,7]

6   [1]Institute of Geological and Mining Research (IRGM), Hydrological Research Centre, Box 4110 Yaoundé,

7   Cameroon

8   [2] PRESS NO & SW, P.O. Box 169 Yaoundé, Cameroon

9   [3] Hiroshima University 1-4-1 Kagamiyama, Higashi-hiroshima, Hiroshima-Japan, 739-8527

10   [4] School of Earth and Ocean Sciences, Institute of Geochemistry and Geobiology, Cardiff University, Cardiff,

11   Park Place, Wales, United Kingdom

12   [5]Department of Geography, University of Yaoundé 1, P.O. Box 812, Yaoundé, Cameroon

13   [6]Department of Earth Sciences, University of Yaoundé 1, P.O. Box 812, Yaoundé, Cameroon

14   [7]Federal Institute of Geoscience and Natural Resources (BGR), Hanover-Germany

15   Corresponding author: fyetoh@yahoo.com; fantongy@gmail.com

16

17   **Abstract**

18   Hydrogeochemical data are required for understanding of water quality, provenance and chemical composition

19   for the 2117700 km^2 Niger River Basin. This study presents hydrogeochemical analysis of the Benue River Basin,

20   a major tributary of the Niger River. The distribution of, major ions, Si, δD and δ^{18}O, Trace and Rare Earth

21   Elements (TE and REEs, respectively) composition in 86 random water samples, revealed mixing of, groundwater

22   with surface water to recharge shallow aquifers by July and September rains. Equilibration of groundwater with

23   kaolinite, and montmorillonites by, incongruent dissolution imprints hydrochemical signatures that vary from

24   Ca+Mg-NO$_3$ in shallow wells to Na+K-HCO$_3$ in boreholes and surface waters, with undesirable concentrations

25   of fluoride identified as major source of fluorosis in the local population. Our results further indicate non-

26   isochemical dissolution of local rocks by water, with springs, wells and borehole waters exhibiting surface water-

27   gaining, weakest water-rock interaction, and strongest water-rock interaction processes, respectively. Poorly

28   mobile elements (Al, Th and Fe) are preferentially retained in the solid residue of incongruent dissolution, while

29   alkalis, alkaline earth and oxo-anion-forming elements (U, Mo, Na, K, Rb, Ca, Li, Sr, Ba, Zn, Pb) are more mobile

30   and enriched in the aqueous phase, whereas transition metals display an intermediate behaviour. Trace elements

31   vary in the order of Ba > Sr > Zn > Li > V > Cu > Ni > Co > As > Cr > Sc > Ti > Be > Pb > Cd, with Potentially

32   Harmful Elements such as Cd, As, and Pb mobilized in acidic media attaining near undesirable levels in populated

33   localities. With the exception of Y, REEs distribution in groundwater in the order of Eu > Sm > Ce >Nd > La >

34   Gd > Pr > Dy > Er > Yb > Ho > Tb > Tm, differ slightly with surface water composition. Post-Archean Average

35   Australian Shale normalized REEs patterns ranging from 1.08-199, point to the dissolution of silicates as key

36   sources of trace elements to groundwater, coupled to deposition by eolian dust.

37

38   **Keywords:** *Recharge periods; Relative mobility of elements; Water-rock interaction; Public health; REEs; Benue*

39   *River Basin.*

40

41   **Introduction**

42   *Scientific background and objectives*

43   The 1400 km long Benue River Basin (BRB) located in the Sahel zone of Northern Cameroon is a major tributary

44   of the Niger River (NR) (Fig.1) marked by a mean aridity index (log [potential evapotranspiration/mean annual

45   rainfall]) of 0.47, and a budyko aridity ratio (solar radiation/amount of rainfall) Budyko (1951) of 2.8. These semi-

46   arid climatic conditions cause surface water scarcity, leaving an estimated 2,500,000 inhabitants to depend on

47   groundwater resources and ephemeral streams for domestic and irrigation purposes. Hence the present study is

48   focused on understanding dry season hydrogeochemical dynamics as the main driver of physical water scarcity-

49   related problems in the BRB. Moreover, the location of the BRB at the upstream of the 2117700 km^2 Niger River

50   Basin, makes Cameroon to be a strategic riparian state for integrated and transboundary water resources

51   management amongst the stakeholders of the Niger Basin Authority (NBA).

52   In order to make useful contributions to the NBA, Cameroon has to furnish comprehensive spatial and temporal

53   data on the chemistry and quantity of water resources in the BRB. In response to the need of generating such data,

54   research work in the BRB has led to exploration of stable environmental isotopes (δD and δ^{18}O) and chloride

55   content in rainwater (Njitchoua et al. 1995), geochemistry, origin and recharge mechanisms of groundwaters in

56   the Garoua Sandstone aquifer in Northern Cameroon (Njitchoua et al. 1997) and climate hydrology and water

57   resources in Cameroon (Molua 2006). Despite increased knowledge on water resources in the study area, the

58   existing data still present the gaps related to (i) major ions and stable environmental isotope data for δD and $\delta^{18}O$

59   generated more than 15 years ago, which fall short of presenting an up-to-date information on water chemistry

60   and groundwater recharge periods, respectively. (ii) There is total absence of data on trace elements (TE) and rare

61   earth elements, thus, obscuring important information on hydrogeochemical and geo-environmental dynamics.

62   (iii) The available data are only on the Garoua sedimentary basin, excluding the other five sedimentary basins

63   (Babouri Figuil, Mayo Oulou Lere, Hamakoussou, Benue, and Koum), which are all in the BRB (Fig. 1).

64   To underscore the feasibility of generating data on water chemistry and its applications, major ions have been

65   used to elucidate groundwater chemistry as a function of water-rock interaction processes (Thomas et al. 1989;

66   Petrides et al. 2006; Srinivasamoorthy et al. 2008), usability for drinking (Nagaraju et al. 2006), and sources of

67   health problems such as fluorosis (e,g., Fantong et al. 2010b). Reporting these characteristics on a river basin scale

68   has also been useful in groundwater supply planning in semi-arid regions (Goni 2006). For surface and

69   groundwater resources to be managed sustainably in semi-arid regions, their origin (e.g., Scalon et al. 2006) and

70   renewability (Leduc et al. 1996; Houston 2007; Shivanna et al. 2008) are important requirements, which can be

71   determined by using the isotopic compositions of oxygen and hydrogen in rain, surface and groundwater (e.g.,

72   Azzaz et al. 2008; Goni 2006; Fantong et al. 2010a; Tsujimura et al. 2007; and Edmunds et al. 2002).

73   In the recharge pathway from rain to groundwater, water molecules interact with minerals that circulate as dust

74   particles in the atmosphere and those within the lithosphere by water-rock interaction, which can also alter the

75   water chemistry by adding TE and REEs (e.g., Rollinson 1993, Vazquez-Ortega et al. 2015; Migaszewski and

76   Galuszka, 2015). Interestingly, "Rare Earths" is a misnomer because they are neither 'earths' nor 'rare', especially

77   as the Earth's upper crust contains 0.015% REEs (Taylor and McLennan 1985), which are referred to as lithophile

78   group 3 lanthanide with atomic numbers 57 (Lanthanum) to 71(Lutetium) and two additional elements, Yttrium

79   (Z=39) and Sc (Z=21). However, most Earth scientists exclude Sc from this group due to its small ionic radius,

80   and classify only lanthanides and Y (with ionic radius similar to that of the REE Ho) into the REEs. Except for

81   Ce (Ce^{3+}, Ce^{4+}) and Eu (Eu^{2+}, Eu^{3+}), the REEs are trivalent, and their ionic radii decrease with increase of atomic

82   number, from 103 pm in La^{3+} to 86 pm in Lu^{3+} ("well known as the lanthanide contraction"). This attribute governs

83   the subtle differences in the REEs geochemical behavior as their respect for the Oddo-Harkins rule provides the

84   basis for dividing the REEs into the following groups: (i) light REE (LREE) including La through Eu or Gd, (ii)

3

85   medium REE (MREE) that comprises Sm through Ho , and (iii) heavy REE (HREE) from Gd or Tb to Lu including

86   Y (Migaszewski et al. 2014).

87   The diagnostic conservative characteristics of the REEs have made them the most useful of all trace elements in

88   igneous, sedimentary and metamorphic petrology (e.g., Migaszewski and Galuszka 2015; Johannesson and Lyon

89   1995; Gimeno et al. 2000; Gammons et al. 2005b; Rollinson 1993; Ndjigui et al. 2014; Houketchang Bouyo et

90   al. 2015), and also in characterizing surface and groundwater geochemistry (e.g., Rollinson 1993; Vazquez-Ortega

91   et al. 2015; Liu et al. 2016; Migaszewski et al. 2014; Chen and Gui 2017; Guo et al. 2010; Munemoto et al. 2015;

92   Pignotti et al. 2017; Zhuravlev et al. 2016; Ferreira et al. 2015; Sultan and Shazili 2009; Censi et al. 2017). Some

93   of the hydro-geochemical signatures that have been underpinned by the REEs include; geo-environmental controls

94   of REEs patterns in surface and groundwater, paleoclimatic conditions, redox and pH conditions, groundwater

95   flow paths, mixing between surface and groundwater, geogenic and anthropogenic inputs into water resources,

96   and water-rock interaction processes.

97   To underpin water-rock interaction processes, the work of Ferreira et al. (2015), and associated references, have

98   shown that groundwater exhibits signatures that closely resemble those for the rocks through which they flow,

99   whereas other investigations (e.g., Masuda et al. 1987; Takahashi et al. 2002) found that REEs pattern in

100   groundwater exhibits the W-type tetrad effects, while the rocks through which they flow exhibit M-type tetrad

101   effects. Despite such usefulness of REEs in hydro-geochemistry, only the work of Ndjigui et al. (2014), has so far

102   attempted to use REEs to characterized water resources in Cameroon. Furthermore, still as a results of water-rock

103   interaction, it has just been over two decades that the International Working Group on Geomedicine (IWGG),

104   now reconstituted into the International Medical Geology Association (IMGA), formalized the study of medical

105   geology as a research discipline, which has continued to develop into a fast-evolving scientific field on the global

106   scene. This is because a tremendous upsurge in research efforts is leading to the decipherment of hitherto "new

107   correlation", spurring fresh promise for success of this science.

108   Consequently, collaboration between geoscientists and medical researchers has led to the identification of

109   potential environmental health problems. In Cameroon, for instance, a link between the chemistry of groundwater

110   for drinking and human health, seems highly plausible, given that majority of the country's population still lives

111   close to the land, subsisting largely on water obtained from their immediate surroundings (Davis 2013 and

112   references there-in). This has caused water-borne diseases such as fluorosis (Fantong et al. 2009; 2010b), whose

113   science and management still require upscaling in Cameroon. Although, the German-Cameroon project code

114   named "PRESS NO and SW", presents a pilot study on pollution of surface and groundwater in the study area

115   (Jokam Nenkam et al. 2019), the data are only as a technical report.

116   Against this backdrop, the overall objective of this study is to evaluate the characteristics of water resources in

117   the Benue River Basin in Northern Cameroon, by using a combination of major ions, δD, $\delta^{18}O$, TEs and REEs.

118   The specific objectives include (1) assessing water chemistry and suitability for drinking, (2) identify groundwater

119   recharge periods and pathways, and (3) characterize REEs patterns for the water resource management in the

120   BRB, with a wider implications for sustainable livelihoods and ecosystem services management in the Niger River

121   Basin (NRB).

122   *Location, drainage, relief and climate of study area*

123   The study area (Fig. 1) is administratively located in the Cameroon's Northern Region, which is bordered to the

124   north, south, east, and west by the Far Northern Region, the Adamawa Region, the Republic of Chad, and the

125   Federal Republic of Nigeria, respectively. Geographically, the study area is located between latitudes 8° and10°N

126   and longitudes 12° and 16°E, with a surface area of 66 263 km². Hillocks by the Mandara, Adamawa Plateaux,

127   and Poli - Alantika Mountains in the north, south and west, respectively, culminate in a maximum height of 1189

128   m.asl, and drops of 165 m.asl. Such a topographic gradient permits the tributaries of river Benue to rise and flow

129   dendritically towards the west to Nigeria (Hervieu 1969). The hydrological network of the Benue River Basin in

130   Cameroon (Fig. 2), is an upstream catchment of River Niger (Fig. 1) . The principal streams that drain BRB are

131   the Mayo Rey and Mayo Godi in the west, the Mayo Louti, Mayo Kebi and Mayo Tiel in the north, and the Faro

132   and Mayo Deo in the south. At the basin midstream is the artificial Lagdo dam that occupies a surface area of

133   about 700 km^2 and has a capacity to retain 7.7 billion m^3 of water for irrigation and hydro-electricity (Blanken

134   and Pecher 2013). During dry months, the surface of the draining channels of almost all the tributaries (except for

135   the Faro and Kebi) run dry, but with underflow at depths of about 0.5 m. Such ephemeral characteristic of the

136   streams obliges the population to depend and rely on groundwater resources for domestic and subsistent

137   agriculture for most part of the year.

138   With respect to climate, the study area is situated in a semi-arid Soudano-Sahelian climatic zone, with a mean

139   annual temperature of 28°C, maximum atmospheric temperature of 45°C that drops to about 19°C in December

140   (Molua 2006). The area is characterized by a rainy and dry season. The rainy season lasts for about 5 months

141   (May to September), and seven months (October-April) for the dry season. The mean annual rainfall has reduced

142   from 1018 mm of rain between 1951-1989 (Njitchoua et al. 2005) to 950 mm in 2000-2014, with about 70 %

143 concentrated between July and September. Rainfall occurs either as low altitude monsoon rains or as occasional

144 high altitude squally showers. Despite the high amount of annual rainfall, contribution to groundwater recharge

145 remains limited because of the incidence of high annual evapotranspiration of 1800 mm, about twice the mean

146 annual rainfall. During the dry season, the harmattan winds blow from the Sahara in the north, causing an

147 estimated 48 % low humidity, and cloud of harmattan eolian dust (Fig. 3). During the rainy season, moisture-

148 laden winds blow from the Gulf of Guinea in the south, bringing higher humidity and rain which flows as runoff

149 into rivers, draining the basin dendritically.

150 *Geological and hydrogeological settings*

151 The Benue River Basin, which is an extension of the Cretaceous to Quaternary marine and continental sediments

152 in Benue trough, constitutes six (Koum, Benue, Garoua, Babouri Figuil, Mayo Oulo-Léré, and Hamakoussou) sub

153 sedimentary basins of carbonated, ferruginous, siliceous and phosphatic sandstones, mudstones, limestone,

154 conglomerates, and alluvial deposits (Nolla et al. 2015; Zaborski et al. 2004; Bessong 2012; Schwoerer 1965;

155 Ntsama et al. 2014; Maurin and Guiraud 1989; Eyong et al. 2013; Brunet et al. 1988; Tillement 1972; Ntsama et

156 al. 2014), that are intruded by basaltic rocks, and they unconformably overlay Neo-Proterozoic basement (Fig. 1)

157 (Ntsama 2013). A N-S cross section of the Mayo-Oulo sedimentary basin is presented in Fig. 4a. The dominant

158 geochemical processes that occur in the basin are compaction, inter-grain pressure, fracturing, precipitation of

159 calcite and hematite cements, kaolinization, and quartz overgrowth (Fig. 4b), which to an extend affects the

160 hydrogeology of the basin by decreasing sediment porosity and permeability together with low groundwater

161 recharge, reduces aquifer yields. According to Bouyo et al. (2015), chondrite normalized plots show enrichment

162 in LREE relative to HREE with an almost flat pattern and slight negative Eu anomaly.

163 To the southwestern border of the study area is the Adamawa massif from where some of the first order tributaries

164 of river Benue originate, and according to Ndjigui et al. (2014), the rock types on this massif do not only exhibit

165 positive Eu anomaly, but are also rich in vivianite ($Fe_3(PO_4)_2 8H_2O$ (Fodoue et al. 2015).

166 In the plains of the Benue river and its tributaries, Quaternary alluvial deposits (sand, gravel and clay) of the

167 Garoua sedimentary basin, with some description in Tillement (1972) and Njitchoua et al. (1995), constitute

168 shallow and unconfined aquifers with transmissivities of 10^{-1} to 10^{-5} m^2/s in the upper horizon, which also provides

169 surfaces on which the harmattan aeolian dust from the Sahara desert accumulates.

170 **Materials and methods**

171   Sampling campaign was undertaken in January (dry season period), during which 86 water samples were

172   randomly collected as shown in Figure 1. The number of samples included 37 from open wells with depths to

173   water ranging from 0.3 to 16.5 m, 34 from sealed wells and boreholes, 12 from surface water, including wadis

174   with depths to underflow from 0.5 to 1 m, and two from lakes. The samples were collected from the Garoua,

175   Benue, Hamakoussou, Mayo-Oulo Lere, and Babouri Figuil sedimentary basins (Fig. 1). Latitudal and longitudal

176   locations of the sample sites were predetermined in the entire catchment with the use of Google Earth, to enable

177   good spatial coverage of the basin for high-resolution hydrogeochemical analysis. Location and altitude were

178   determined on the field using a 3 m precision Garmin 64 Global Positioning System (GPS). Open wells were

179   sampled using drawing buckets anchored by ropes. Hand pump wells and boreholes were pumped for 5 - 15

180   minutes before sampling. The waters were collected into a collector after thorough rinsing with large volume of

181   sample water. Water from the collector was filled into four new 100 ml polyethylene bottles after rinsing with the

182   sample and one filtered through 0.45 μm cellulose filters and preserved unacidified for the determination of the

183   dissolved anions of SO_4^{2-}, Cl^-, F^-, Br^-, NO_3^-, NO_2^-, and PO_4^{3-} from each site. The second bottle was filled with

184   filtered and acidified water that was used for cations (Ca^{2+}, Mg^{2+}, Na^+, K^+, NH_4^+, and H_4SiO_4) and trace elements

185   (Fe^{2+}, Mn^{2+}, Al^{3+}, Pb, Cd, Ni, Zn, Cu, Ti, Sn, Mo, As, Co, Sb, Ba, U, Sr , La, Ce, Pr, Nd, Sm, Eu, Gd, Tb, Dy, Ho,

186   Er, Tm, Yb, Lu, and Y) determination. Acidification was done to pH~2 with supra-pure HNO_3 for the sampled

187   water. The third and fourth bottles for ^{18}O and ^2H and alkalinity determination were properly corked to avoid

188   evaporation. while the fourth bottle contained water that was used for alkalinity measurement. Electrical

189   conductivity (EC), pH, and water temperature were measured immediately in the field before sample collection,

190   using a Hanna made pH meter model HI 991001, pH/EC waterproof meter and a custom CT-450WR thermometer,

191   respectively. Atmospheric temperature was measured with a custom CT- 450WR thermometer. Land use, human

192   activities and rock type were noted at each sampling site using a mobile Open Data Kit (ODK) smartphone

193   application. Alkalinity measurements were carried out within 10 hours of sample collection by acid titration from

194   the volume of 0.02 N HCl added to the sample to reach the end -point titration, which was marked by a pH of 4.5.

195   Samples for anions, cations and TE, and stable environmental isotope determination were labeled, preserved in

196   ice-chilled boxes and dispatched to Federal Institute of Geoscience and Natural Resources (BGR), Hanover-

197   Germany for analyses.

198   Major elements (anions and cations) were quantified using a Spectro Ciros ICP-AES and a DIONEX ICS 3000

199   ion chromatography. Silica (H_4SiO_4) was analyzed by the molybdenum-blue method using spectrophotometry.

200   Stable environmental isotopes ratios were determined on a PICARRO cavity ringdown spectrometer (CRDS

7

201   model L2120-i), following the procedures described by Brand et al. (2009) and Lis et al. (2008).Trace elements,

202   including the REEs content were measured on an Agilent 7500ce ICP-MS. Details on the analytical

203   instrumentation and methods can be found in Birke et al. (2010). For the major elements, reliabilities of the

204   chemical measurements were verified by using a charge balance equation (Appelo and Postma 1993), and they

205   were within the limit of less than ±10 % for all the investigated samples. The obtained stable isotope ratios were

206   given in the conventional delta (δ) expression in parts per mil (‰) relative to Vienna Standard Mean Ocean Water

207   (VSMOW) with analytical precisions of ±1‰ for δD and ±1.5‰ for $\delta^{18}O$. For TEs, the analytical accuracy was

208   checked from replicate measurement of several samples and by measuring the certified reference materials (CRM)

209   standard of, River Water (SLRS-4), produced by the National Research Council of Canada. The detection limits

210   were 1 ng/L for all REEs. Analytical precision for the REEs, except for Ce and Pr, was better than 5% relative

211   standard deviation (RSD), with a 10 and 11 % RSD precision for Ce and Pr, respectively.

212   **2.1. Data processing and quantification of REEs anomalies**

213   Box and whisker plots were used to analyze the distribution of observed variables. All statistical analyses were

214   performed with R software. Aquachem software was used to draw Pipers' diagram to identify water facies, and

215   REE patterns and δD versus $\delta^{18}O$ space diagrams were drawn using Microsoft excel, while maps were established

216   with ArcGIS version 10.2 and QGIS 2.18.X softwares.

217   Although the distribution and geochemical behavior of REEs in natural materials can be illustrated by plotting the

218   relative abundances versus the atomic number, such a plot produces a saw tooth pattern (the Oddo Harkins Rule

219   effects), with decreasing slope toward the highest atomic numbers. Thus, the REEs behavior is better presented

220   if the values are normalized and reported as a relative abundance plot on a logarithmic scale . This means that the

221   concentrations of REEs found in the sample are normalized to their concentrations in a reference material such as

222   Cl chondrite, the chondritic meteorite, and the Post Archaean Australian Shales (PAAS) (Edet 2004). The

223   advantage of this process is that the Oddo Harkins Rule effect is eliminated, and any fractionation that has occurred

224   among the REEs will be detected. Hence, the abundance of positive peaks and negative troughs in the normalized

225   REE pattern reflect the geochemical history of the sample. Generally, the abundance of REEs in natural waters is

226   extremely low in comparison to the levels found in most rocks. In this investigation, the Post-Archean Average

227   Australian Shale (PAAS) (McLennan 1989), was chosen as a reference standard because 'shales' are widely used

228   in hypergene processes and environmental studies (Migaszewski et al. 2014) such as surface and shallow

229   groundwater systems affected by weathering. Detection of anomalies is based on the presence of individual

230 elements that are higher or lower than the corresponding shale-normalized patterns. For example, Eu and Ce

231 anomalies were quantified, according to Noak et al. (2014), in which the geogenic value of each element was

232 obtained by interpolation of the neighbor normalized REE elements of Ce and Eu, by using the equations presented

233 in equations (1) and (2), respectively.

234 $Ce/Ce^* = Ce_{PAAS}/(La_{PAAS} + Pr_{PAAS})^{0.5}$…………………….....(1)

235 $Eu/Eu^* = Eu_{PAAS}/(Sm_{PAAS} + Gd_{PAAS})^{0.5}$………………………..(2)

236 It is worth mentioning that the last two indexes could be influenced in some situations by anomalies in La and Gd.

237 Nevertheless, their calculation can be useful in discriminating   sampled water types.

238 **Results**

239   *Geochemistry*

240 The laboratory results for the content of major cations and anions, including EC, pH, water temperature, δD,

241 $\delta^{18}O$, TEs and REEs are presented in Tables 1a, 1b, and 1c, respectively. The elements data for rock in any of

242 the Tables are from Ndjigui et al. (2014).

243 The data shows that water temperature ranged from 24.1 to 32.2°C and 23.9 to 32.3°C in surface and groundwater,

244 respectively. In decreasing order, water temperature followed the pattern boreholes > hand dug wells > lakes >

245 rivers > springs, with a mean value of 31°C, similar to groundwater temperature reported 22 years ago by

246 Njitchoua et al. (1997). pH values ranged from acidic (5.7) to basic (8.9), declining according to the following

247 trend, lake water > rivers > springs > boreholes > dug wells. Electrical conductivity (EC) showed a wide range

248 from 35 to 2500 μS/cm, with mean values for surface and groundwater being 106 and 376 μS/cm, respectively,

249 and varied in the observed sample as, dug wells > boreholes > rivers > lakes > springs.

250 The values of major ions (anions and cations) shows that concentrations are higher in groundwater samples than

251 in surface water samples. Such observation depicts that the observed groundwater has a longer residence time in

252 the aquifer than surface water (Kazemi et al. 2006), and that the hydrological regime is dominantly a stream

253 loosing system by surface water recharging the groundwater aquifer. The concentration of anions were distributed

254 in the order of $NO_3^- > HCO_3^- > Cl^- > SO_4^{2-} > F^- > PO_4 > Br^-$ in groundwater, compared to $HCO_3^- > NO_3^- > Cl^- >$

255 $SO_4^{2-} > PO_4 > NO_2 > F^- > Br^-$ in surface water. Relative concentration of cations in both groundwater and surface

256 water was in the order of $Ca^{2+} > Na^+ > Mg^{2+} > K^+ > NH_4$. Piper's diagram (Piper 1944) plots (Fig. 5) suggest,

257   that the hydro-chemical facies evolved predominantly from Ca+Mg-NO$_3$ rich water in shallow wells to Na+K-

258   HCO$_3$ rich water in boreholes, and surface waters.

Stable environmental isotopes distribution

260   The δD values in ‰ ranged from -42 to -18 in boreholes, -32 to -16 in hand dug wells, -18 to 3 in rivers, and -27

261   in the only spring sample analysed. The δ^{18}O values in ‰ ranged from -6.62 to -2.94 in boreholes, -5.37 to -2.94

262   in hand dug wells, -3.37 to 0.55 in rivers, and -5.10 in the spring. The δD and δ^{18}O cross plots of these values are

263   presented in the delta space (Fig. 6a). The Global Meteoric Water Line (GMWL) of Craig (1961), was used for

264   comparative purposes because of the acute lack of regular rainfall measurements in the BRB. Deuterium excess

265   (d-excess) values were more than 10 ‰ in ca.70 % groundwater (hand dug wells and boreholes) samples, with

266   only the exception of one borehole that was > 15 ‰, whilst all surface waters were < 10 ‰ (Fig. 6b).

Trace elements (TEs and REEs) distribution

268   Selected trace elements concentrations are in the order of Ba > Sr >Zn > Li > V > Cu > Ni > Co > As > Cr > Sc

269   > Ti > Be > Pb > Cd, in both groundwater and surface water samples, with relatively higher concentrations in

270   groundwater compared to surface water. Figure 7 is a scatter plot of the average concentration of each metal in

271   water and in BRB sandy clay. As purported by Aiuppa et al. (2000), a good correlation between the two variables

272   suggests that composition of local sediments contribute to the water chemistry. Figure 7 also indicates that metal

273   partitioning between the sediments and solution depends on the chemical behaviour of the elements. With respect

274   to the general trend, Al, Fe, Ti, Ta, Hf, Ga, Y, Cr, and Zr appear to be depleted in water, due probably to their

275   concentration in secondary product of weathering such as oxides and clays. On the contrary, the alkalis, alkaline

276   earth and lithophile elements (Na, Mg, Ca, Sr) are shifted towards the lower axis, depicting their preferential

277   solution during weathering. A similar trend is also observed for U and Mo, called "oxo-hydroxo anion forming

278   elements" (indicated as OHA elements), due to their tendency to form water soluble anion complexes (Aiuppa et

279   al. 2000). Transition metals plot in an intermediate position.

280   Individual REEs, total REEs, LREEs, HREEs, MREEs concentrations, as well as LREEs/HREEs ratios, selected

281   raw data, and PAAS-normalized values presented in Table 1c, suggest REEs concentrations are generally low,

282   and broadly consistent with circumneutral pH waters (e.g., Johannesson et al. 1999; Guo et al. 2010). Total REEs

283   (ΣREEs) varied widely from 0.007 to15.02 μg/L with concentrations in boreholes, hand dug wells, rivers and

284   spring from 0.044 to 2.12 μg/L , 0.086 to 0.36 μg/L, and 0.149 μg/L, respectively. With the exception of Y, the

285   concentrations of REE in groundwater (boreholes and hand dug wells) followed the order Eu > Sm > Ce >Nd >

286   La > Gd > Pr > Dy > Er > Yb > Ho > Tb > Tm and these differed from the surface water rivers and spring trends

287   with concentrations in the order of Eu > Sm > Ce > Nd > La > Gd > Pr > Dy > Tb > Er > Yb > Ho. The MREE

288   (Sm-Ho) were the most abundant elements, followed by the LREE (La-Gd), with the HREE (Tb-Lu) being the

289   least abundant

290   *PAAS normalized REEs patterns*

291   To enable comparison across the full suite of sample types, the REE concentrations were normalized with respect

292   to Post-Archean Average Australian Shale (PAAS) (Fig. 8 a-g), employed extensively in groundwater studies

293   (e.g., McLennan 1989; Sholkovitz et al. 1994; Tang and Johannesson 2006; Rollinson 1993). With exception of

294   samples from boreholes 25 (BO 25) and 37 (BO 37) (Fig. 8b), which show a relatively monotonous flat pattern,

295   all the waters mostly exhibit enrichment in the HREEs relative to the LREEs. Positive Eu anomalies (Eu/Eu* =

296    $Eu_{PAAS}/(Sm_{PAAS} + Gd_{PAAS})^{0.5}$) with values of 1.08-199 in boreholes, 6.26-171 in the hand dug wells, 72.9-107.6 in

297   rivers and 30.58 in spring, impose a distinctly steep roof - shaped PAAS-normalized REE patterns, masking the

298   commonly observed "W and M" types tetrad REE patterns.

299   **Interpretation and discussion**

300   *Groundwater recharge mechanisms and period*

301   With the low temperature (~24-32°C) of water samples in the study area (Table 1a), the observed $\delta^{18}O$ and δD

302   values can be regarded as conservative during water-rock interaction reaction (e.g., Gat 2010;Taylor and Howard

303   1996). Thus, the δ-values of the groundwater would be expected to be almost similar to that of the recharging

304   meteoric water. Factors that can affect the recharging rainfall are soil-zone processes and direct

305   heterogeneous/diffuse or localized/focused rainfall infiltration (Taylor and Howard 1996). The clustering of

306   observed groundwater and surface water along the GMWL (Global Meteoric Water Line) in Fig. 6a indicates that

307   soil-zone evaporation prior to rainfall infiltration is not a significant process in the area. However, a few surface

308   water samples plot to the right of the GMWL, indicating that within the rainwater-surface water-groundwater

309   system, the incidence of evaporation prior to groundwater recharge was not totally absent. Such a pattern suggests

310   that in the study area, the mechanism of preferential flow pass (e.g. Tsujimura et al. 2007, Asai et al. 2010)

311   dominates groundwater recharge after localized evaporation (Edmunds et al. 2002, Tsujimura et al. 2007, Fantong

312   et al. 2010a). The suggestion of a preferential flow pass hypothesis indicates that irrespective of reduced porosity

313   in the study area as (Fig. 4b) illustrates, local occurrences of effective porosity in the sand-rich sediment, which

314   favors rapid infiltration of rainwater into the aquifer, cannot be totally denied. Similar recharge mechanism was

11

315 identified in part of the study area by Njitchoua et al. (1995), and in the Lake Chad (Fantong et al. 2010a), coastal

316 (Fantong et al. 2016) sedimentary basins of Cameroon, and also in the semi-arid sediments in Mongolia

317 (Tsujimura et al. 2007). The high d-excess in groundwater (with ca. 75 % of the groundwater samples having

318 values above 10 ‰) does not only confirm direct infiltration of rainwater into the shallow aquifer (Kebede et al.

319 2005), but also suggests that groundwater recharge occurred under low relative humidity conditions (Kendall and

320 Doctor 2011). The implications from the δ-space diagram (Fig. 6a) and d-excess (Fig. 6b) indicate hydraulic

321 connectivity within the shallow aquifer that favors mixing between surface and the shallow groundwater over the

322 entire region. A comparison of isotopic compositions between monthly local rainfall and groundwater on a δ-

323 space can be employed to identify the period(s) of groundwater recharge (e.g., Mbonu and Travi 1994; Nkotagu

324 1996; Taylor and Howard 1996; Deshpande et al. 2003). The δ values for monthly rainfall co-opted from

325 Njitchoua et al. (1995) and plotted together with measured (Fig. 6a) and as observed, the $\delta^{18}O$ and δD in

326 groundwaters clustered between those of July and September abundant monsoon rains, indicating that the

327 groundwater is predominantly recharged in the months of July and September. This groundwater recharge period

328 is similar to that in the Lake Chad basin (Fantong et al. 2010a), but differs from the recharge period of June to

329 August in the Lakes Monoun and Nyos volcanic aquifer (Kamnctueng et al. 2014), May to June in the Quaternary

330 sediment in Ndop plain (Wirmvem et al. 2015), and May to September in the volcano-sedimentary aquifers of

331 Mt. Cameroon and Douala (Fantong et al. 2016). As the rainwater circulates to recharge the groundwater, water-

332 rock interaction occurs, which result in geogenic sources of ions in water (e.g., Faure 1991; Fantong et al. 2009;

333 Fantong et al. 2010b) .

334 ***Geogenic controls on the chemical composition of water***

335 Gibbs (1970) used the chemical composition of freshwater to identify major processes controlling dissolved ions

336 in water based on the concentration of total dissolved solids (TDS) and $(Na^+ + K^+)/(Na^+ + K^+ + Ca^{2+})$ and $Cl^-/(Cl^-$

337 $+ HCO_3^-)$ ratios. Similarly, Gibbs diagram (Fig. 9) for sites dominantly within the rock domain, suggests

338 incongruent dissolution of silicates as the provenance of Ca, Mg, Na, K, and HCO_3 to groundwater according to

339 the following reactions (3), (4) and (5) (Nesbitt and Wilson 1992; Subramani et al. 2010; Faure 1991), which

340 could be promoted by root respiration (Fantong et al. 2009):

341 $CaAl_2SiO_2O_8 + 2CO_2 + 3H_2O = Al_2SiO_5 (OH)_4 + Ca^{2+} + 2HCO_3$ ………………………..(3)

342 $2NaAlSi_3O_8 + 2H_2CO_3 + 9H_2O = 2Na^+ + 2HCO_3^- + Al_2Si_2O_5(OH)_4 + 4H_4SiO_4$…………..(4)

343 $2KAl Si_3 O8 + 2H^+ + 2H_2O = Al_2 Si_2 O_5 (OH)_4 + 4SiO_2 + 2K^+$…………………………..(5)
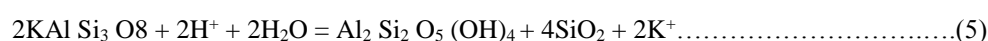
344 Although such incongruent dissolution depicts that weathering of rock-forming minerals is a controlling factor

345 for the major ion chemistry of groundwater in the area, the Ca and Na systems stability diagrams (Fig. 10 a-b)

346 further clarify the equilibrium states between the secondary minerals and the circulating water (Tardy 1971;

347 Appelo and Postma 1993). For example, the stability of albite, anorthite, kaolinite, and montmorillonite in the

348 waters was evaluated in this study by plotting log (aNa^+/aH^+) vs Log (aH_4SiO_4) and Log $(a Ca^{2+}/a2H^+)$ versus log

349 (aH_4SiO_4). The diagrams were drawn with the assumption that Al was preserved in the weathering product

350 (Appelo and Postma 1993; Faure 1991). End member compositions were also assumed using equilibrium

351 relationship for standard temperature (25^oC) and pressure (1 atmosphere), which approximately reflect the

352 groundwater conditions. Constituents' activities computed using Phreeqc for Windows version 2.1 (Appelo and

353 Postma 1993), show that groundwater and surface water from the study area span the stability fields of Na-

354 montmorillonite (Fig.10 a), Ca-montmorillonite (Fig.10 b), kaolinite and amorphous silica. These observations

355 do not only concur with the occurrence of clay minerals in the study area, but are also similar to findings from

356 areas such as the Lake Chad basin (e.g., Fantong et al. 2009) and the Lake Nyos catchment (e.g., Fantong et al.

357 2015), where granites constitute the fresh rock suites. Moreover, with saturation index (SI) it is possible to predict

358 the reactive mineralogy of the subsurface from groundwater data without collecting the samples of the solid phase

359 and analyzing the mineralogy (Deutsch 1997). The saturation index (SI) of a given mineral is defined in Eq. (6)

360 (Garrels and Mackenzie, 1967) SI = $\log_{10}$(IAP/Ksp)…………………………………………….(6)

361 IAP is the ion activity product of the solution and Ksp is the solubility product at a given temperature (the

362 thermodynamic equilibrium constant adjusted to the temperature of a given sample). The thermodynamic data

363 used in this computation are those contained in the default database of the 'Phreeqc for Windows'. Supersaturation

364 (SI > 0) indicates that precipitation is thermodynamically favorable. On the other hand, undersaturation (SI < 0)

365 signifies that dissolution is favored. Using this guideline, a plot of SI against TDS indicates that all the samples

366 were undersaturated with respect to gypsum and anhydrites relative to some crossing the undersaturation threshold

367 into the supersaturation zone for the carbonates of calcite, aragonite, and dolomite (Fig. 10 c). This may reflect

368 the incongruent re-dissolution of calcium carbonates that commonly occur as cementing material within the

369 sediments as shown in Fig. 4b. However, the strong evidence for incongruent dissolution, imply favorable

370 environmental conditions such as pH, reduction, oxidation, residence time, enabled the selective enrichment of

371 water with major cations, Si, trace elements and REEs.

372 *Geo-environmental controls and implications for REEs patterns*

13

373 As shown in Figure 8, the REE patterns in groundwater (boreholes and hand dug wells) fall within the same range

374 and are spatially the same as for surface waters (rivers, springs), where both show distinct but similar positive Eu

375 positive anomalies. This similarity suggests that hydraulic connectivity between groundwater and surface water

376 result in mixing. Further the generally flat PAAS normalized REEs pattern of samples BO37 and BO25 (Fig. 8b),

377 is interpreted as groundwater sourced from deeper aquifer that do not mix with the surface water. Moreover, the

378 clustering of groundwater $\delta^{18}O$ and δD values with surface waters (Fig. 6a) and their similar water chemistries

379 support spatial mixing enabled by aquifer interconnectivity (Fig. 5). To further verify such aquifer

380 interconnectivity, the log-log plots for trace elements in different types of waters in boreholes (BO) that showed

381 absence and presence of EU anomaly, and for a hand dug well and borehole are presented in Fig. 11a and 11b,

382 respectively. According to Taran et al. (2008), such correlation plots can be used for the estimation , at least ,

383 qualitative, whether waters from different sources originate from the same aquifer or not. The two plots show very

384 good correlation between major and trace elements, suggesting that irrespective of slight differences in REE

385 patterns of sample BO25 and BO37, all waters are from the same aquifer or a part of a bigger aquifer.

386 Such a mixing-based REEs pattern has been reported in the North China plain (Liu et al. 2016), and Australian

387 catchment (Duvert et al. 2015). The characteristic steep-roof-shaped PAAS normalized pattern may hints that

388 MREEs are more easily leached from parent rocks (Migaszewski et al. 2014), through preferential dissolution of

389 feldspars (Guo et al. 2010), because, bivalent Eu (an MREE) is selectively enriched and incorporated into primary

390 tectosilicates. For example, MREE enrichment in K-felspars and plagioclases is achieved by preferential

391 substitution into Ca^{2+}, Na^+, and K^+ sites. Moreover, preferential dissolution of feldspars relative to other REE-

392 bearing primary minerals, should result in positive aqueous Eu-anomalies (Ma et al. 2011; Brioschi et al. 2013).

393 Such positive Eu anomaly in freshwater has also been attributed to dissolution of phosphate mineral and eolian

394 deposition (Vazquez-Ortega et al. 2015).

395 Considering that phosphate-Feldspar-rich minerals (e.g., vivianite) have been located in the western upstream of

396 our study area (Fodoue et al. 2015; Bouyo et al. 2015), and that the fresh granitoids in the study area have similar

397 positive Eu anomalies (Ndjigui et al. 2014), while the sediments express negative Eu anomalies (Ndjigui et al.

398 2014; Bouyo et al. 2015), point to incongruent dissolution of silicates, followed by enrichment in water and

399 depletion in sediments. It has also been reported that influent atmospheric aeolian dust contains substantial total

400 phosphorous, which can be associated with phosphate and alkali feldspars (Nash 1984). Hence, dust inputs may

401 contribute significantly to the near surface REEs measurements. As shown in Fig. 3, the study area is markedly

14

402 influenced by eolian dust storm, and eventually deposited as sediments in which the shallow groundwater and

403 surface water circulates to acquire a positive Eu anomaly.

404 It is worth noting that the observed positive Eu anomalies in freshwater within the study area contradicts

405 observations in high temperature hydrothermal waters (Rollinson 1993; Bau 1991) and in fresh water from the

406 Terengganu River basin, Malaysia (Sultan and Shazili 2009) and Tono in central Japan (Munemoto et al. 2015).

407 However, the patterns are similar to freshwater from New Northern Mexico, South central Poland, Northern

408 Anhui Province in China, Ukraine, Israel, Romagna in Italy, North China plain, and Inner Mongolia |(Vazque-

409 Ortega et al. 2015; Migaszewski et al. 2014; Chen and Geu 2017; Zhuravlev et al. 2016; Censi et al. 2017; Pignotti

410 et al. 2017; Liu et al. 2016; and Guo et al. 2010). Although most of the latter work attributed their REEs patterns

411 to redox conditions, our investigation did not measure the Eh of sampled waters, thus falling short of defining the

412 precise redox conditions that controlled REEs concentrations in the BRB. However, the biplots of La/Yb ratio

413 against HCO_3 (Fig. 12), show that La/Yb ratio in surface water increased at low HCO_3 concentration, while the

414 ratio dropped significantly in groundwater as HCO_3 concentration increases. Such plots suggest that acidic

415 conditions most likely favoured the enrichment of HREEs and MREEs concentrations in surface waters, while

416 enriching LREEs under alkaline conditions. This observation, however, is in disagreement with the suggestion

417 of Johannesson and Hendry (2000) that higher carbonate ion concentrations would promote greater stability of

418 the REEs in solution, and lead to their elevated concentrations.

419 **Potentially Harmful Elements (PHEs) and health impacts**

420 An interplay of geogenic and anthropic factors is suggested to mobilize potentially harmful elements (PHEs) such

421 as fluoride (F-), cadmium (Cd), lead (Pb), and arsenic (As) to water reaching levels that expose the local population

422 to various unhealthy clinical phenomena.

423 Contextually, PHEs are elements whose concentrations in water are toxic to consumers (Davies 2013), for

424 example F-, Cd, Pb, and As. Most fluoride-related health studies pay more attention to endemic fluoride exposure

425 from drinking water because that is the easiest pathway to quantify the impact on a community served by public

426 water supply. Considering that the maximum permissible level of fluoride in drinking water is set at 1.5 mg/L by

427 WHO (WHO 2004) and an optimum level of 0.7 mg/L for the semi-arid Northern regions of Cameroon (Fantong

428 et al. 2010b), the concentrations of fluoride measured in the water samples (Table 1a; Fig. 13) show an undesirable

429 concentrations of fluoride in drinking water sources from both the sedimentary basins (Garoua, Hamakoussou,

430 Mayo Oulo Lere, and Babouri Figuil) and the granitic Precambrian basement, where children from these localities

431 (Barnake, Garoua, Pitoa, and Figuil) manifest chronic incidences of fluorosis (pitted teeth with white horizontal

432 striations, pitted brown teeth, and unpitted teeth with black, brown, and chalky coats). Considering that the study

433 area is just to the south of the Mayo Tsanaga River Basin, where Fantong et al. (2010b), identified alkaline-

434 mobililized geogenic (mica and fluorapatite) provenance of fluoride in groundwater exploited for drinking, it is

435 most likely that similar geochemical factors control the origin and mobilization of fluoride in the Benue River

436 basin. However, a site-specific investigation is hereby proposed to underpin the origin and factors that mobilize

437 fluoride in groundwater within the study area.

438 With respect to metalloids and heavy metals such as As, and Cd, and Pb, respectively, which have been found to

439 cause lung and bladder cancers (Silvera and Rohan 2007), kidney damage (Davies 2013), and blockage of the

440 large intestine (Tayie 2004), respectively, their concentrations in the study area (Table 1b) were found to be below,

441 but close to the WHO (2004) threshold limits in some of the drinking water sources observed (Fig. 14). Although,

442 the values of As, Cd and Pb (Fig. 14a-c), increase in the populated locality of Garoua, relative to sites with limited

443 human influence, suggest a more likely anthropogenic origin for As, Cd and Pb, for instance from smelting, open-

444 air burning of E-waste, and poorly disposed batteries (Davies 2013), a positive correlation of As, Cd, and Pb with

445 HCO_3 in some samples (Fig. 15 a, b, and c), still suggests contribution from water-rock interaction processes.

446 Evidence for anthropogenic input into the observed water samples can also be observed by a positive correlation

447 between As, Cd and Pb versus NO_3 in some samples (Fig. 15 d, e and f), and a sturdy positive correlation between

448 nitrate and chloride (Fig. 16), as explained in Fantong et al. (2016 and references there-in). Thus, a combination

449 of conditions for water-rock interaction and anthropogenic input mobilizes elements in water, and determines the

450 degree to health impacts on the population within the BRB.

451 **Relative Mobility of metals in waters within the Benue River Basin**

452 The extend to which major and trace elements enter the aqueous phase during weathering is called " relative

453 mobility" (RM), which was computed from Eqn. 7 (Meybeck 1987; Gislason et al. 1996).

454 $RM = (X/Mg)_w/(X/Mg)_r$………………………………………………………………………7

455 Where w and r refer to the solution and the rock, respectively. Considering that this approach has been successfully

456 applied to rivers draining basaltic terrains in Iceland (e.g., Louvat 1997), Mt. Etna-Sicily (Aiuppa et al. 2000), and

457 Mount Vesuvius volcanic aquifer in Italy (Aiuppa et al. 2005), in this study, the relative mobility of elements was

458 calculated for 10 samples (representing boreholes (BO), hand dug wells (W), rivers (R), Spring (Sp), no EU

459 anomaly samples (BO 25; and 37), and EU anomaly samples (e.g., BO 53)) from their water/rock concentration

16

460   ratio, normalized to magnesium, because of its strong chemical mobility during weathering. The results, which

461   are presented in Table 2, are plotted in Figure 17 a, b, in which elements are ranked with RMs increasing from

462   left to right with the groupings (1), (2), (3), and (4) representing the OHA (oxo-hydroxo anion) elements, alkalis

463   and alkaline earths, transition metals, and immobile metals, respectively. The main information therefrom are

464   summarized as follows:

465   (i)   The spike-shaped data pattern reveals that the dissolution of BRB lithology is not isochemical with

466   relative mobility values ranging from 0.01-2.48 for OHA elements; 0.01-24.3 for alkalis and alkaline

467   earths; 0.01 to 76.33 for transition metals, and 0.01-0.15 for immobile metals.

468   (ii)   Aqueous mobility of redox-sensitive elements such as Mn and Fe is weak, disagreeing with the

469   findings of Aiuppa et al. (2005), in the volcanic aquifer of Versuvius, where their mobility was

470   significantly enhanced.

471   (iii)   The mean mobility sequence for alkalis is Na > K > Rb, and that for alkaline earth elements is Ca >

472   Ba. In agreement with the observation of Aiuppa et al. (2005), both sequences are similar to the

473   Hofmeister series, which refer to the relative affinity of cations for clay minerals and oxides (e.g.,

474   Stumm and Morgan 1996). Thus, water-rock interaction is a controlling factor for the distribution of

475   these elements between the aqueous and solid phase in the BRB, probably enriching the aqueous

476   phase in lithogenic fluoride that is consumed via drinking water sources and leading to observed

477   fluorosis.

478   (iv)   Lead, Cu, Zn, Mo, U, Ca, and Sr are among the most mobile elements in the BRB.

479   (v)   Aluminum is shown to be the most immobile element , probably because it is retained in the product

480   of incongruent dissolution such as hydroxides and clay minerals. Moreover, Cr, Mn, Rb, and V are

481   among the least mobile elements in the BRB.

482   (vi)   For the only spring source that was sampled (Sp001), the analyzed elements show relative mobility

483   values ranging in between those of hand dug wells and boreholes, indicating that the spring water

484   was more or less draining an aquifer, thus a "surface water gaining system".

485   (vii)   The hand dug wells (W028; W038), are characterized by lowest elements mobility, suggesting that

486   among the selected samples, they harbor the weakest water-rock interaction (WRI) process.

487   (viii)   The boreholes (B025 and B037), on the other hand are characterized by highest elements mobility

488   (Fig. 17a), suggesting that they harbor the strongest water-rock interaction processes. This trend

489   supports the speculation that their flat REE patterns (Fig. 8b) may be attributed to deeper aquifer

490   sources.

491   When these heavy metal (loid)s dissolve in water bodies, their mobility and dispersion are partly controlled by

492   pH. To check this assertion, the sum of Pb, Cd, Cu, Zn, and Co was plotted against pH (Fig. 18), which depicts

493   that in acidic pH < 6, condition the concentration of the heavy metal (loid)s increased in groundwater. On the

494   other hand, a pH > 6, causes the concentrations to drop below 250 µg/L in both groundwater and surface waters.

495   **Conclusions**

496   In the Benue River Basin, Cameroon, one of the major upstream catchments of river Niger, groundwater is

497   recharged by monsoon rainwater from July to September via a permeable clayey sandy lithology that favours

498   hydraulic connectivity, preferential flow pass mechanism, but minimizes evaporation. High d-excess values (>10

499   ‰) in groundwater indicate that the recharge occur under low relative humidity conditions. Major ions plots on a

500   Piper`s diagram, δD versus $\delta^{18}O$ plots, and PAAS normalized REEs patterns, depict mixing of surface and

501   groundwater within a shallow aquifer system. The aquifer minerals interact with the circulating water

502   incongruently, in an acidic-basic media, resulting in equilibrium between secondary clay minerals (kaolinite, Ca-

503   montmorillonite, and Na-montmorillonite) and the groundwater, which becomes loaded with dissolved major

504   ions, TEs and REEs. The results further indicate non-isochemical dissolution of local rocks by water, with springs,

505   wells and borehole waters exhibiting surface water-gaining, weakest water-rock interaction, and strongest water-

506   rock interaction processes, respectively. Poorly mobile elements (Al, Th and Fe) are preferentially retained in the

507   solid residue of incongruent dissolution, while alkalis, alkaline earth and oxo-anion-forming elements (U, Mo,

508   Na, K, Rb, Ca, Li, Sr, Ba, Zn, Pb) are more mobile and enriched in the aqueous phase, whereas transition metals

509   display an intermediate behaviour. The dominantly geogenic processes imprint hydro-chemical signatures that

510   varied from Ca+Mg-NO$_3$ type in shallow wells to Na+K-HCO$_3$ type in boreholes, and surface waters, with

511   undesired concentrations of fluoride along the southwest-northeast corridor of the study area, where children

512   manifest fluorosis in the localities of Barnake, Garoua, Pitoa, and Figuil. In addition to the fluoride-based health

513   impacts, geogenic and anthropogenic concentrations of potentially harmful Cd, Pb and As are mobilized in acidic

514   media attaining near-undesirable levels in and around populated localities. The data suggest that these localities

515   should be actively monitored for As, Cd and Pb vulnerability linked to chronic toxicity, which could turn acute

516   along the Niger river following population expansion and industrialization. The observed surface and groundwater

517   samples had acidic-mobilized, low REEs concentrations with a wide range (0.007 to15.02 µg/L) in total REEs

518 (ΣREEs), and "steep roof-shaped" PAAS normalized positive Eu anomalies that could be attributed to preferential

519 dissolution of feldspars relative to other REE-bearing primary minerals, the dissolution of phosphate-rich

520 minerals, and the deposition of eolian dust. This work suggests important tenets for sustainable management of

521 groundwater resources in other headwater basins in Sub-Saharan Africa.

522

523

529

530

531

532 **References**

533 Asai, K., Satake, H., and Tsujimura, M. (2010). Isotopic approach to understanding the groundwater flow system

534   within the andesitic strato-volcano in a temperate humid region: case study of Ontake volcano, Central

535   Japan. Hydrological Processes, 23, 559–571.

536 Appelo, C.A.J., & Postma, D. (1993). Geochemistry, groundwater, and pollution. Balkema, Netherlands, p 536.

537 Aiuppa, A., Allard, P., D'Alessandro, W., Michel, A., Parello, F., Trueil, M., and Valenza, M. (2000). Mobility

538   and fluxesof major, minor and trace metals during basalt weathering and groundwater transport at Mt. Etna

539   volcano (Sicily). Geochemica et Cosmochimica Acta. Vol. 64, No. 11, 1827-1841.

540 Aiuppa, A., Federico, C., Allard, P., Gurrieri, S., and Valenza, M. (2005). Trace metal modelling of groundwater-

541   gas-rock interactions in a volcanic aquifer: Mount Vesuvius, Southern Italy. Chemical Geology. 216, 289-

542   311.

19

543   Azzaz, H., Cherchali, M., Meddi, M., Houha, B., Puig, J.M., Achachi, A. (2008). The use of environmental
544   isotopic and hydrochemical tracers to characterize the functioning of karst systems in the Tlemcen
545   Mountains, northwest Algeria. Hydrogeol J. 16, 593– 607.

546   Bau, M. (1991). Rare-earth element mobility during hydrothermal and metamorphic fluid-rock interaction and the
547   significance of the oxidation state of europium. Chem. Geol. 93, 219–230.

548   Bessong, M. (2012). Paléoenvironnements et diagenèse dans un réservoir gréseux d'âge crétacé du fossé de la
549   Bénoué au Nord Cameroun : les grès de Garoua. Thèse de Doctorat, Université de Poitiers, 197 p.

550   Birke, M., Reimann, C., Demetriades, A., Rauch, U., Lorenz, H., Harazim, B., Glatte, W. (2010). Determination
551   of major and trace elements in European bottled mineral water—analytical methods. J Geochem Explor
552   107:217–226. doi:10.1016/j.gexplo.2010.05. 005

553   Blanken, J., and Pecher, S. (2013). Programme "changements climatiques, gestion des ressources naturelles et
554   securite alimentaire dans le bassin versant de la Bénoué" Technical Report.

555   Bouyo, M. H., Zhao, Y., Penaye, J., Zhang, S.H., Njel, U.O. (2015). Neoproterozoic subduction-related
556   metavolcanics and metasedimentary rocks from the Rey Bouba Greenstone Belt of north-central Cameroon
557   in the Central African Fold Belt: New insights into a continental arc geodynamic setting. Precambrian
558   Research. 261, 40-53.

559   Brand, W.A., et al. (2009). Cavity ring-down spectroscopy versus high temperature conversion isotope ratio mass
560   spectrometry; a case study on δ^2H and δ^{18}O of pure water samples and alcohol/water mixtures. Rapid
561   Communication in Mass Spectrometer, 23, 1879-1884. doi:10.1002/rcm.4083

562   Brioschi, L., Steinmann, M., Lucot, E., Pierret, M.C., Stille, P., Prunier, J., Badot, P.M. (2013). Transfer of rare
563   earth elements (REE) from natural soil to plant systems: implications for the environmental availability of
564   anthropogenic REE. Plant Soil 366, 143–163.

565   Brunet, M., Dejax J., Brillanceau ,A., Congleton, J ., Downs, W., Duperon-Laudoueneix M., Eisenmann V.,
566   Flanagan, K., Flynn, L., Heintz, E., Hell, J., Jacobs, L., Jehenne, Y., Ndjeng, E., Mouchelin, G., et Pilbeam,
567   D. (1988). Mise en évidence d'une sédimentation précoce d'âge Barrémien dans le fossé de la Bénoué en
568   Afrique occidentale (Bassin du Mayo Oulo Léré, Cameroun), en relation avec l'ouverture de l'Atlantique
569   Sud. C.R. Acad. Sci. Paris, 306 (II), pp. 1125-1130).

570 Budyko, M.I. (1951). On climate factors of runoff. Prob. Fiz. Geogr. 16 in Russian Canadian Council of Ministers

571   of the Environment (2001a) Canadian water quality guidelines for the protection of aquatic life. CCME

572   water quality index 1.0, Technical report. http://www.ccme.ca

573 Censi, P., Raso, M., Yechieli, Y., Ginat, H., Saiano, F., Zuddas, P., Brusca, L., D'Alessandro, W., and

574   Inguaggiato, C. (2017). Geochemistry of Zr, Hf, and REE in a wide spectrum of Eh and water

575   composition: The case of Dead Sea Fault system (Israel), Geochem. Geophys. Geosyst., 18, 844–857,

576   doi:10.1002/2016GC006704.

577 Chen, S., and Gui1, H. (2017). Hydrogeochemical characteristics of groundwater in the coal-bearing aquifer of

578   the Wugou coal mine, northern Anhui Province, China. Appl. Water Sci. 7, 1903-1910.

579 Craig, H. (1961). Isotopic variation in meteoric water. Science. 133,1702–1703.

580 Davies, T.C. (2013). Geochemical variables as plausible aetiological cofactors in the incidence of some common

581   environmental diseases in Africa. Journal of African Earth Sciences. 79, 24-49.

582 Deshpande, R.D., Bhattacharya, S.K., Jani, R.A., Gupta, S.K. (2003). Distribution of oxygen and hydrogen

583   isotopes in shallow groundwaters from southern India: influence of a dual monsoon system. J Hydrol. 271,

584   226–239.

585 Deutsch, W.J.(1997). Groundwater geochemistry: fundamentals and applications to contamination. Lewis, New

586   York, p 221.

587 Duvert, C., Cendón, D.I., Raiber, M., Seidel, J., Cox, M.E. (2015). Seasonal and spatial variations in rare earth

588   elements to identify inter-aquifer linkages and recharge processes in an Australian catchment. Chem. Geol.

589   369, 83–97.

590 Edet, A.E. (2004). A preliminary assessment of the concentrations of rare earth elements in an acidic fresh

591   groundwater (south-eastern Nigeria), Applied Earth Science, 113, 100-109.

592 Edmunds, W.M., Carrillo-Rivera, J.J., Cardona, A. (2002). Geochemical evolution of groundwater beneath

593   Mexico city. J Hydrol. 258,1–24.

594 Eyong, J.T., Bessong. M., Hell, J.V., Mfoumbeng, M.P., Ntsama, A.J., Ngjeng, E. (2013). Lithostratigraphy of

595   the Mayo Oulo-Lere basin Northern Cameroon (W. Africa). Journal of Geological Resource and

596   Engineering. 1, 2328 – 2193.

21

597   Fantong, W.Y., Satake, H., Ayonghe, S.N., Aka, F.T., Kazuyoshi, A.(2009). Hydrogeochemical controls and
598   usability of groundwater in the semi-arid Mayo Tsanaga River Basin: Far north province, Cameroon. J.
599   Environ. Geol. 58, 1281–1293.

600   Fantong, W.Y., Satake, H., Aka, F.T., Ayonghe, S.N., Asai, K., Mandal, A., Ako, A.A. (2010a). Hydrochemical
601   and isotopic evidence of recharge, apparent age, and flow direction of groundwater in Mayo Tsanaga River
602   Basin, Cameroon: bearings on contamination. Environ. Earth Sci. 60, 107–120.

603   Fantong, W.Y., Satake, H., Ayonghe, S.N., Suh, C.E., Adelana, S.M.A., Fantong, E.B.S., Banseka, S.H.,
604   Gwanfogbe, C.D., Woincham, L.N., Uehara, Y., Zhang, J. (2010b). Geochemical provenance and spatial
605   distribution of fluoride in groundwater of Mayo Tsanaga River Basin, Far North Region, Cameroon:
606   implications for incidence of fluorosis and optimal consumption dose. Environ Geochem Health. 32,147–
607   163.

608   Fantong, W.Y., Kamtchueng, B.T.,Yamaguchi, K.,, Ueda, A., Issa., Ntchantchoa, R., Wirmvem, M.J., Kusakabe,
609   M.,Ohba, T., Zhang, J., Aka, F.T., Tanyileke, G., Joseph V. Hell, J.V. (2015). Characteristics of chemical
610   weathering and water–rock interaction in Lake Nyos dam (Cameroon): Implications for vulnerability to
611   failure and re-enforcement. Journal of African Earth Sciences. 101, 42-55.

612   Fantong, W.Y., Fouepe, A.T., Ketchemen-Tandia, B., Kuitcha, D., Ndjama, J., Fouepe, T.A., Takem, G.E., Issa
613   Wirmvem, M.J., Bopda Djomou, S.L., Ako, A.A., Nkeng, G.E., Kusakabe, M., Ohba, T. (2016). Variation
614   of hydrogeochemical characteristics of water in surface flows, shallow wells, and boreholes in the coastal
615   city of Douala (Cameroon). Hydrol. Sci. J. http://dx.doi.org/10.1080/0262666720161173789.

616   Faure, G. (1991). Principles and Applications of Inorganic Geochemistry. Macmillan publishing, New York, pp.
617   626.

618   Ferreira, C.A., Helena, E. L., Palmieri., Maria Ângela de B. C. M. (2015). Rare Earth Elements And Uranium In
619   Fountain Waters From Different Towns Of The Iron Quadrangle, Mg, Brazil. International Nuclear Atlantic
620   Conference. Associação Brasileira De Energia Nuclear - ABEN ISBN: 978-85-99141-06-9

621   Fodoue, Y., Nguetnkam, J.P., Tchameni, R., Basga, S.D., and Penaye, J. (2015). Assessment of the Fertilizing
622   effect of Vivianite on the growth and yield of the Bean "Phaseolus vulgaris" on oxisoils from Ngaoundere
623   (central North Cameroon). International Research Journal of Earth Sciences. 3 (4), 18-26.

624 Garrels, R.M., Mackenzie, F.T. (1967). Origin of the chemical composition of some springs and lakes. In: Gould
625   RF (ed) Equillibrium concepts in natural water systems. American Chemical society, Washington, DC, pp
626   222–242.

627 Gammons, C. H., Wood, S. A., Pedrozo, F., Varekamp, J. C., Nelson, B. J., Shope, C. L., & Baffico, G. (2005b).
628   Hydrogeochemistry and rare earth element behavior in a volcanically acidified watershed in Patagonia,
629   Argentina. Chemical Geology, 222, 249–267.

630 Gat, J.R. (2010). Isotope hydrology: a study of the water cycle. Series on environmental science and
631   management, vol 6. Imperial College Press, London

632 Gibbs, R.J. (1970). Mechanisms controlling World water chemistry. Science, 170, 1088–1090. American
633   Association for the Advancement of Science, Washington DC. doi:10.1126/science.170.3962.1088.

634 Gimeno, M. J., Auqué, L. F., & Nordstrom, D. K. (2000). REE speciation in low-temperature acidic waters and
635   the competitive effects of aluminium. Chemical Geology, 165, 167–180.

636 Gislason, S.R., Arnorsson, S., Armannsson, H. (1996). Chemical weathering of basalts in southwest Iceland:
637   effects of runoff,, age of rocks and vegetative/glacial cover. Am. J. Sci. 296, 837-907

638 Goni, I.B. (2006). Tracing stable isotope values from meteoric water to groundwater in the south western part of
639   the Chad basin. Hydrogeol. J. 14, 4331–4339.

640 Guo, H.M., Zhang, B., Wang, G.C., Shen, Z.L. (2010). Geochemical controls on arsenic and rare earth elements
641   approximately along a groundwater flow path in the shallow aquifer of the Hetao Basin, Inner Mongolia.
642   Chem. Geol. 270, 117–125.

643 Herczeg, A.L., Simpson, H.J., Mazor, E. (1993). Transport of soluble salts in a large semiarid basin. River
644   Murray, Australia. J Hydrol. 144, 59–84.

645 Houston, J. (2007). Recharge to groundwater in the Turi basin, northern Chile: an evaluation based on tritium and
646   chloride mass balance techniques. J Hydrol. 334, 534-544.

647 Johannesson, K. H., & Lyons, W. B. (1995) . Rare-earth element geochemistry of Colour Lake, an acidic
648   freshwater lake on Axel Heiberg Island, Northwest Territories, Canada. Chemical Geology, 119, 209-223.

649 Johannesson, K.H., Farham, I.M., Guo, C.X., and Stetzenbach, K.J.(1999). Rare earth element fractionation and

650 concentration variations along a groundwater flow path within a shallow, basin-fill aquifer, southern

651 Nevada, USA. Geochemica et Cosmochima Acta. 63, 2697-2708.

652 Johannesson, K.H., Hendry, M.J. (2000). Rare earth element geochemistry of groundwaters from a thick till and

653 clay-rich aquitard sequence, Saskatchewan, Canada. Geochim. Cosmochim. Acta 64 (9), 1493–1509.

654 Jokam Nenkam, T. L. L., Nbendah, P., Fantong, W.Y., Takoundjou, A. F. (2019). Etude Pilote sur la Pollution

655 des Eaux de Surface et Souterraines a Garoua et ses environs et son Impact sur la Sante des Populations

656 Riveraines (EPESS Garoua). Federal Institute for Geosciences and Natural Resources (BGR) Technical

657 Report No. 05-2388. Edited by Kringel Robert, Vassolo Sarah, and Wilczok Charlotte. 125 pages.

658 Kamtchueng, B.T., Fantong, W.Y., Ueda, A., Tiodjio, E.R., Anazawa, K., Wirmvem, M.J., Mvondo, J.O.,

659 Nkamdjou, L.S., Kusakabe, M., Ohba, T., Tanyileke, G., Hell, J.V. (2014). Assessment of shallow

660 groundwater in Lake Nyos catchment (Cameroon, central Africa): Implications for hydrogeochemical

661 controls and uses. Environ. Earth Sci. http://dx.doi.org/10.1007/s12665-014-3278-6.

662 Kazemi, G.A., Lehr, J.H., Perrochet. P. (eds) (2006). Groundwater age. Wiley, Hoboken, New Jersey, 325 pp

663 Kebede, S., Travi, Y., Alemayehu, T., Ayenew, T. (2005). Groundwater recharge, circulation and geochemical

664 evolution in the source region of the Blue Nile River, Ethiopia. Appl Geochem. 20,1658– 1676.

665 Kendall, C., Doctor, D.H. (2011). Stable isotope applications in hydrologic studies. In: Holland HD, Turekian KK

666 (eds) Isotope geochemistry, 1st edn. Academic Press, London, pp 181-220.

667 Leduc, C., Taupin, J.D., Gal La Salle, C. (1996). Estimation de la recharge de la nappe phreatique du Continental

668 Terminal (Niamey, Niger). C R Acad Sci Paris Ser IIa 323, 599-605.

669 Lis, G., Wassenaar, L.L., and Hendry, M.J. (2008). High precision laser spectrometry D/H and $^{18}O/^{16}O$

670 measurements of microliter natural water samples. Analytical Chemistry, 80, 287–293. doi:10.1021/

671 ac701716q

672 Liu, H., Guo, H., Xing, L., Zhan, Y., Li, F., Shao, J., Niu. H., Liang, X., Li, C. (2016). Geochemical behaviours

673 of rare earth elements in groundwater along a flow path in the North China Plain. Journ. Asian Earth

674 Sciences. 117, 33-51.

24

675   Louvat, P. (1997). Etude geochemique de l`erosion fluviale des iles volcaniques : l`aide des bilans d`elements

676   majeurs et traces. These de doctorat, Universite Paris VII.

677   Ma, L., Jin, L., Brantley, S.L. (2011). How mineralogy and slope aspect affect REE release and fractionation

678   during shale weathering in the Susquehanna/Shale Hills Critical Zone Observatory. Chem. Geol. 290, 31–

679   49.

680   Masuda, A., Kawakami, O., Dohmoto, Y., and Takenaka, T. (1987). Lanthanide tetrad effects in nature: Two

681   mutually opposite types, W and M. Geochemical Journal. 21, 119-124.

682   Maurin, J.C., and Guiraud, R. (1989). Relations entre tectonique et sédimentation dans les bassins barrémo-aptiens

683   du Nord Cameroun. C.R. Acad. Sci. Paris 308, Sér. II, pp. 787-792.

684   Mbonu, M., Travi, Y. (1994). Labelling of precipitation by stable isotopes (^{18}O, ^{2}H) over the Jos Plateau and the

685   surrounding plains (north-central Nigeria). J Afr. Earth Sci. 19, 91-98.

686   McLennan, S.M.(1989). Rare earth elements in sedimentary rocks; influence of provenance and sedimentary

687   processes. In Liplin BR and McKay GA (eds) Geochemistry and mineralogy of rare earth elements.

688   Reviews in Mineralogy and Geochemistry 21. Mineralogical Society of America, pp 169–200.

689   Meybeck, M. (1997). Global chemical weathering of surficial rocks estimated from river dissolved loads. Am. J.

690   Sci. 287, 401-428.

691   Migaszewski, Z.M., Gałuszka, A., Migaszewski. (2014). The study of rare earth elements in farmer's well

692   waters of the Podwiśniówka acid mine drainage area (south-central Poland). Environ Monit Assess.

693   186,1609–1622.

694   Migaszewski, Z. M., and Galuszka, A. (2015). The Characteristics, Occurrence, and Geochemical Behaviour of

695   Rare Earth Elements in the Environment: A Review. Critical Reviews in Environmental Science and

696   Technology. 45, 492-471.

697   Molua, E.L. (2006). Climatic trends in Cameroon: implications for agricultural management. Clim. Res. 30,

698   255–262.

699   Munemoto, T., Ohmori, K., Iwatsuki. (2015). Rare earth elements (REE) in deep groundwater from granite and

700   fracture-filling calcite in the Tono area, central Japan: Prediction of REE fractionation in paleo- to present

701   -day groundwater. Chem. Geol. 417,58-67.

702   Nagaraju, A., Surresh, S., Killam, K., Hudson-Edwards, K. (2006). Hydrogeochemistry of waters of Mangampeta
703   Barite Mining Area, Cuddapach Basin, Andhra Pradesh, India. Turk J Environ Sci. 30, 203–219.

704   Nash, W.P. (1984). Phosphate minerals in terrestrial igneous and metamorphic rocks. In: Nriagu, J.O., Moore,
705   P.B. (Eds.), Phosphate minerals. Springer, Berlin Heidelberg, pp. 215-241.

706   Ndjigui, P.D., Beauvais, A., Fadil-Djenabou, S., Ambrosi, J-P. (2014). Origin and evolution of Ngaye River
707   alluvial sediments, Northern Cameroon: Geochemical constraints. Journal of African Earth Sciences. 100,
708   164-178.

709   Nesbitt, H.W., Wilson, R.E. (1992). Recent chemical weathering of basalts. Am J Sci 292:740–777.

710   Njitchoua, R., Aranyossy, J.F., Fontes, J.C., Michelot, J.L., Naah, E., Zuppi, G.M. (1995). Oxygen-18, deuterium
711   et chlorures dans les precipitations a Garoua (Nord-Cameroon): implications meteorolgiques. CR Acad Sci
712   Paris, t 321, serie IIa: 853–860.

713   Njitchoua, R., Dever, L., Fontes, J-C., Naah, E. (1997). Geochemistry, origin and recharge mechanisms of
714   groundwaters from the Garoua Sandstone aquifer, northen Cameroon. J Hydrol. 190,123–140.

715   Nkotagu, H. (1996). Application of environmental isotopes to groundwater recharge studies in a semi-arid
716   fractured crystalline basement area of Dodoma, Tanzania. J Afr Earth Sci. 22, 443–457.

717   Noak, C.W., Dzombak, D.A., Karamalidis, A.K. (2014). Rare earth element distributions and trends in natural
718   waters with a focus on groundwater. Environ. Sci. Technol. 48, 4317–4326.

719   Nolla, J.D., Hell, J.V., Ngos, S., Bessong, M., Mfoumbeng, M. P., Eyong, T. J., Dissombo, E.A.N., Mbang, A.
720   R., Engombi, G., Ndjeng, E. (2015). Lithostratigraphy of the Koum Basin (Northern Cameroon).
721   International Journal of Multidisciplinary Research and Development. 2 (6), 103-114.

722   Ntsama, J.A. (2013). Magnétostratigraphie et sédimentologie des formations crétacées des bassins sédimentaires
723   d'Hamakoussou et du Mayo Oulo-Léré au Nord-Cameroun (Fossé de la Bénoué). Thèse Terre solide et
724   enveloppes superficielles. Poitiers : Université de Poitiers. 193 pp.

725   Ntsama, A. J., Bessong, M., Hell, J. V., Mbesse, C. O., Nolla, J. D., Dissombo, E. A. N., Eyong, J.T., Mbassa,
726   B.J., Mouloud, B., Vignaud, P., Mfoumbeng, M.P. (2014). The Importance of Diagenetic Processes in
727   Sandstones Facies of the Hamakoussou Sedimentary Basin in North Cameroon: Influence on Reservoir
728   Quality. International Journal of Sciences: Basic and Applied Research. 13, 220-230.

729   Petrides, B., Cartwright, I., Weaver, T.R. (2006). The evolution of groundwater in the Tyrell catchment, south-

730   central Murray Basin, Victoria, Australia. Hydrogeol J. 14,1522-1543.

731   Pignotti, E., Dinelli, E., Birke, M. (2017). Geochemical characterization and rare earth elements anomalies in

732   surface- and groundwaters of the Romagna area (Italy). Rend. Fis. Acc. Lincei. 28, 265-279.

733   Piper, A. M. (1944). A graphic procedure in the geochemical interpretation of water analyses. American

734   Geophysical Union Transactions. 25, 914–923.

735   Rollinson, H. R. (1993). Using Geochemical data: Evaluation, Presentation, Interpretation. Longman Singapore

736   Publishers Ltd. Singapore. 352 pp.

737   Scalon, B.R., et al. (2006). Global synthesis of groundwater recharge in semi-arid and arid regions. Hydrol

738   Process, 20, 3335–3370. doi:10.1002/hyp.6335

739   Schwoerer, P. (1965). Carte de reconnaissance à l'échelle du 1/500 000. Notice explicative sur la feuille Garoua-

740   Est. Direction des Mines et de la Géologie du Cameroun (éd) Yaoundé, 49 p.

741   Shivanna, K., Tirumalesh, K., Noble, J., Joseph, T.B., Singh ,G., Joshi, A.P., Khati, V.S. (2008). Isotope

742   techniques to identify recharge areas of springs for rainwater harvesting in the mountainous region of

743   Gaucher area, Chamoli District, Uttarakhand. Curr Sci. 94,1003–1011.

744   Sholkovitz, E.R., Landing, W.M., and Lewis, B.L. (1994). Ocean particle chemistry: The fractionation of rare

745   earth elements between suspended particles and seawater. Geochimica et Cosmochimica Acta. 58, 1567-

746   1579.

747   Silvera, S., Rohan, T. (2007). Trace elements and cancer risk: a review of the epidemiological evidence.

748   Cancer causes and control. 18 (1), 7-27.

749   Srinivasamoorthy, K., Chindambaram, S., Prasanna, M.V., Vasanthavihar, M., Peter, J., Anandhan, P. (2008).

750   Identification of major sources controlling groundwater chemistry from a hard rock terrain-A case study

751   from Mettur taluk, Salem district, Tamil Nadu, India. J Earth Syst Sci. 117(1), 49–58.

752   Stumm, W., Morgan, J.J. (1996). Aquatic Chemistry: Chemical Equillibria and rates in Natural Waters. Wiley

753   Interscience Publication, New Jersey.

754   Subramani, T., Rajmohan, N., Elango, L. (2010). Groundwater geochemistry and identification of

755   hydrogeochemical processes in hard rock region, Southern India. Environ Monit Assess. 162,123-137.

756   Sultan, K., Shazilli, A.A. (2009). Rare earth elements in tropical surface water, soil and sediments of the
757   Terengganu River Basin, Malaysia. Journal of Rare Earths. 27, 1073-1078.

758   Takahashi, Y., Yoshida, H., Sato, N., Hama, K., Yasu, Y., and Shimizu, H. (2002). W-and M- type tetrad effects
759   in REE patterns for water-rock system in the Tono uranium deposit, central Japan. Chemical Geology. 184,
760   311-335.

761   Tang, J., and Johannesson, K.H. (2006). Controls on the geochemistry of rare earth elements along a groundwater
762   flow path in the Carrizo Sand aquifer, Texas, USA. Chem. Geol. 225, 156–171.

763   Taran, Y., Rouwet, D., Inguaggiato, S., Aiuppa, A. (2008). Major and trace element geochemistry of neutral and
764   acidic thermal springs at El Chichon volcano, Mexico: Implications for monitoring of the volcanic
765   activity. Journal of Volcanology and Geothermal Research. 178, 224-236

766   Tardy, Y. (1971). Characterization of the principal weathering types by the geochemistry of waters from some
767   European and African crystalline massifs. Chem. Geol. 7, 253–271.

768   Tayie, F. (2004). Pica: motivating factors and health issues. African Journal of Food, Agriculture, Nutrition and
769   Development 4 (1) <http://www.bioline.org.br/ (accessed 18.07.2019).

770   Taylor, R.G., Howard, K.W.F. (1996). Groundwater recharge in the Victoria Nile basin of East Africa: support
771   for the soil moisture balance method using stable isotope and flow modelling studies. J Hydrol. 180,
772   31–53.

773   Thomas, J.M., Welch, A.H., Preissler, A.M. (1989). Geochemical evolution of groundwater in Smith Creek
774   Valley—a hydrologically closed basin in central Nevada, USA. Appl Geochem. 4, 493–510.

775   Tillement, B. (1972). Hydrogeologie du Nord—Cameroun. Rapport 6, 294p. Direction des Mines et de la
776   Geologie, Yaounde, Cameroon

777   Tsujimura, M., Abe, Y., Tanaka, T., Shimada, J., Higuchi, S., Yamanaka, T., Davaa, G., Oyunbaatar, D. (2007).
778   Stable isotopic and geochemical characteristics of groundwater in Kherlin River Basin: a semiarid region
779   in Eastern Mongolia. J. Hydrol. 333, 47–57.

780   Vázquez-Ortega, A., Perdrial, J., Harpold, A., Zapata-Ríos, X., Rasmussen, C., McIntosh, J., Schaap, M., Pelletier,
781   J.D., Brook, P.D., Amistadi, M.K., Chorover, J. (2015). Rare earth elements as reactive tracers of
782   biogeochemical weathering in forested rhyolitic terrain. Chem. Geol. 391, 19–32.

783   WHO (World Health Organization). (2004). Guidelines for drinkingwater quality: training pack. WHO, Geneva

784   Wirmvem, M.J., Mimba, M.E., Kamtchueng, B.T., Wotany, E.R., Bafon, T.G., Asaah, A.N.E., Fantong, W.Y.,

785   Ayonghe, S.N., Ohba, T. (2015). Shallow groundwater recharge mechanism and apparent age in the Ndop

786   plain, northwest Cameroon. Appl Water Sci. doi:10.1007/ s13201-015-0268-0

787   Zaborski, P., Ugodunlunwa, F., Idornigie, A., Nnabo, P., Ibe, K. (1997). Stratigraphy and structure of the

788   Cretaceous Gongola Basin 'N.E. Nigeria). Bulletin des Centres de Recherches Exploitation-Production Elf-

789   Aquitaine 21(1), 153-177.

790   Zhuravlev, A., Berto, M., Arabadzhi,, M., Gabrieli, J., Turreta, C., Cozz, G.m Barbante, C. (2016). Trace and

791   Rare Earth Elements in Natural Ground Waters: Weathering Effect of Water-Rock Interaction. Int. J.

792   Environ. Res. 10 (4), 561-574.

793

794   **Figure Captions**

795   **Fig. 1** Location of study area in the Northern Region of Cameroon and within the River Niger system in Africa.

796   It also shows the spatial locations of the 5 sub sedimentary basins that constitute the extension of the

797   Benue Trough in Cameroon, and sample collection sites

798   **Fig. 2** Topography (Digital Elevation Model) of study area, showing the hydrographic network

799   **Fig. 3** Incidence of Aeolian harmattan dust, which reduce visibility to less than 15 meters

800   **Fig. 4** North-South correlation panel of Mayo-Oulo sedimentary Basin (a), and geochemical diagenetic processes

801   of the Hamakoussou sedimentary Basin (b)

802   **Fig. 5** Pipers` plots of observed water samples, showing $Ca+Mg-NO_3$ water facies in shallow wells (group1),

803        $Na+K-HCO_3$ facies in boreholes (group 2), and $Na+K-HCO_3$ (group 3) type in surface water. The cluster

804   of the plots indicates mixing of the surface and groundwater resources

805

806   **Fig. 6** A $\delta^{18}O$-δD relationship of groundwater, surface water and rainfall in the Benue River basin. There is an

807   almost dominant cluster of observed water samples between July and September rains and along the

808   Global Meteoric Water Line (GMWL) of Craig (1961), indicating groundwater recharge months are

809   mainly July and September, with little or no evaporation. The cluster of the plots are also indicative of

810   mixing between surface and groundwater. The monthly rainfall data are from Njitchoua et al. 1995. Plots

811   of some surface water to the right of the GMWL indicate evaporation effect (a). More than 60 % of

812   groundwater plot show d-excess greater than 10 ‰ indicating recharge under low humidity conditions

813   (b).

814

815   **Fig. 7** Average metal concentrations in water within the Benue River Basin (Cw, μg/l) versus average

816   concentrations in local lithology (sandy clay) (Cs, mg/kg). The abbreviation "OHA" stands for oxo-

817   hydroxo anion forming elements. Water and rock data are presented in Tables 1a, b and c, and original

818   rock data were gotten from Ndjigui et al. (2014).

819   **Fig. 8** PAAS normalize patterns of rare earth elements in observed water samples. (a)-(c) in boreholes, (d)-(f) in

820   hand dug wells, and (g) in spring. All samples, except (BO 25 and 37) show a "steep roof-shaped" positive

821   Eu anomaly

822

823   **Fig. 9** Gibbs plots indicating rock domain (water-rock interaction) as main process controlling groundwater

824   chemistry in the study area

825   **Fig. 10** Stability diagrams for some minerals in the systems $Na_2-Al_2O_3-SiO_2-H_2O$ (a) and $CaO-Al_2O_3-SiO_2-H_2O$

826   (b) at 25ºC and pressure of 1 bar, showing that observed water samples are in equilibrium with

827   montmorillonites and kaolinite, and the plots of saturation index versus TDS (c) showed that some samples

828   were supersaturated with respect to carbonate phases, while all samples were undersaturated with respect

829   to gypsum and anhydrite

830

831   **Fig. 11** Log-log plots for major and trace elements in selected water samples within the Benue River Basin

832   **Fig. 12** Biplots of La/Yb ratio against HCO_3 show that La/Yb ratio in surface water increased at low HCO_3

833   concentration (group 1), suggesting that acidic conditions may favour REEs concentration in surface

834   waters than alkaline conditions will do

835   **Fig. 13** Spatial distribution of mg/l concentrations of fluoride in observed water samples. Sites with high (> 1.5

836   mg/l) fluoride concentration cause fluorosis on children teeth

837

838   **Fig. 14** Spatial distributions of Potentially Harmful Elements (PHEs) showed that the values (μg/L) of As (a), Cd

839   (b), and Pb (c) increase in relatively populated locality (Garoua) within the study area. This suggests that

840   their origin may be associated to anthropogenic activities

841   **Fig. 15** Scatter diagrams plotting HCO_3 versus As (a), Cd (b), Pb (c), and NO_3 versus As (d), Cd (e), and Pb (f).

842   The diagrams depict water rock interaction (WRI) and anthropogenic input (AI) as contributing factors to

843   the incidence of As, Cd, and Pb in waters within the Benue River Basin

844   **Fig. 16** Chloride versus nitrate plots, indicate the incident of anthropogenic input into the water resources

845   observed

846   **Fig. 17** Relative mobility of metals in selected groundwater samples in Benue River Basin. RM values were

847   normalized to magnesium and computed from equation 7 (see text). Elements are arranged in four groups

848   based on increasing mobility (1. OHA elements; 2, alkalis and alkaline earths; 3, transition metals; 4,

849   immobile metals). Relative metal mobilities in the selected samples are compared to the average trend

850   **Fig. 18** Biplots of the sum of Pb, Cd, Cu, Zn, and Co against pH, depict that at acidic pH of less than 6, the

851   concentration of the heavy metals increased in groundwater (group (a)), whereas above pH 6, the

852   concentrations drop (group (b))

853

854

855

856   **Table Captions**

857   **Table1a** Sample location and physico-chemical (majors ions and stable isotopes) results of groundwater (n=72)

858   and surface water (n=14) in the Benue River Basin

Table 1b Sample location and trace elements results of groundwater (n=72) and surface water (n=14) in the

Benue River Basin

859

860   **Table 1c** Rare earth elements results of observed water (B=borehole; W= hand dug well; R= rivers; S= spring)

861   (n=86) in Benue River Basin

862   **Table 2** Relative mobility of elements in selected water samples in Benue River basin.
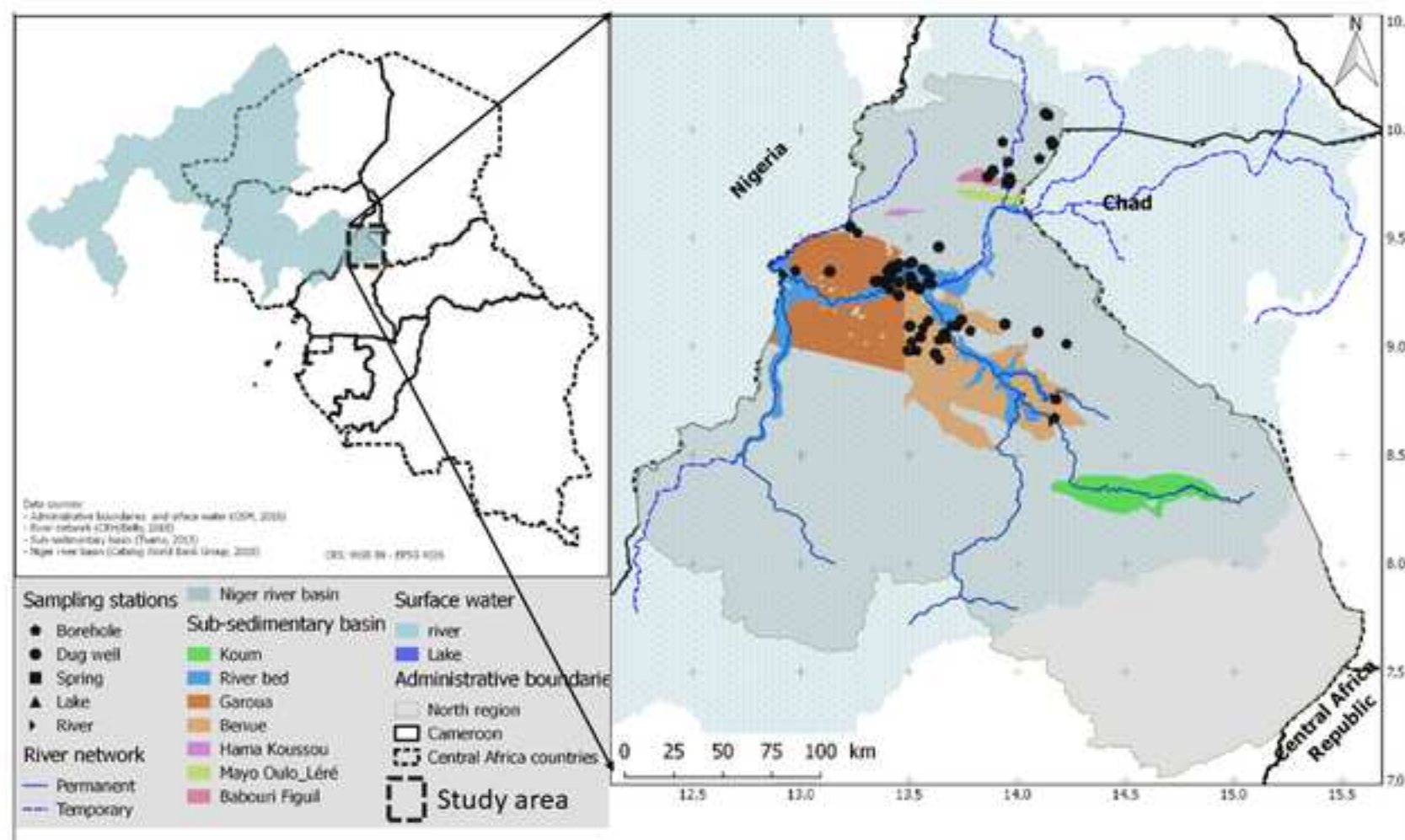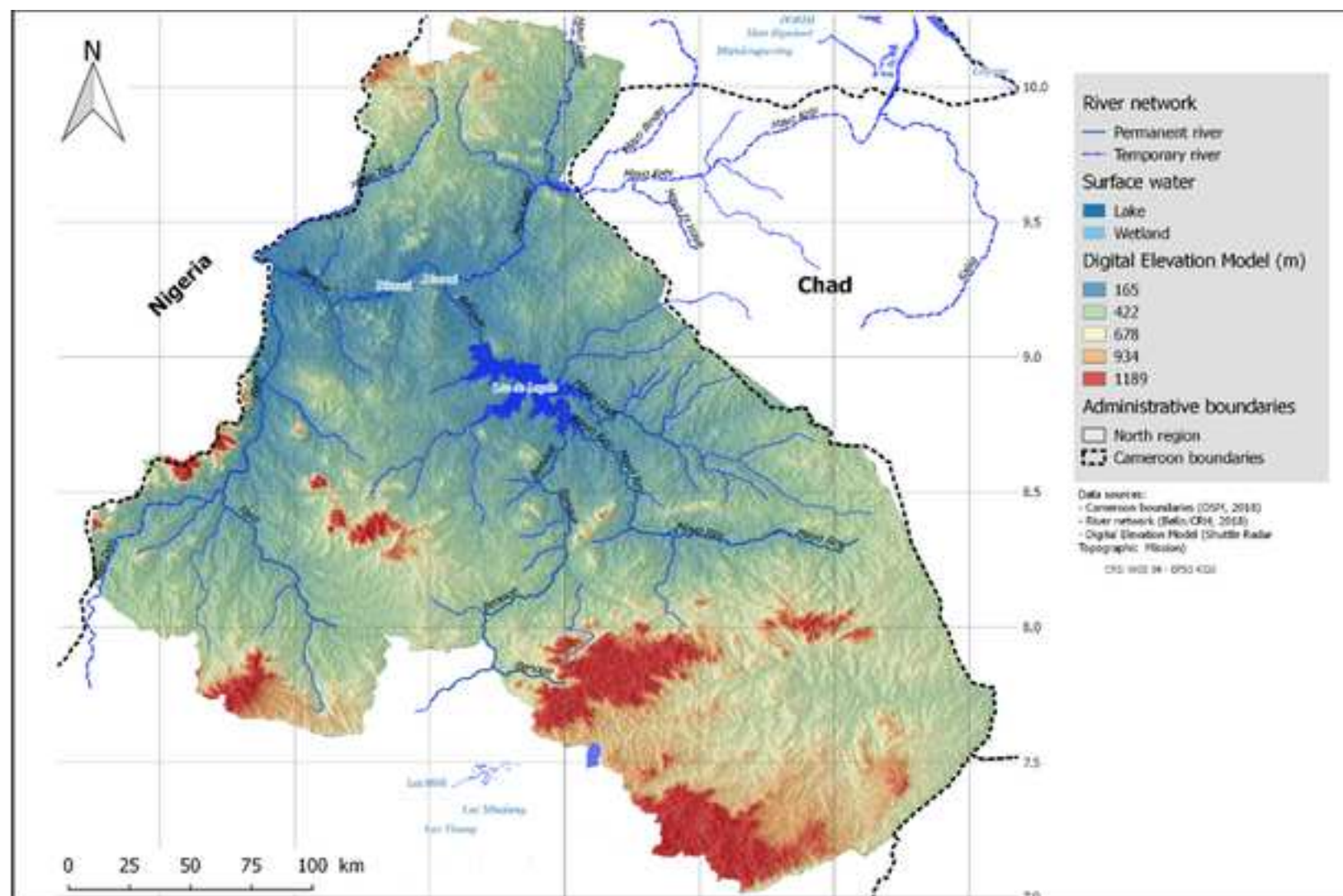
863

864

865

866

867

868

869

870

871

872

873

874

875

876

877

878

Figure 1

Figure 3

Figure 4a
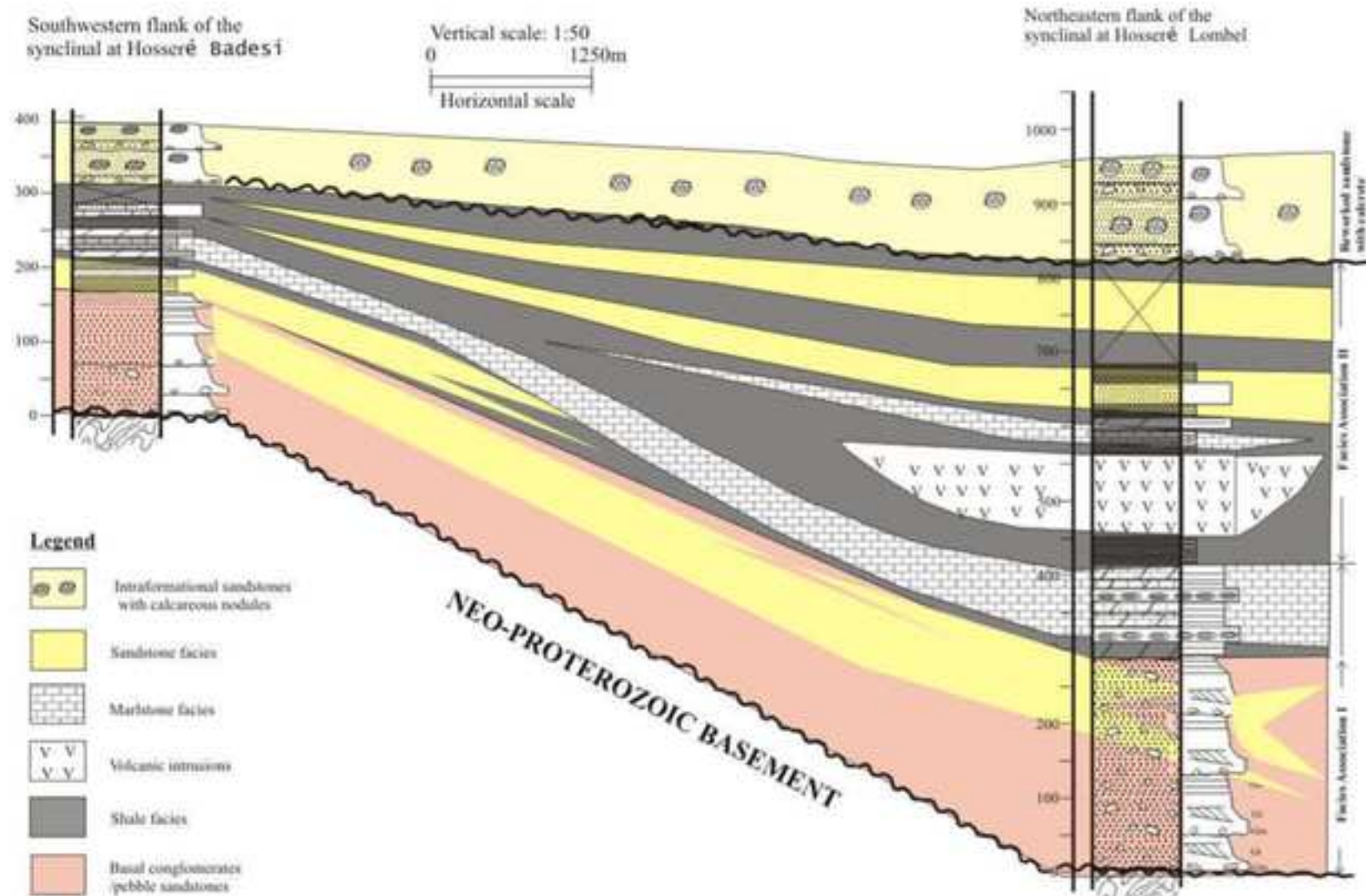
Diagenetic Events	Early ⟶ Late	Porosity incease(+), decrease(-)
Sediment compaction		−
Grain to grain pressure		−
Fracturation		+
Precipitation of calcite cement		−
Dissolution of K- feldspar		+
Precipitation of kaolinite		−
Precipitation of hematite		−
Quartz overgrowth		−

Figure 5
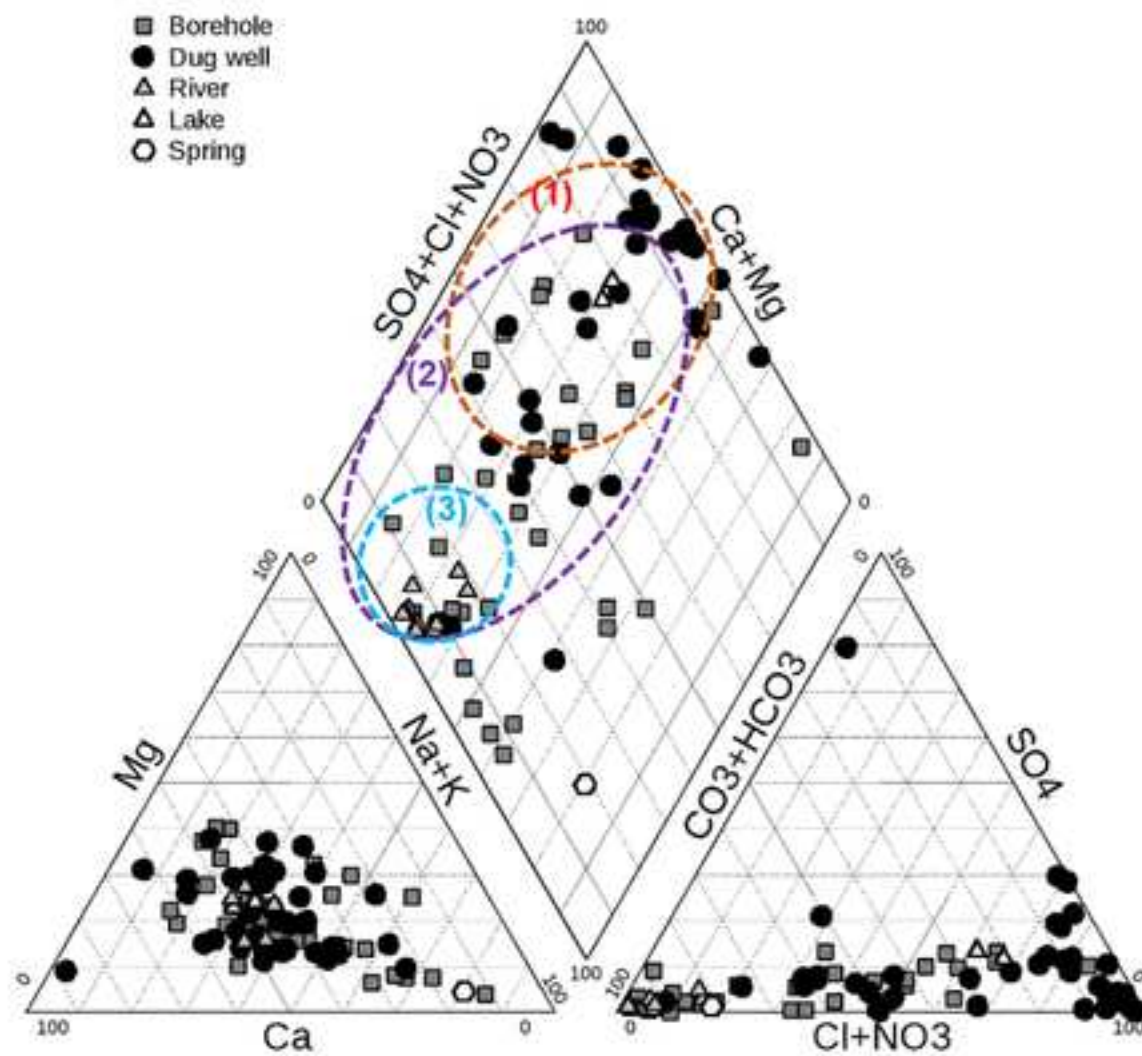
Figure 7
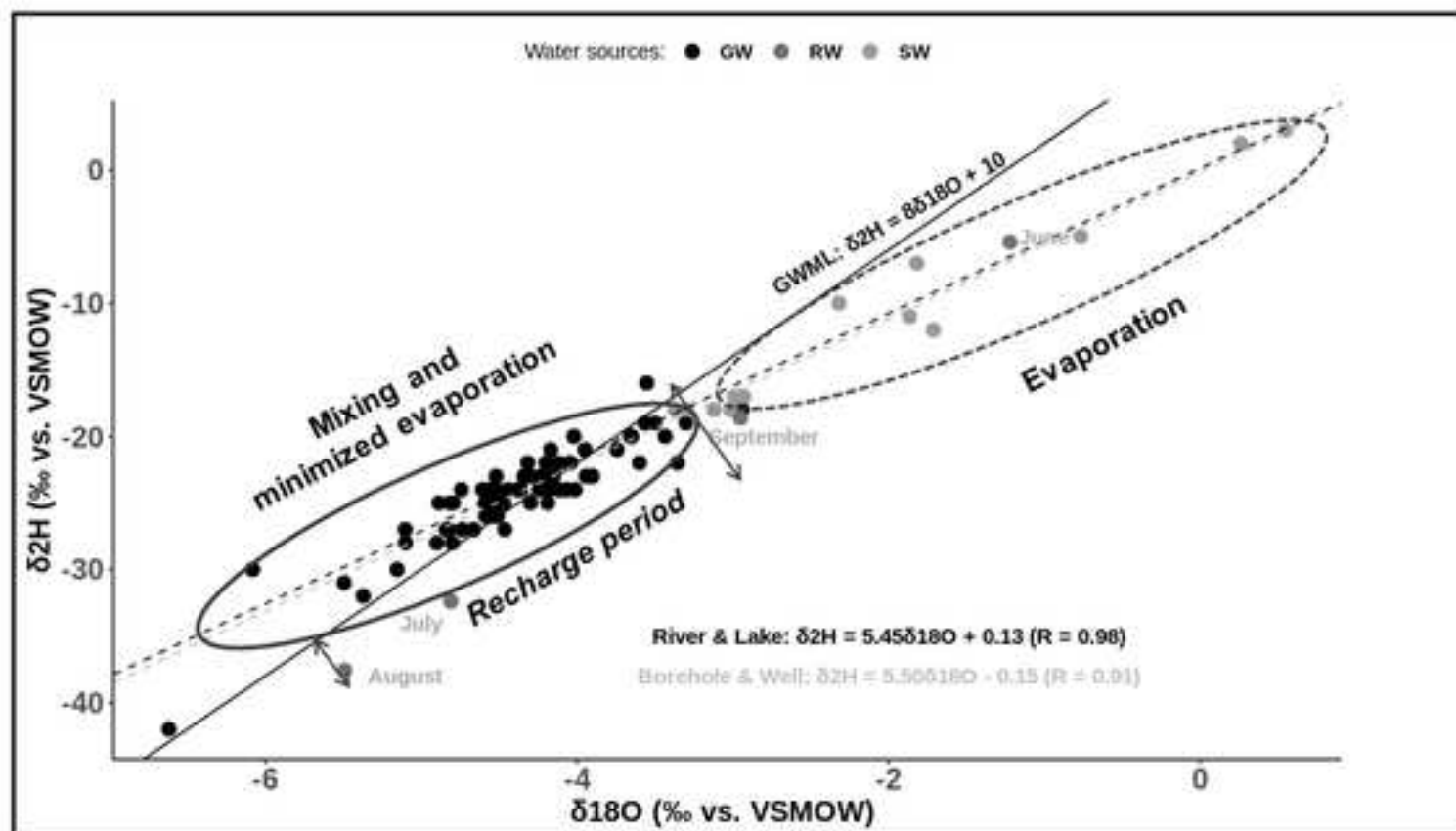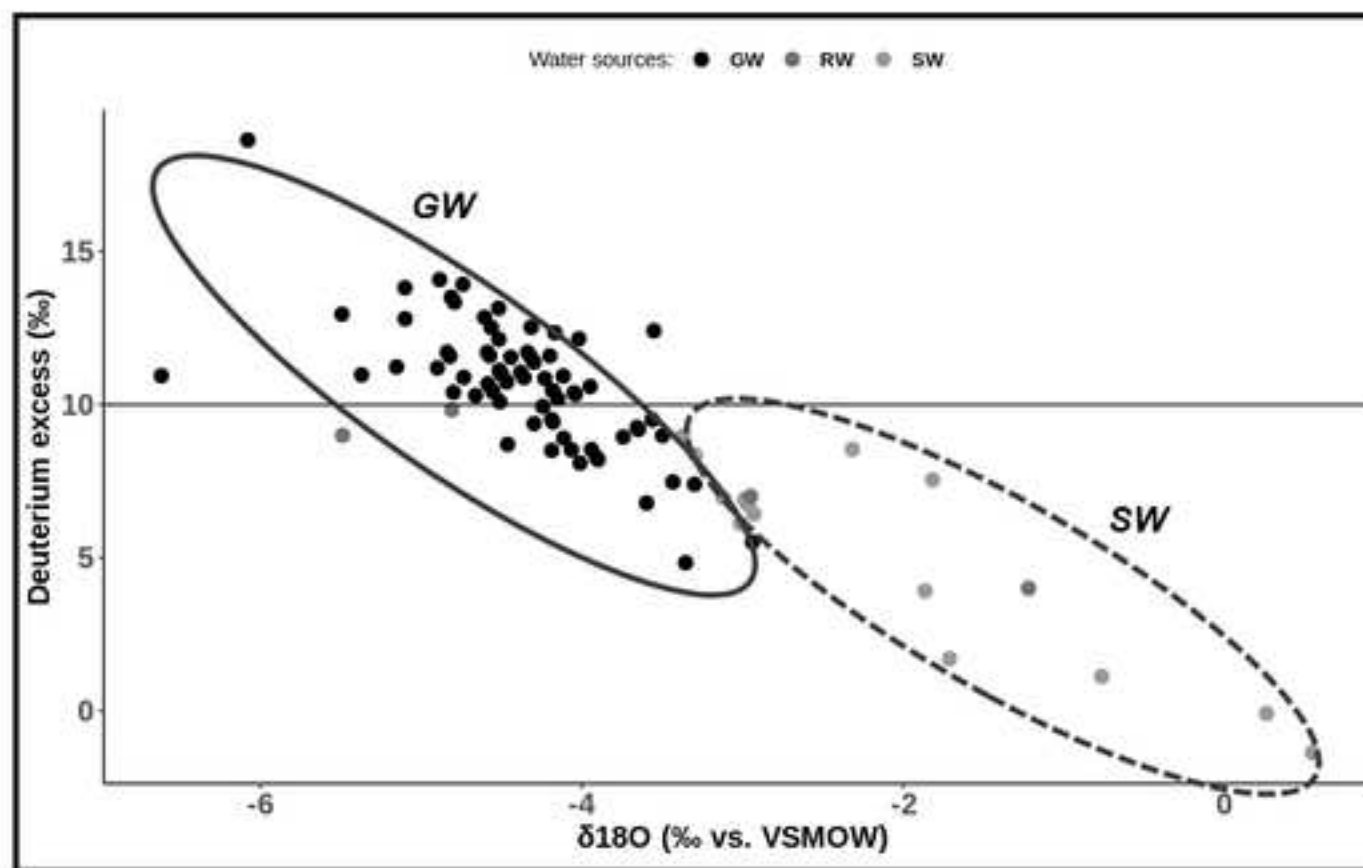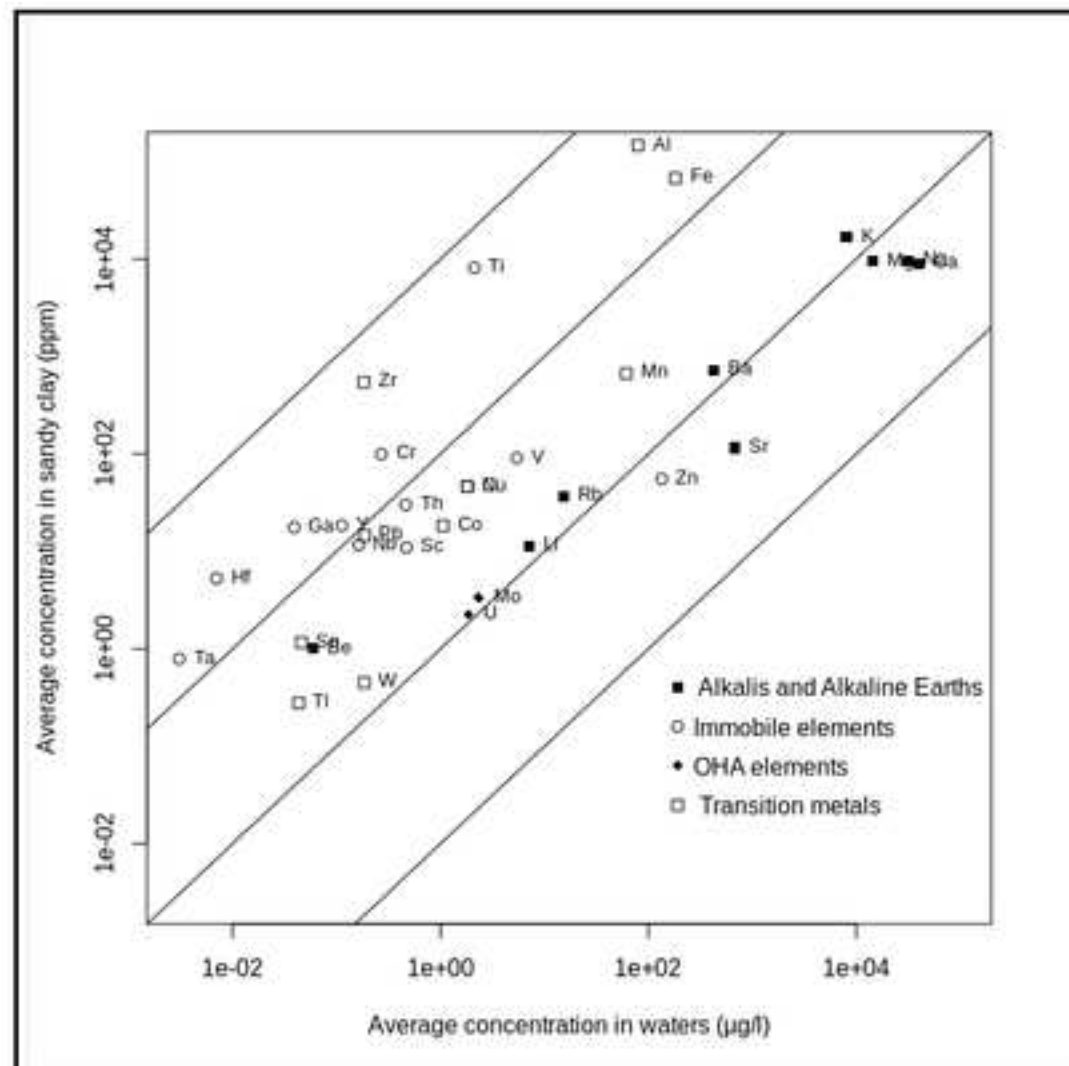
Figure 7

Figure 8

Click here to access/download;Figure;Fig. 8..jpg ⬇

Figure 9

Figure 10

Figure 10

Figure 11

Click here to access/download;Figure;Fig. 11 a and b.tif

(a)

(b)
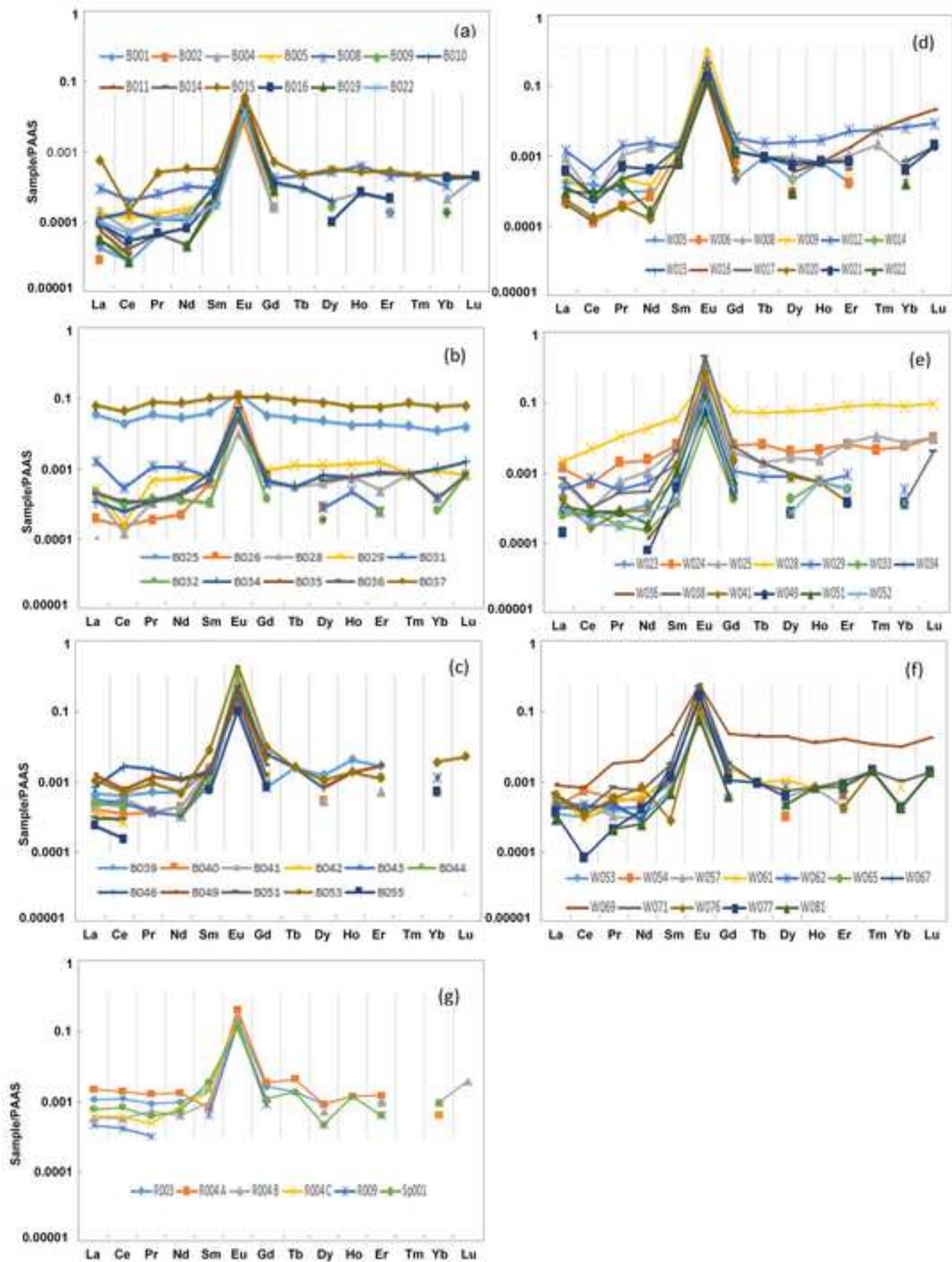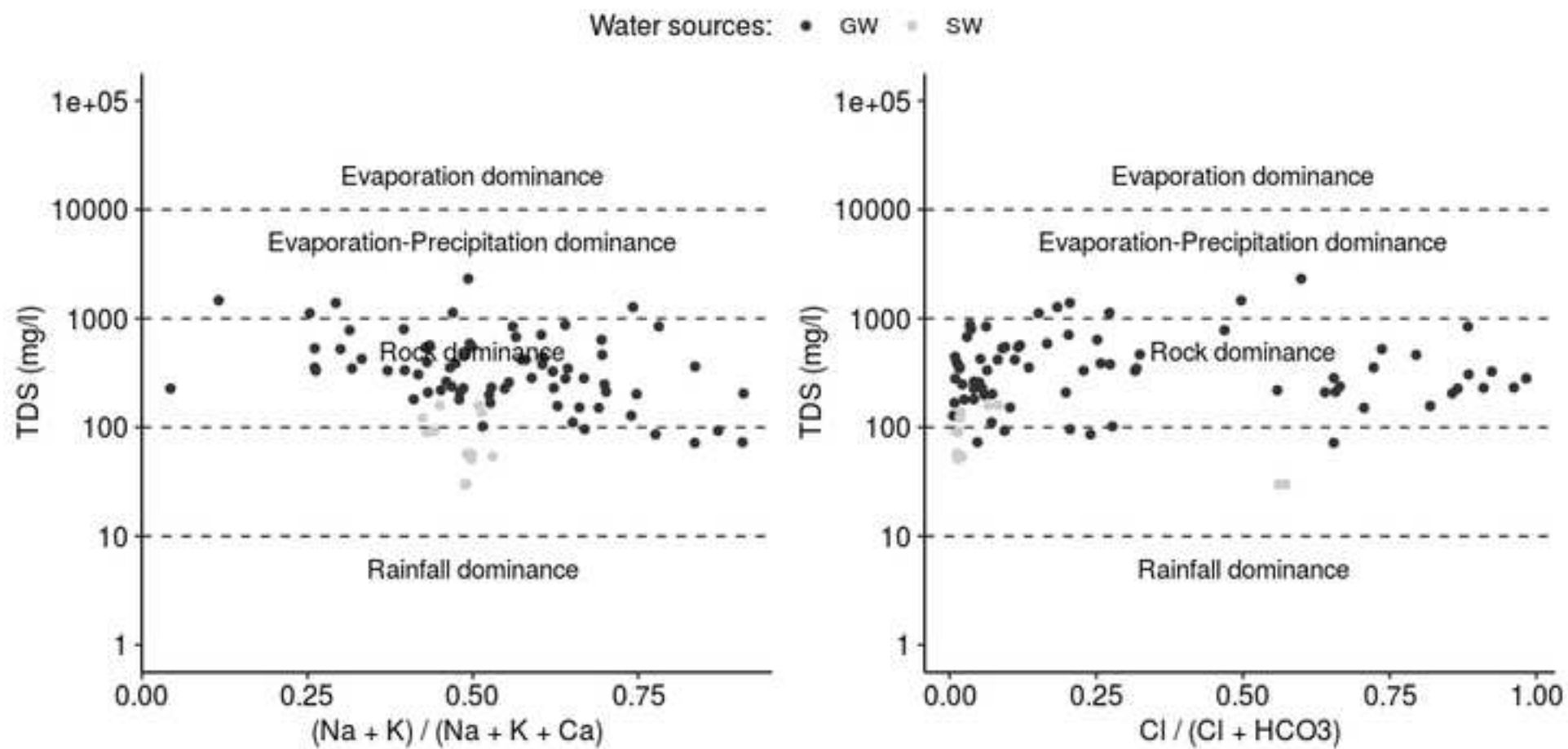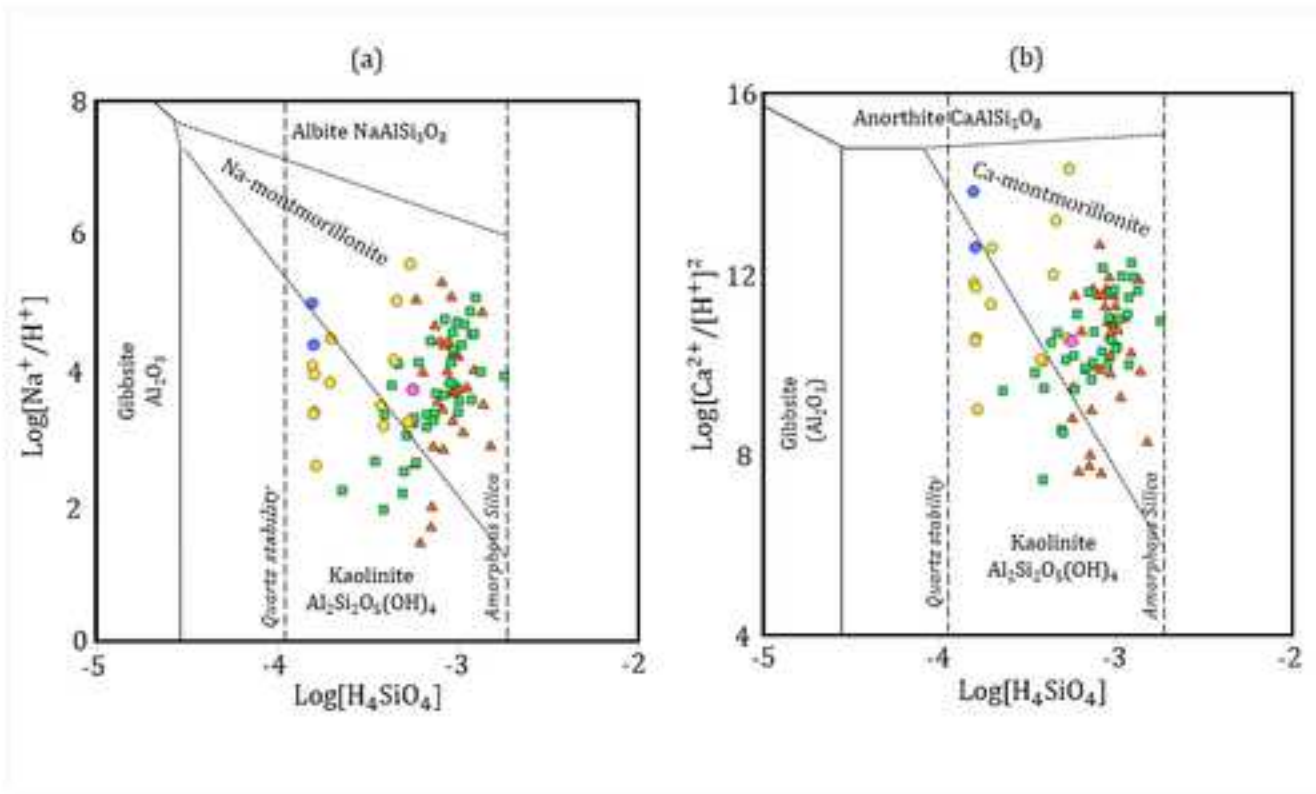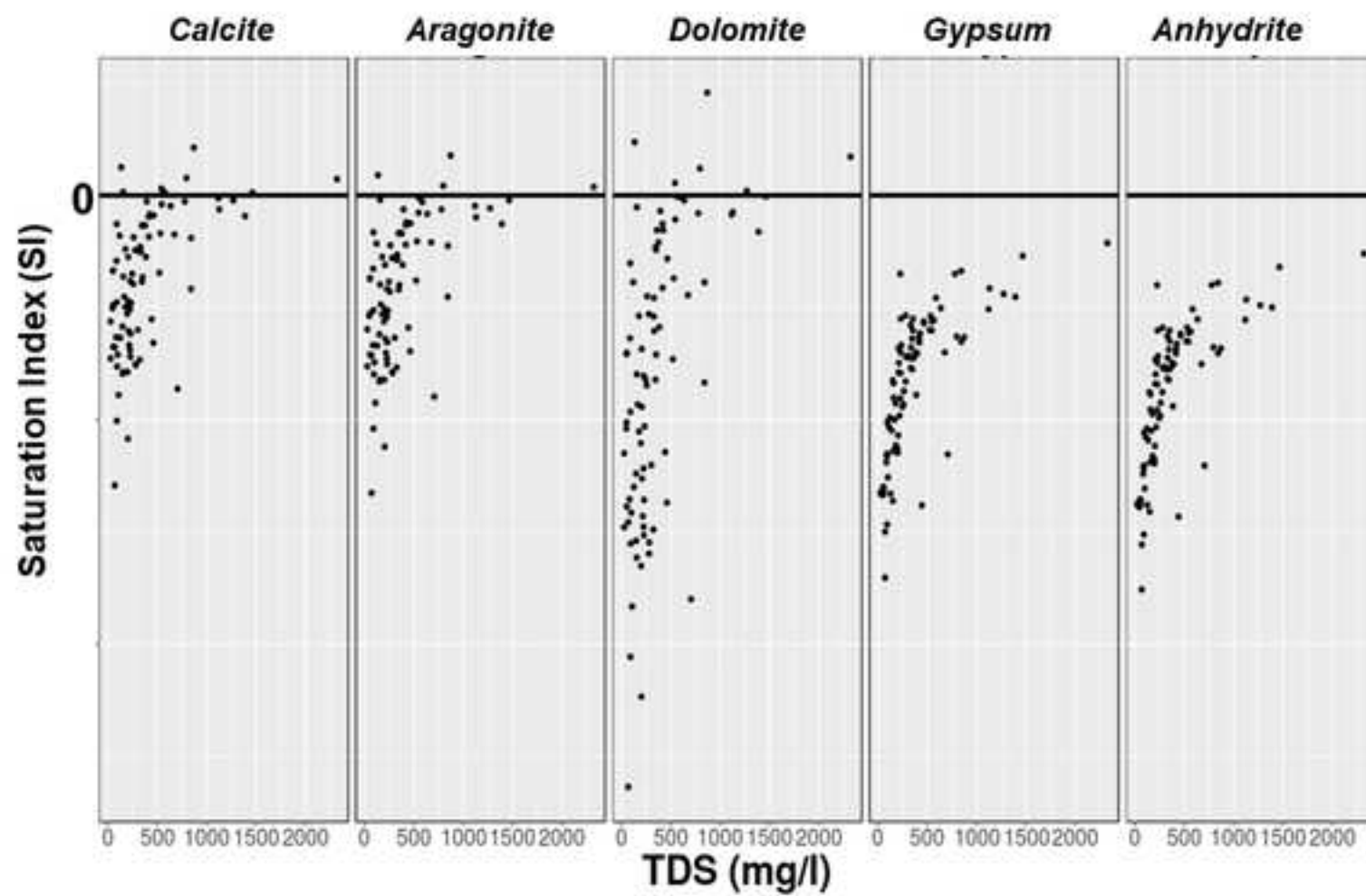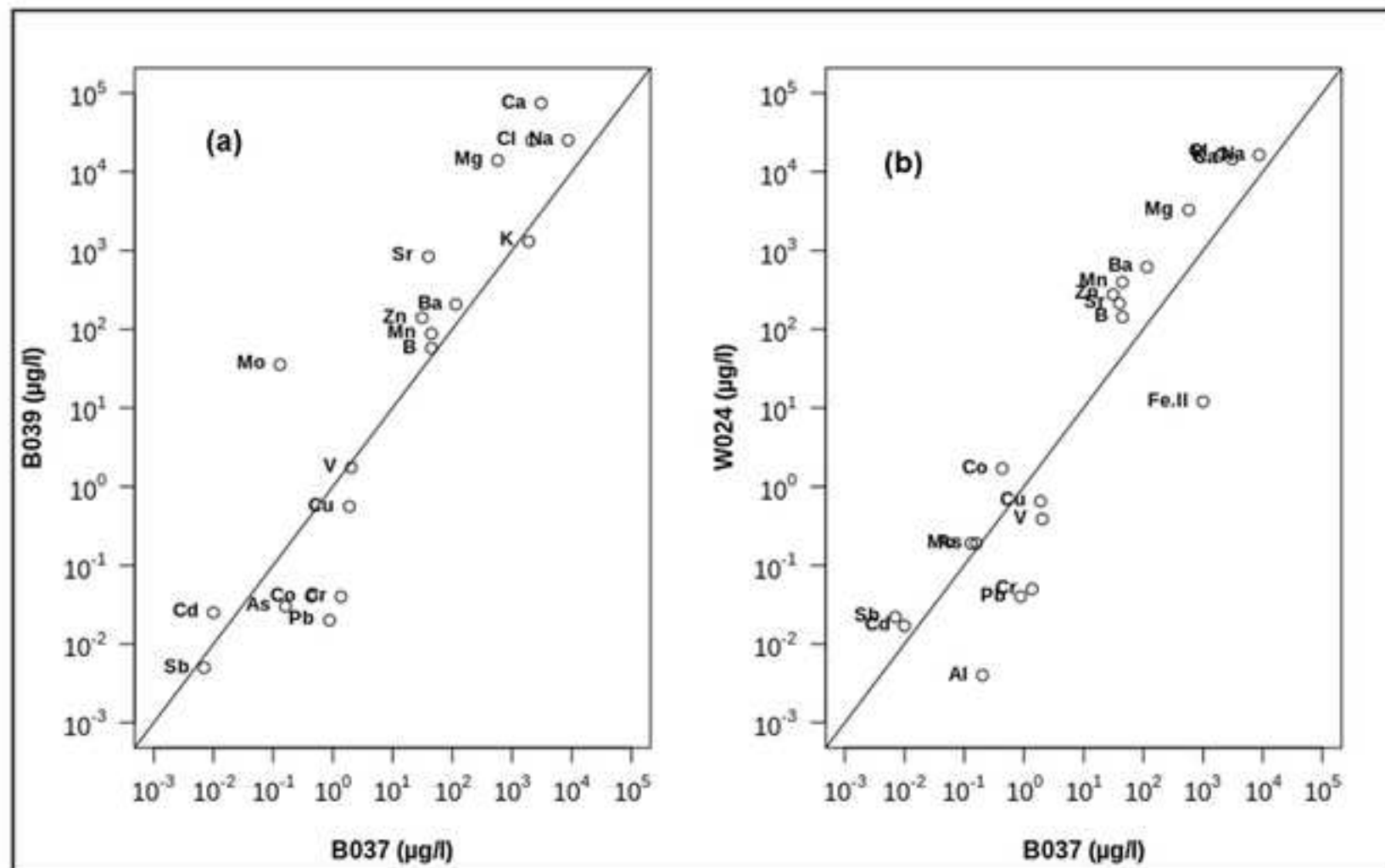
Figure 12

Click here to access/download;Figure;Fig. 12..tif

Figure 13
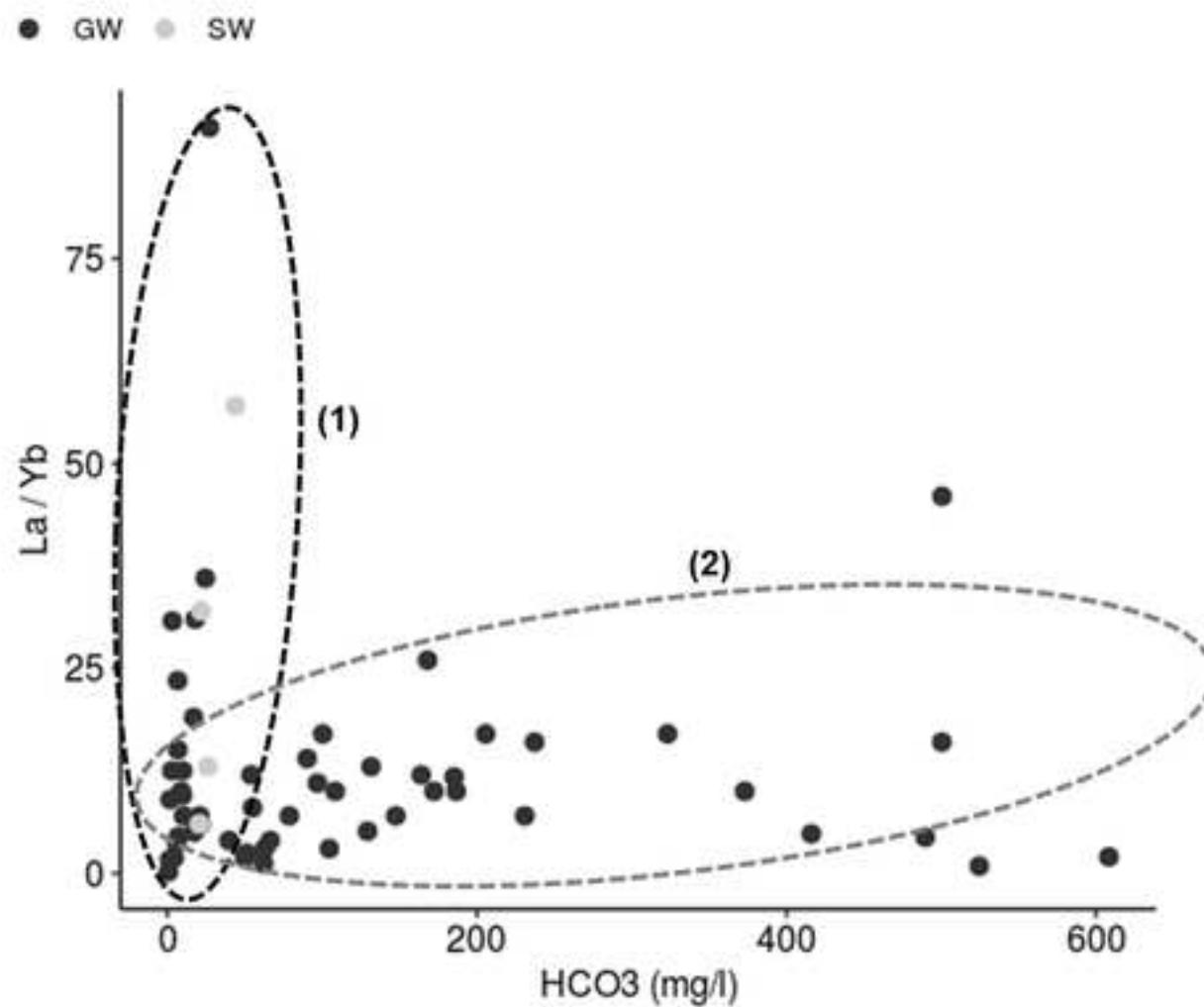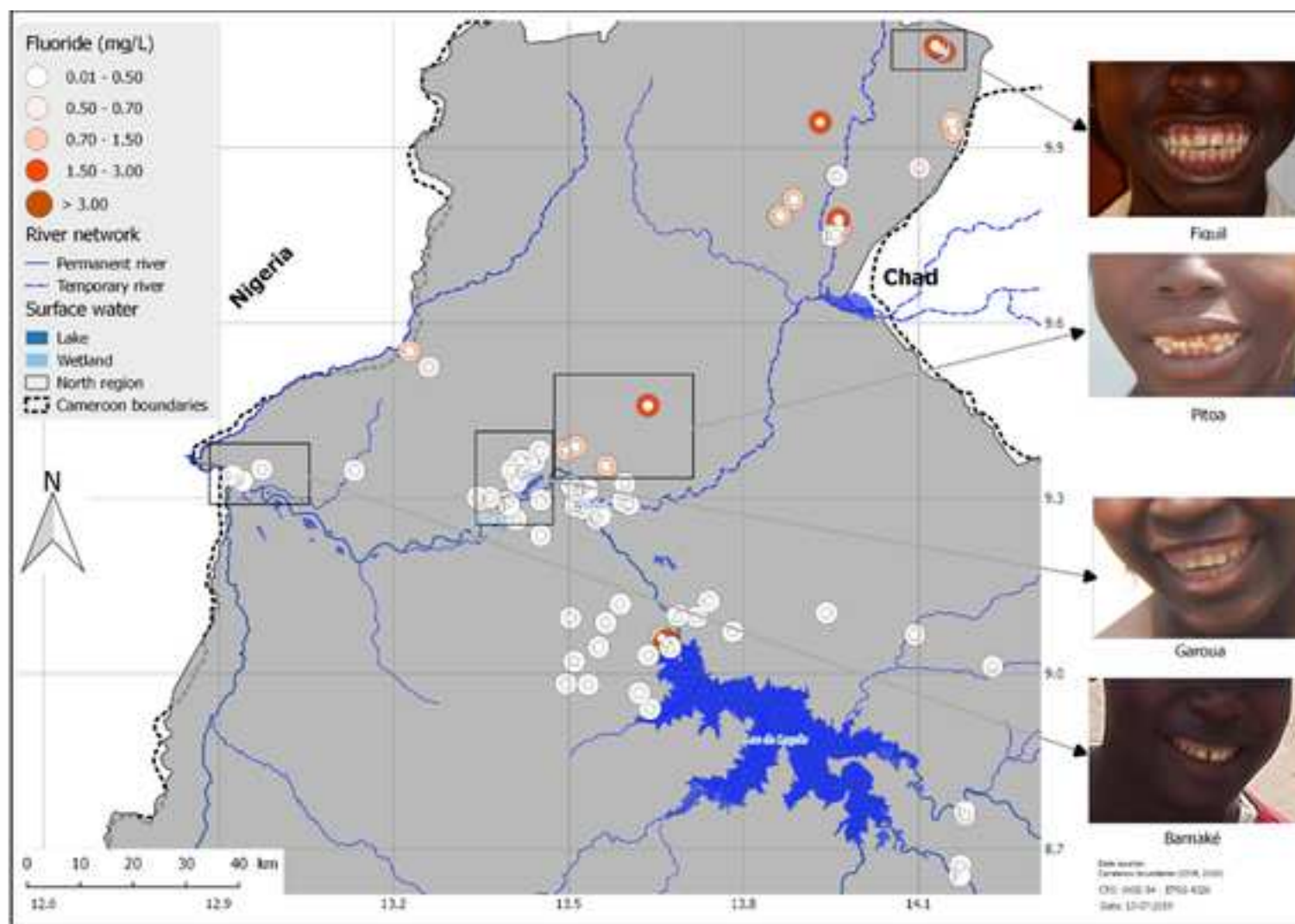
Figure 14

Figure 15

Click here to access/download;Figure;Fig. 15a-f.tif ±
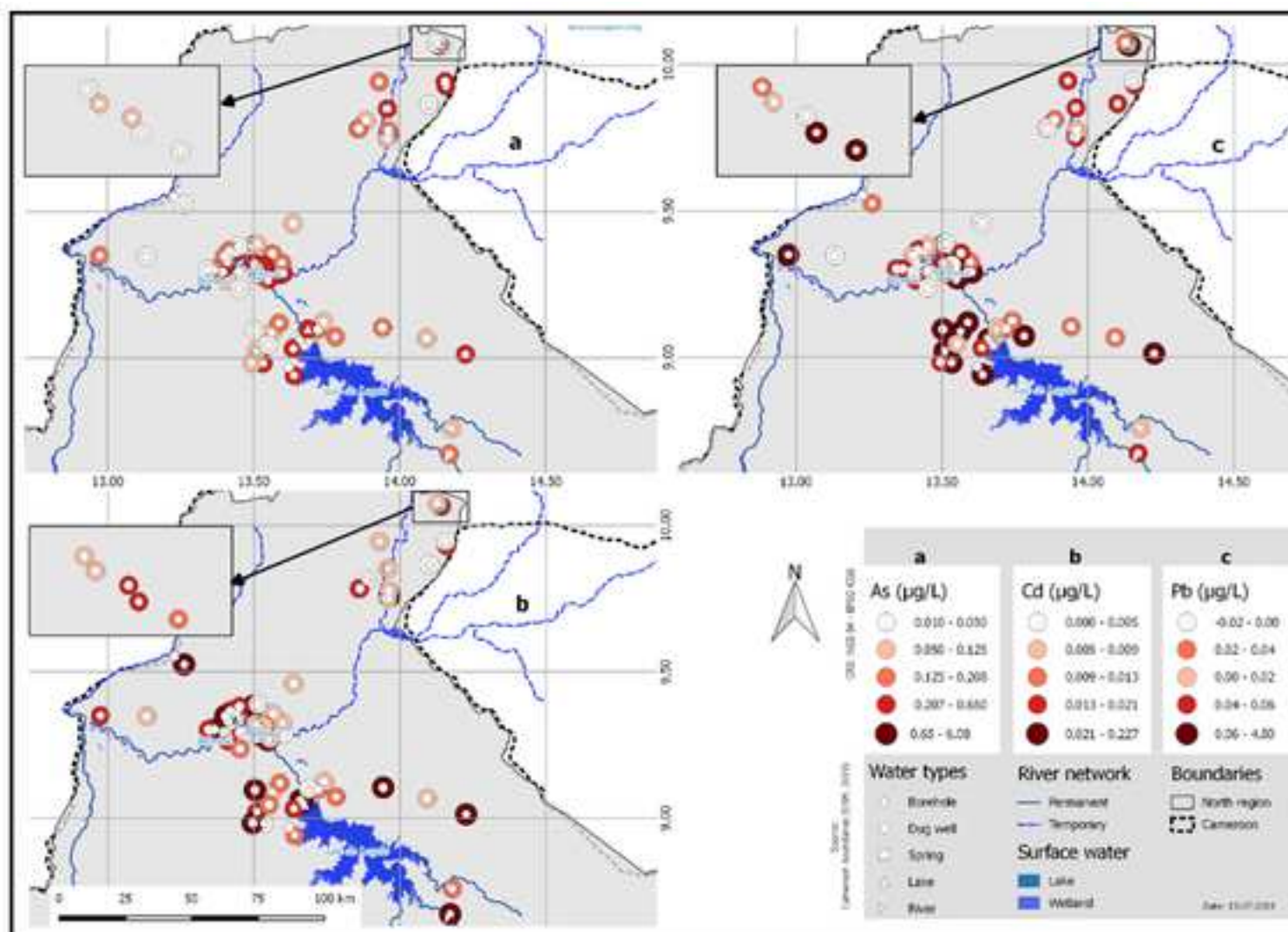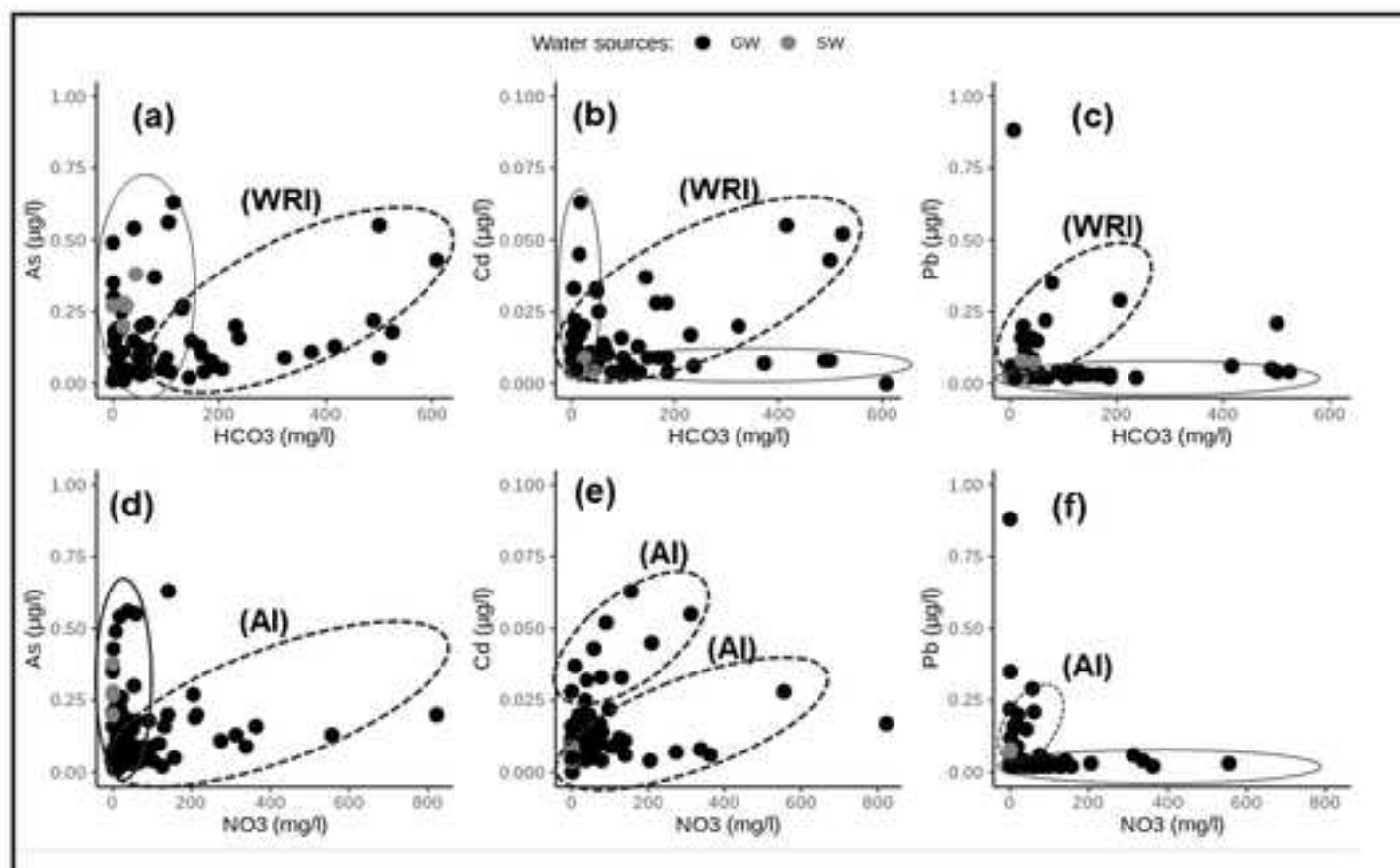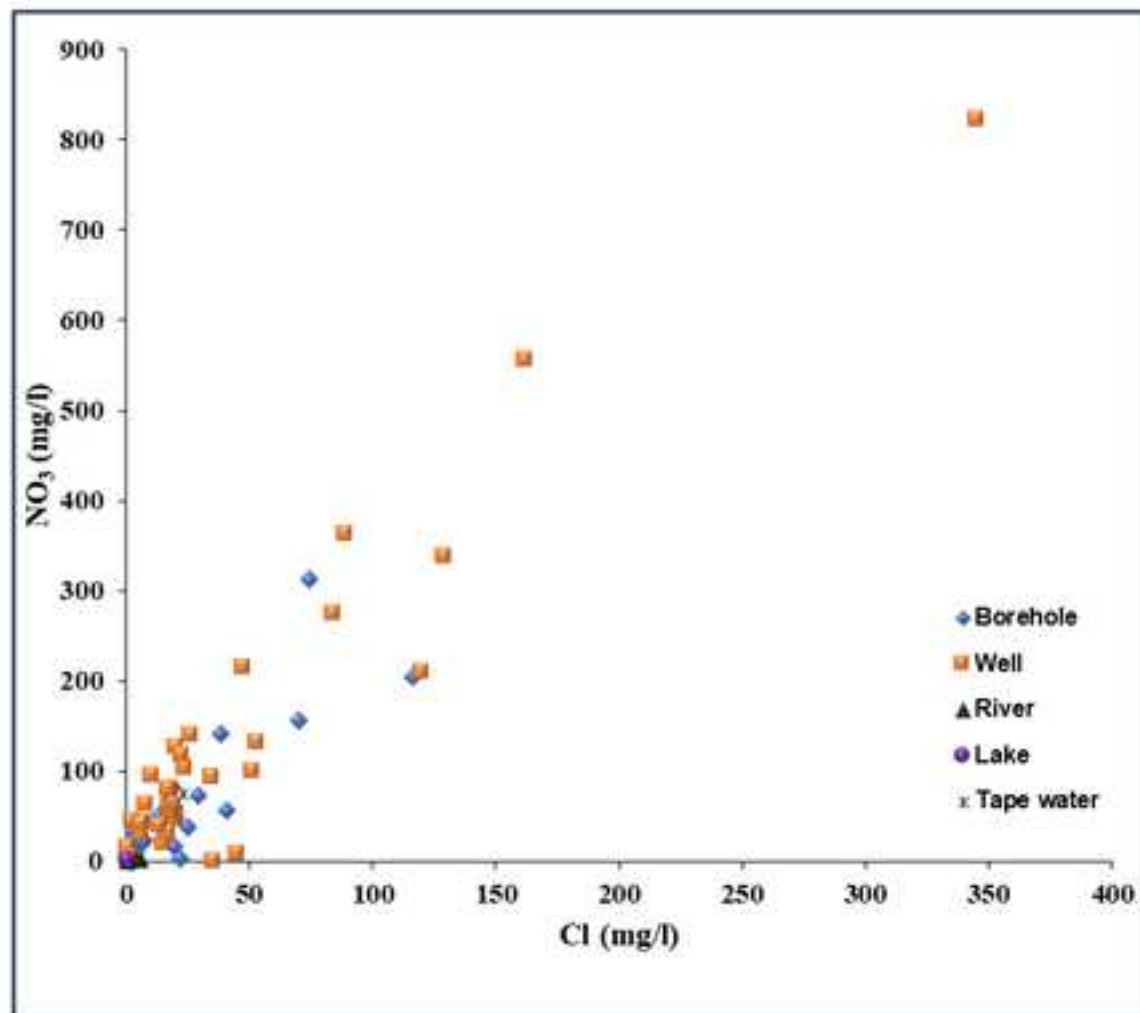
Figure 16

Figure 17

Figure 18
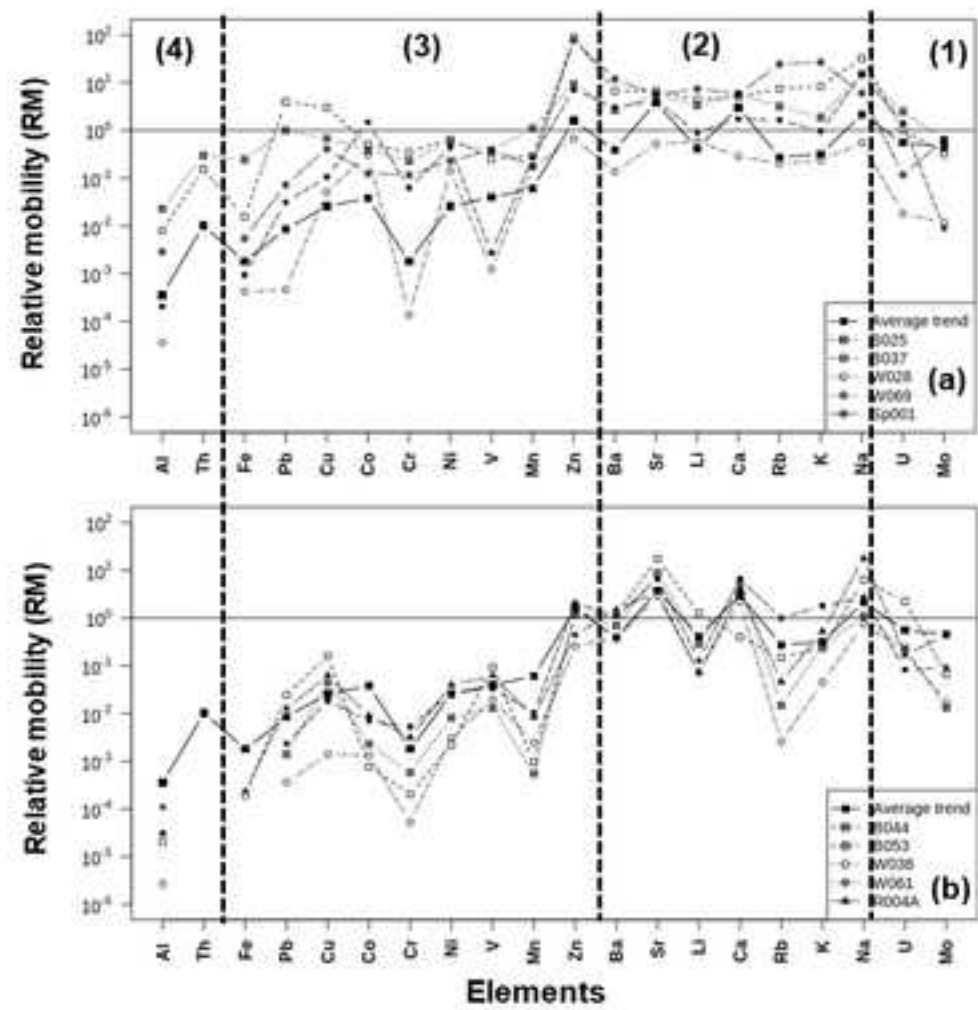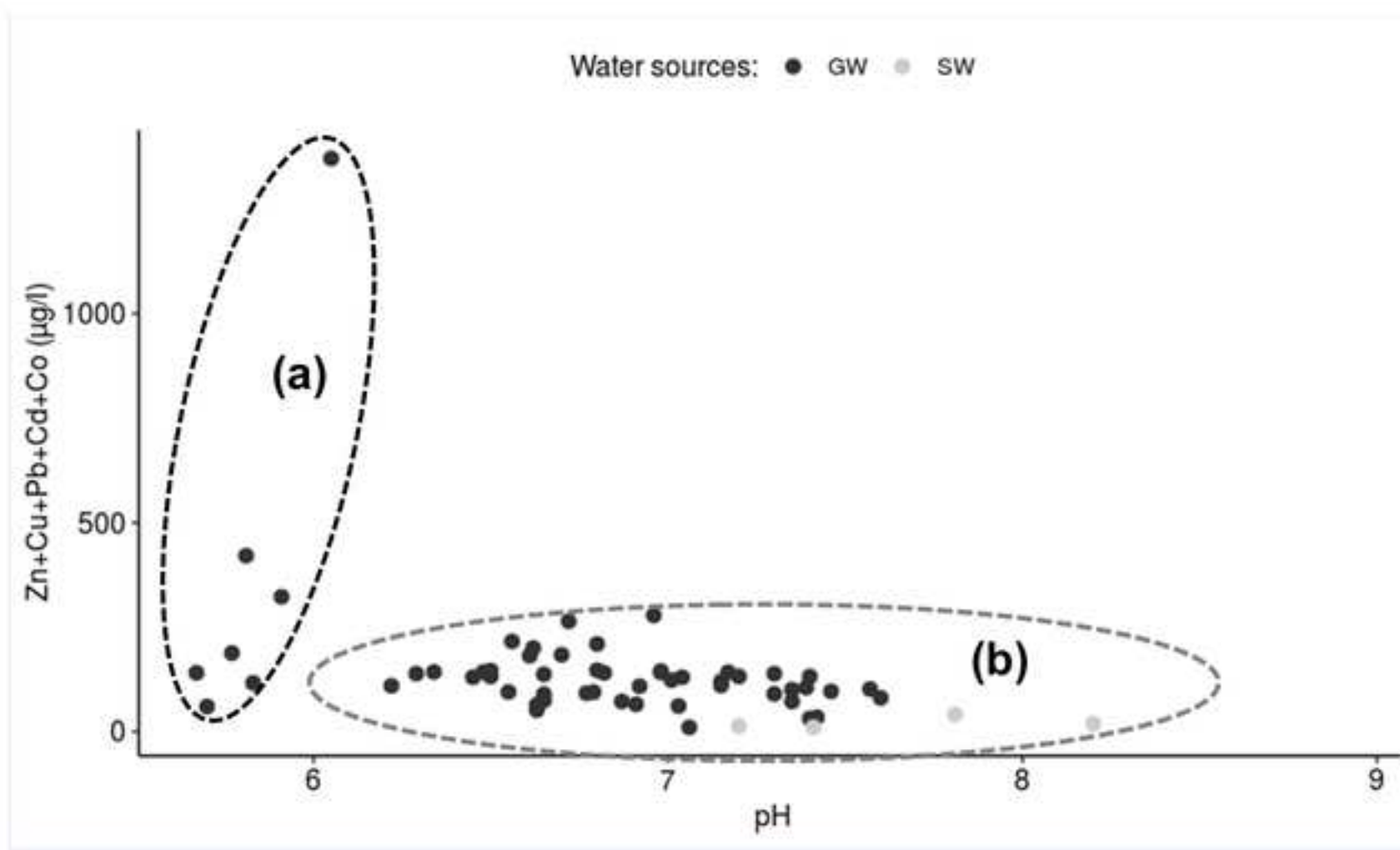
Table 1a*:*

Sample ID	Long (dd.dd)	Lat (dd.dd)	Temp (°C)	PH	EC (µS/cm)	HCO_3 (mg/l)	K (mg/l)	Na (mg/l)	Cl (mg/l)	Mg (mg/l)	Ca (mg/l)	SO_4 (mg/l)	NO_3 (mg/l)	Br (mg/l)	NH_4 (mg/l)	F (mg/l)	SiO_2 (mg/l)	$\delta^{18}O$ (‰)	δ^2H (‰)	DE (‰)
B001	13.59	9.29	30.2	6.63	214	36.42	1.5	19.5	0.31	5.63	18.9	0.774	4.52	0.009	0.01	0.321	46.4	-2.94	-18	6
B002	13.6	9.29	30.2	6.63	332	40.75	5.1	26.6	2.39	9.09	33.6	3.13	17.9	0.017	0.01	0.498	56.0	-3.43	-20	8
B004	13.6	9.33	30.8	6.8	474	147.62	3.1	52.8	13.2	10.9	40.5	10.2	51.1	0.042	0.03	0.367	55.1	-4.18	-24	10
B005	13.5	9.39	28.3	7.06	1266	131.58	1.7	65.5	116	47.9	147	64.0	205	bdl	0.02	1.10	bdl	-4.17	-21	12
B008	13.5	9.38	31.1	7.17	549	185.26	1.6	44.0	2.28	20.2	60.3	4.59	0.025	0.022	bdl	1.09	47.4	-4.57	-25	12
B009	13.55	9.27	31.1	6.98	378	62.83	7.1	12.5	18.6	19.3	33.2	4.19	81.4	0.040	0.02	0.292	58.1	-4.59	-25	11
B010	13.52	9.28	30.9	7.35	741	108.46	11.8	120	1.82	28.0	25.9	8.83	0.017	0.016	0.01	0.768	35.0	-6.62	-42	11
B011	13.5	9.32	30.7	6.7	71	5.92	8.1	2.0	1.53	1.49	5.00	2.30	14.9	0.010	0.02	0.079	34.3	-5.10	-28	13
B014	13.41	9.26	32	5.7	82	13.24	11.0	1.4	1.02	1.57	6.65	1.43	14.7	0.009	bdl	0.099	37.1	-6.08	-30	19
B015	13.39	9.3	26.9	5.91	648	18.06	39.7	49.1	70.1	10.1	38.9	26.3	156	0.206	0.01	0.090	33.8	-4.24	-24	10
B016	13.42	9.34	30.9	6.5	244	62.22	32.4	20.3	29.1	7.04	29.2	15.5	72.3	0.033	0.01	0.272	49.2	-4.19	-25	8
B019	13.42	9.37	32.3	6.17	50	5.55	10.3	1.6	0.574	0.425	1.77	0.090	4.38	0.005	bdl	0.074	42.7	-4.84	-27	12
B022	13.35	9.3	30.6	6.48	68	38.74	5.7	6.1	0.242	1.21	4.16	0.145	2.01	0.004	0.01	0.152	43.5	-4.90	-28	11
B025	12.97	9.35	31.8	5.81	192	3.23	11.6	25.8	19.3	0.793	3.75	1.95	58.5	0.028	0.02	0.036	49.7	-4.59	-26	11
B026	13.26	9.52	31.1	7.01	383	143.53	5.3	13.2	2.46	21.9	39.8	3.39	9.01	0.007	0.01	0.576	67.3	-5.15	-30	12
B028	14.1	9.87	31.7	7.03	571	90.28	0.5	22.0	14.1	30.0	63.7	11.0	37.7	0.038	0.01	0.632	52.4	-4.79	-25	13
B029	14.16	9.93	31.2	6.98	771	129.32	0.4	40.9	7.17	36.5	83.1	8.03	23.1	0.012	0.01	1.03	59.7	-4.18	-23	10
B031	14.14	10.06	31.5	7.4	285	27.27	1.0	25.9	0.699	6.66	29.2	1.00	1.49	0.017	0.01	1.56	53.2	-3.35	-22	5
B032	14.14	10.07	30.2	7.3	279	24.52	2.0	21.9	6.06	3.54	31.4	3.33	19.9	0.032	0.01	1.14	58.5	-4.34	-23	12
B034	13.93	9.94	31.5	7.39	734	51.24	4.0	70.9	19.3	32.3	48.9	5.85	15.5	0.022	0.01	1.87	81.1	-3.60	-22	7
B035	13.96	9.85	30.7	7.4	840	113.95	3.8	118	38.3	40.9	53.6	37.0	141	bdl	0.01	2.78	54.8	-4.19	-24	10
B036	13.66	9.06	30.7	7.2	840	205.63	4.1	68.9	41.0	25.1	74.4	39.3	55.9	0.039	0.01	1.32	44.5	-4.05	-22	10
B037	13.78	9.07	26.9	7.42	67	6.77	1.9	8.7	2.14	0.575	3.06	0.699	0.007	0.018	0.04	0.051	38.2	-5.49	-31	13
B039	13.67	9.05	29.7	6.82	580	54.11	1.3	25.2	25.0	14.0	74.4	11.7	36.8	0.043	0.01	3.34	53.4	-3.95	-21	11

B040	13.64	9.03	31.8	6.05	130	17.32	1.3	16.5	1.36	1.13	6.02	0.559	9.80	0.005	0.01	0.268	91.0	-4.80	-28	10
B041	13.56	9.09	31.7	6.45	272	21.47	6.0	15.6	0.927	6.75	31.0	0.165	9.08	0.004	0.01	0.235	56.1	-4.74	-27	11
B042	13.59	9.12	31.7	6.34	174	39.89	3.6	13.5	2.51	3.73	15.5	0.273	18.0	0.006	0.02	0.304	63.4	-4.56	-26	11
B043	13.64	8.94	30.6	6.8	267	66.49	1.8	38.8	1.49	2.24	17.5	1.41	0.374	0.011	0.03	0.417	73.0	-3.91	-23	9
B044	13.53	8.98	31.2	6.87	479	78.81	3.8	59.3	0.770	9.34	35.5	2.21	0.750	0.005	0.01	0.163	55.8	-4.46	-27	9
B046	13.51	9.02	29.9	5.77	92	323.18	7.8	2.0	3.06	1.77	6.36	0.072	31.9	0.011	0.03	0.041	42.4	-4.04	-22	11
B049	14.23	9.01	31.2	7.15	620	500.38	3.7	39.5	19.0	18.6	66.0	9.15	59.9	0.020	0.01	0.277	50.5	-4.18	-23	10
B051	14.18	8.76	31.1	6.61	188	71	1.6	18.8	3.77	3.75	16.4	1.62	9.19	0.005	0.01	0.221	82.7	-4.51	-26	11
B053	14.17	8.67	31.5	6.62	1030	416.02	12.8	31.0	74.5	28.1	129	16.3	313	0.099	0.01	0.116	61.4	-4.47	-25	11
B055	13.86	9.78	30	7.8	610	608.29	2.3	76.8	21.9	23.5	44.6	13.3	1.73	0.037	0.05	1.26	48.8	-3.30	-19	7
W005	13.56	9.36	28.9	7.3	463	3.36	4.8	33.3	5.97	17.2	41.2	7.49	28.7	0.018	bdl	1.07	42.0	-4.30	-25	10
W006	13.51	9.39	28	7.17	804	7.99	2.1	60.9	20.8	35.7	72.4	16.6	46.6	0.045	bdl	1.38	56.1	-4.38	-24	11
W008	13.55	9.27	30	6.56	378	6.65	8.7	15.8	50.9	13.1	34.2	6.66	99.3	0.030	0.01	0.100	44.1	-4.51	-25	11
W009	13.52	9.28	29.3	6.84	765	17.02	14.1	22.1	47.6	23.2	84.5	9.21	214	0.086	0.02	0.197	56.3	-4.11	-24	9
W012	13.5	9.32	27.7	6.5	320	489.65	29.0	11.4	15.0	5.31	31.1	9.34	19.9	0.012	0.01	0.249	40.0	-4.01	-24	8
W014	13.45	9.3	28.9	6.83	160	1.77	14.9	4.0	8.01	3.16	11.2	0.348	62.9	0.029	0.02	0.029	31.0	-4.66	-27	11
W015	13.45	9.24	29.9	6.8	95	6.04	5.3	1.8	2.32	2.75	6.69	0.183	43.5	0.022	0.03	0.015	20.8	-4.82	-27	12
W016	13.39	9.29	25.5	6.81	638	0.79	50.5	47.0	44.9	9.01	48.5	26.6	7.91	0.048	bdl	0.518	27.9	-4.55	-26	11
W017	13.41	9.33	28.8	7	512	1.40	25.7	32.6	35.1	7.05	52.1	20.4	0.016	0.049	bdl	0.360	35.9	-4.52	-25	11
W020	13.42	9.35	29.5	6.5	44	0.24	6.2	1.2	0.455	0.360	1.46	0.012	14.5	0.008	bdl	0.027	29.5	-4.44	-24	12
W021	13.43	9.36	29.3	6.65	268	9.88	27.6	12.3	19.0	4.19	17.0	9.01	47.9	0.032	0.01	0.094	40.3	-4.36	-24	11
W022	13.44	9.36	31.5	6.65	374	1.77	41.8	10.9	17.9	6.04	32.0	7.83	54.6	0.050	0.03	0.261	34.6	-4.50	-25	11
W023	13.45	9.38	30.3	6.91	319	8.97	14.4	14.0	17.8	6.67	32.3	10.3	60.3	0.036	bdl	0.366	45.0	-4.52	-24	12
W024	13.42	9.37	26.7	6.96	228	7.20	15.9	16.4	17.3	3.28	14.5	5.03	30.7	0.034	0.02	0.101	25.6	-4.20	-22	11
W025	13.4	9.35	27.8	6.29	480	4.39	22.9	28.5	53.2	10.1	31.4	6.78	131	0.049	0.01	0.063	23.4	-4.02	-20	12
W028	13.36	9.3	28.8	6.72	367	524.54	23.0	30.8	34.9	5.59	15.1	30.6	91.7	0.072	0.03	0.393	53.9	-4.81	-25	14
W029	13.34	9.3	27	6.79	241	2.93	7.2	17.3	18.9	3.52	20.2	1.79	74.9	0.021	0.02	0.050	50.1	-4.30	-23	11
W033	13.13	9.35	30	6.03	310	20.86	0.2	3.9	0.9	5.68	91.2	78.0	3.46	0.008	0.01	0.141	13.7	-3.55	-16	12

W034	13.23	9.55	28.8	6.75	55	3.11	1.2	7.9	0.791	1.21	5.98	1.01	0.396	0.004	0.05	0.990	43.4	-5.37	-32	11
W036	13.97	9.76	26.8	6.54	1310	15.86	3.0	146	120	49.5	117	91.0	209	bdl	0.01	1.34	56.2	-3.65	-20	9
W038	13.96	9.75	29.9	6.22	1540	500.51	5.7	55.2	129	72.4	147	26.8	338	bdl	bdl	0.756	71.5	-3.74	-21	9
W041	13.96	9.78	29.2	6.77	1421	237.23	2.8	99.9	88.8	72.9	116	45.9	363	bdl	0.02	1.60	62.8	-3.94	-23	9
W049	14.16	9.94	28.4	7.28	743	104.68	0.3	66.7	13.1	36.9	49.8	11.2	39.9	0.021	0.01	1.43	58.9	-3.66	-20	9
W051	14.14	10.07	28	7.05	338	96.99	0.9	28.9	4.20	7.23	35.0	1.48	0.008	0.005	0.01	1.36	54.3	-3.50	-19	9
W052	14.13	10.07	29.1	7.15	670	186.66	2.2	58.7	19.5	19.5	61.2	17.4	65.1	0.030	0.01	2.68	71.4	-3.90	-23	8
W053	14.13	10.07	29.9	7.35	708	172.26	2.0	52.9	23.5	19.2	71.3	16.0	102	0.084	0.01	2.28	64.8	-4.07	-24	8
W054	13.89	9.81	27.9	6.55	655	187.51	2.8	24.8	18.5	24.9	78.1	17.6	79.9	0.005	0.01	1.12	60.6	-4.15	-23	10
W057	13.94	9.1	29.5	6.92	1967	164.03	5.1	28.2	162	76.9	254	89.6	556	0.194	0.01	0.484	79.8	-3.56	-19	9
W061	13.72	9.1	26.9	7.57	524	55.02	26.3	23.0	26.4	8.37	51.7	18.0	140	0.094	0.02	0.128	73.8	-4.32	-23	12
W062	13.74	9.12	30.5	6.65	368	100.41	16.2	13.1	6.86	6.84	44.5	7.28	41.9	0.019	0.04	0.243	60.1	-4.61	-24	12
W065	13.62	8.97	28.5	6.34	242	8.30	14.7	4.9	10.5	4.04	23.8	0.745	94.4	0.015	bdl	0.038	35.2	-4.89	-25	14
W067	13.5	8.98	29.5	7.04	225	49.29	8.6	18.5	17.1	8.56	30.1	1.47	79.1	0.018	0.06	0.318	108	-4.57	-24	13
W069	13.5	9.1	29.9	5.67	106	50.02	5.3	4.7	5.75	3.14	5.13	0.095	40.6	0.019	bdl	0.010	23.2	-4.74	-24	14
W071	13.55	9.05	30.3	5.83	356	10.49	26.0	11.8	19.9	7.60	26.4	7.96	126	0.059	0.09	0.042	29.9	-4.52	-23	13
W076	14.09	9.07	28.5	7.46	660	168.12	2.1	48.2	22.2	25.6	67.0	11.3	118	bdl	0.01	0.585	50.5	-4.12	-22	11
W077	13.64	9.46	28.8	6.9	1600	373.02	2.0	230	83.9	58.5	80.7	53.1	275	bdl	bdl	2.82	69.9	-4.32	-22	13
W081	13.86	9.78	29.8	7.07	2500	230.89	1.0	244	345	124	252	177	823	0.663	0.02	0.820	75.1	-4.23	-23	11
R001	13.59	9.3	26.1	8.04	115	43.68	3.5	6.7	0.68	3.77	13.2	0.234	0.547	0.004	0.02	0.207	11.8	0.55	3	-1
R003	13.55	9.27	25.7	7.81	50	21.84	2.5	4.5	0.48	2.04	6.21	0.114	0.680	bdl	0.01	0.129	9.4	-3.37	-18	9
R004 A	13.54	9.32	24.4	7.41	154	44.04	3.3	6.5	0.652	3.63	13.0	0.252	0.138	0.004	0.06	0.204	11.7	0.26	2	0
R004 B	13.53	9.32	24.1	7.2	63	20.74	2.3	3.8	0.281	2.03	6.16	0.095	0.218	bdl	bdl	0.130	9.6	-3.29	-18	9
R004 C	13.53	9.32	24.8	7.76	63	26.23	2.3	3.8	0.33	2.03	6.17	0.110	0.146	bdl	0.02	0.132	9.6	-3.12	-18	7
R005	13.4	9.29	24.8	6.4	65	24.83	2.4	3.9	0.345	2.09	6.54	0.124	0.422	bdl	0.02	0.133	9.8	-2.99	-17	7
R006 A	12.94	9.33	25.6	7.16	65	23.49	2.4	3.9	0.326	2.11	6.34	0.124	0.141	bdl	0.01	0.138	9.5	-2.97	-17	7
R006 B	12.92	9.34	28.8	6.86	90	35.01	1.9	5.2	0.321	3.28	8.95	0.364	0.011	bdl	0.07	0.165	23.1	-1.82	-7	7
R007	13.95	9.75	28.7	6.71	222	69.24	5.5	14.9	6.27	4.07	19.7	1.82	1.68	0.011	0.01	0.325	22.3	-0.77	-5	2

R008	13.96	9.85	30	8.2	193	56.06	3.8	16.5	3.96	4.55	24.8	2.65	2.08	0.009	0.01	0.297	27.4	-2.32	-10	8
R012	14.18	8.76	29.8	7.72	134	46.60	4.0	6.6	0.827	4.42	14.4	1.05	1.14	0.004	bdl	0.136	26.3	-1.71	-12	2
R013	14.17	8.65	32.2	8.92	139	50.51	2.5	10.9	1	4.34	12.7	0.709	1.80	0.004	0.01	0.308	32.5	-1.86	-11	4
R009	13.69	9.1	29.3	8.2	72	0.21	2.3	3.7	0.27	2.05	6.30	0.092	0.214	bdl	0.01	0.132	9.5	-3.01	-18	6
R010	13.67	9.05	28.7	8.81	65	0.24	2.4	3.7	0.322	2.06	6.35	0.101	0.039	bdl	0.01	0.135	9.3	-2.93	-17	6
Sp001	13.51	9.29	23.9	7.6	35	9.76	8.5	1.1	0.487	0.181	0.98	0.119	1.26	0.004	0.03	0.042	31.7	-5.10	-27	14
Rk	-	-	-	-	-	-	16673.3	9606.7	-	9520.0	8926.7	-	-	-	-	-	636686.7	-	-	-

B = borehole, W = dug-well, R = river or lake, Rk = rock, Temp. = Temperature, EC = electrical conductivity, n = number of samples, bdl = below detection limit, letter following R004 and R006 represent the sample station. Data for rocks (which are presented here as average) are from Ndjigui et al. (2014)

Table 1b

Sample ID	Long (dd.dd)	Lat (dd.dd)	Fe(II) (mg/l)	Mn (mg/l)	Al (mg/l)	As (µg/l)	Ba (µg/l)	BO2 (mg/l)	Br (mg/l)	Cd (µg/l)	Co (µg/l)	Cr (µg/l)	Cu (µg/l)	Li (µg/l)	Ni (µg/l)	Pb (µg/l)	V (µg/l)	Zn (µg/l)
B001	13.59	9.29	3.13	0.397	0.007	6.08	209	0.02	0.009	0.003	0.066	0.04	0.15	0.5	bdl	0.02	0.046	51.2
B002	13.6	9.29	0.005	0.024	bdl	0.54	166	0.06	0.017	0.005	0.549	0.03	1.71	1.0	1.1	0.09	19.3	61.9
B004	13.6	9.33	0.017	0.001	bdl	0.15	332	0.29	0.042	0.009	0.046	0.24	5.70	0.7	0.3	0.03	6.75	204
B005	13.5	9.39	bdl	bdl	bdl	0.27	245	bdl	bdl	0.004	0.026	0.10	0.48	0.2	0.2	0.03	0.486	9.61
B008	13.5	9.38	0.003	0.501	bdl	0.08	285	0.11	0.022	0.028	1.34	0.05	1.85	0.5	0.7	0.03	8.11	139
B009	13.55	9.27	bdl	bdl	0.003	0.08	397	0.12	0.040	0.014	0.030	0.21	2.60	4.7	0.4	0.02	6.84	139
B010	13.52	9.28	bdl	0.015	bdl	0.04	605	0.11	0.016	0.004	0.165	0.02	0.61	30.0	0.2	0.02	6.02	71.4
B011	13.5	9.32	bdl	0.001	bdl	0.16	762	0.10	0.010	0.015	0.112	0.08	1.76	2.4	0.7	0.02	0.694	182
B014	13.41	9.26	bdl	0.000	bdl	0.06	325	0.02	0.009	0.018	1.09	1.84	1.37	1.8	2.4	0.04	0.454	57.6
B015	13.39	9.3	0.021	0.023	bdl	0.05	720	0.26	0.206	0.063	3.12	0.63	0.64	2.2	4.5	0.02	0.316	319
B016	13.42	9.34	bdl	0.002	bdl	0.04	288	0.16	0.033	0.012	0.298	0.33	1.72	1.3	1.3	bdl	0.860	195
B019	13.42	9.37	bdl	0.001	bdl	0.02	363	0.18	0.005	0.016	0.829	0.16	0.21	2.0	1.1	bdl	0.835	173
B022	13.35	9.3	bdl	0.001	bdl	0.04	307	0.27	0.004	0.011	0.153	0.31	1.86	1.3	0.9	0.04	0.229	141
B025	12.97	9.35	0.087	0.013	0.098	0.18	401	0.86	0.028	0.017	0.774	2.92	11.6	4.2	2.5	4.80	1.90	404
B026	13.26	9.52	0.003	0.001	bdl	0.02	630	0.15	0.007	0.037	0.024	0.15	3.16	7.4	0.2	0.03	1.54	120
B028	14.1	9.87	bdl	0.001	bdl	0.05	87.4	0.07	0.038	0.004	0.035	0.05	2.82	2.7	0.2	0.04	12.4	58.3
B029	14.16	9.93	bdl	0.000	bdl	0.26	181	0.13	0.012	0.013	0.050	0.07	0.85	5.8	0.1	0.04	10.1	144
B031	14.14	10.06	0.330	0.026	bdl	0.03	255	0.11	0.017	0.010	0.053	0.04	0.78	14.5	0.1	0.12	0.658	131
B032	14.14	10.07	0.715	0.087	0.003	0.05	220	0.07	0.032	0.020	0.166	0.06	0.39	17.8	0.8	0.20	0.206	138
B034	13.93	9.94	0.001	0.001	0.003	0.13	309	0.09	0.022	0.007	0.033	0.47	0.39	8.6	0.2	0.04	37.7	105
B035	13.96	9.85	bdl	0.002	0.003	0.63	177	0.06	bdl	0.006	0.052	0.07	0.26	15.8	0.2	0.04	23.9	31.3
B036	13.66	9.06	bdl	0.098	0.003	0.05	171	0.14	0.039	0.206	0.070	0.30	1.49	22.4	0.4	0.29	6.76	130
B037	13.78	9.07	0.999	0.035	0.202	0.16	115	0.11	0.018	0.010	0.433	1.37	1.89	2.3	1.6	0.88	2.03	31.1
B039	13.67	9.05	bdl	0.082		0.03	207	0.16	0.043	0.025	0.040	0.04	0.56	86.2	0.1	0.02	1.75	140
B040	13.64	9.03	bdl	0.008	bdl	0.25	237	0.41	0.005	0.017	0.042	0.50	2.99	1.8	0.3	0.06	4.20	1369

B041	13.56	9.09	0.031	0.009	bdl	0.11	372	0.06	0.004	0.007	0.027	0.08	1.98	4.6	0.3	0.16	2.28	128
B042	13.59	9.12	0.078	0.003	bdl	0.15	358	0.20	0.006	0.010	0.029	0.15	1.65	14.9	0.4	0.16	3.37	141
B043	13.64	8.94	0.078	0.012	bdl	0.21	409	0.17	0.011	0.012	0.023	0.04	2.70	21.0	0.2	0.22	1.48	144
B044	13.53	8.98	bdl	0.001	0.003	0.37	880	0.09	0.005	0.004	0.014	0.02	7.17	14.1	0.1	0.35	8.22	64.7
B046	13.51	9.02	0.006	0.005	0.009	0.09	460	0.08	0.011	0.020	0.655	0.88	26.6	3.3	2.7	1.87	0.136	159
B049	14.23	9.01	bdl	0.119	bdl	0.55	428	0.09	0.020	0.043	0.080	0.03	0.33	19.3	0.1	0.21	5.66	110
B051	14.18	8.76	bdl	0.041	bdl	0.12	254	0.22	0.005	0.010	0.243	0.10	1.37	0.4	0.3	0.02	3.20	180
B053	14.17	8.67	0.013	0.001	bdl	0.13	1480	0.27	0.099	0.055	0.124	0.17	6.04	9.7	1.1	0.06	3.47	194
B055	13.86	9.78	0.045	0.040	0.004	0.43	123	0.41	0.037	0.000	0.037	bdl	0.08	9.1	0.4	bdl	2.23	68.0
W005	13.56	9.36	0.006	0.011	0.005	0.14	228	0.13	0.018	0.006	0.075	0.23	0.44	0.7	0.4	0.04	11.2	89.7
W006	13.51	9.39	bdl	0.011	bdl	0.09	298	0.12	0.045	0.005	0.082	0.03	0.22	3.0	0.2	bdl	19.0	95.1
W008	13.55	9.27	0.004	0.032	bdl	0.09	635	0.12	0.030	0.022	0.384	0.04	0.56	1.1	2.3	0.02	1.12	215
W009	13.52	9.28	bdl	0.033	bdl	0.20	1177	0.13	0.086	0.227	0.201	0.08	0.45	6.6	2.8	bdl	2.41	142
W012	13.5	9.32	0.003	0.004	0.011	0.22	320	0.47	0.012	0.008	0.108	0.06	1.12	0.2	0.4	0.05	2.56	145
W014	13.45	9.3	0.748	0.062	0.334	bdl	bdl	bdl	0.029	bdl	bdl	bdl	bdl	bdl	bdl	bdl	bdl	bdl
W015	13.45	9.24	bdl	0.025	bdl	0.03	547	0.19	0.022	0.012	4.15	0.19	0.48	2.3	5.8		0.105	126
W016	13.39	9.29	bdl	0.008	bdl	0.49	209	0.23	0.048	0.008	0.316	0.06	1.14	0.1	1.2		7.04	119
W017	13.41	9.33	0.003	0.273	bdl	0.35	439	0.16	0.049	0.004	1.26	0.03	0.42	1.0	0.7		0.215	116
W020	13.42	9.35	bdl	0.001	bdl	0.01	331	0.24	0.008	0.012	0.978	0.45	1.11	1.7	1.5	0.03	0.104	130
W021	13.43	9.36	0.006	0.007	0.003	0.10	268	0.18	0.032	0.020	0.087	0.06	1.14	1.2	1.2	0.03	0.983	136
W022	13.44	9.36	bdl	0.001	0.005	0.30	213	0.11	0.050	0.005	0.074	0.57	0.76	4.0	0.2	0.02	4.78	73.6
W023	13.45	9.38	0.006	0.011	0.005	0.03	433	0.04	0.036	0.013	0.153	0.11	0.66	0.9	2.0	0.02	0.490	64.6
W024	13.42	9.37	0.012	0.347	0.004	0.19	615	0.50	0.034	0.017	1.70	0.05	0.65	0.6	3.2	0.04	0.386	276
W025	13.4	9.35	bdl	0.037	0.004	0.16	1269	0.20	0.049	0.033	1.39	0.06	1.27	1.4	6.9	0.02	0.883	136
W028	13.36	9.3	0.167	0.607	0.031	0.18	583	0.46	0.072	0.052	33.3	0.08	13.9	39.3	39.2	0.04	0.667	217
W029	13.34	9.3	bdl	0.295	0.007	0.04	467	0.14	0.021	0.017	10.2	0.93	0.75	13.3	11.6	0.06	1.44	83.5
W033	13.13	9.35	bdl	0.001	bdl	0.01	74.3	0.13	0.008	0.008	0.031	0.04	0.48	0.2	0.2		0.691	141
W034	13.23	9.55	0.612	0.046	2.04	bdl	bdl	bdl	0.004	bdl	bdl	bdl	bdl	bdl	bdl	bdl	bdl	bdl

W036	13.97	9.76	bdl	0.160	bdl	0.19	250	0.15	bdl	0.045	0.244	0.07	1.21	16.1	4.0		8.10	96.5
W038	13.96	9.75	bdl	0.011	0.003	0.09	2058	0.14	bdl	0.008	0.184	0.04	0.49	6.5	0.3	0.04	13.5	109
W041	13.96	9.78	bdl	0.003	0.003	0.16	861	0.16	bdl	0.006	0.191	0.73	0.73	8.4	0.4	0.02	17.6	91.2
W049	14.16	9.94	bdl	0.018	bdl	0.56	131	0.11	0.021	0.005	0.042	0.10	0.29	2.9	0.3		21.3	87.5
W051	14.14	10.07	0.021	0.410	bdl	0.07	269	0.15	0.005	0.016	1.13	0.03	0.26	7.4	1.3		0.677	166
W052	14.13	10.07	bdl	0.042	bdl	0.06	213	0.19	0.030	0.009	0.078	0.02	0.34	17.8	0.5	0.02	6.98	120
W053	14.13	10.07	bdl	0.011	bdl	0.04	171	0.14	0.084	0.009	0.088	0.04	0.29	12.8	0.2	0.03	7.10	100
W054	13.89	9.81	bdl	0.001	bdl	0.07	324	0.11	0.005	0.004	0.071	0.23	0.47	2.0	0.2	0.03	20.6	94.3
W057	13.94	9.1	bdl	0.005	bdl	0.13	203	0.24	0.194	0.028	0.082	0.19	0.48	9.4	0.7	0.03	5.98	108
W061	13.72	9.1	bdl	0.006	0.004	0.20	692	0.17	0.094	0.011	0.113	0.46	0.74	1.3	1.1	0.03	2.59	101
W062	13.74	9.12	bdl	0.007	0.003	0.09	487	0.08	0.019	0.009	0.063	0.03	0.36	0.5	0.4	0.03	4.44	89.2
W065	13.62	8.97	0.140	0.063	0.129	bdl	bdl	bdl	0.015	bdl	bdl	bdl	bdl	bdl	bdl	bdl	bdl	bdl
W067	13.5	8.98	0.006	0.032	0.007	0.09	892	0.14	0.018	0.033	0.612	0.04	0.46	4.5	1.2	0.04	5.32	129
W069	13.5	9.1	0.021	0.056	0.010	0.05	725	0.30	0.019	0.032	9.02	2.05	1.60	3.4	6.7	0.15	0.083	130
W071	13.55	9.05	0.007	0.004	0.006	0.02	754	0.24	0.059	0.012	0.068	0.05	0.50	1.4	2.3	0.02	0.437	116
W076	14.09	9.07	0.004	0.004	0.004	0.10	236	0.11	bdl	0.009	0.100	0.03	0.38	9.3	0.4	0.03	11.2	95.9
W077	13.64	9.46	0.004	0.022	0.006	0.11	431	0.15	bdl	0.007	0.235	0.07	0.84	4.9	0.5	bdl	14.7	33.4
W081	13.86	9.78	0.004	0.006	0.003	0.20	132	0.10	0.663	0.017	0.248	0.29	0.43	8.6	4.0	bdl	19.2	73.4
R001	13.59	9.3	0.128	0.021	0.106	bdl	bdl	0.02	0.004	bdl	bdl	bdl	bdl	bdl	bdl	bdl	bdl	bdl
R003	13.55	9.27	0.009	0.001	0.010	0.28	257	0.18		0.007	0.038	0.09	0.46	0.2	0.3	0.08	0.465	40.4
R004 A	13.54	9.32	0.006	0.002	0.006	0.38	409	0.28	0.004	0.004	0.063	0.12	1.09	0.3	0.7	0.07	2.12	9.23
R004 B	13.53	9.32	0.009	0.001	0.006	0.20	214	0.21		0.004	0.024	0.06	0.36	0.2	0.2	0.02	0.532	12.9
R004 C	13.53	9.32	0.006	0.001	0.003	0.27	243	0.12		0.009	0.026	0.05	0.39	0.2	0.2		0.508	16.4
R005	13.4	9.29	0.222	0.051	0.107	bdl	bdl	bdl	bdl	bdl	bdl	bdl	bdl	bdl	bdl	bdl	bdl	bdl
R006 A	12.94	9.33	0.200	0.047	0.131	bdl	bdl	bdl	bdl	bdl	bdl	bdl	bdl	bdl	bdl	bdl	bdl	bdl
R006 B	12.92	9.34	0.389	0.031	0.381	bdl	bdl	bdl	bdl	bdl	bdl	bdl	bdl	bdl	bdl	bdl	bdl	bdl
R007	13.95	9.75	0.072	0.185	0.007	bdl	bdl	0.13	0.011	bdl	bdl	bdl	bdl	bdl	bdl	bdl	bdl	bdl
R008	13.96	9.85	0.122	0.837	0.006	bdl	bdl	0.17	0.009	bdl	bdl	bdl	bdl	bdl	bdl	bdl	bdl	bdl

R012	14.18	8.76	0.022	0.323	0.005	bdl	bdl	0.33	0.004	bdl	bdl	bdl	bdl	bdl	bdl	bdl	bdl	bdl
R013	14.17	8.65	0.691	0.565	0.059	bdl	bdl	bdl	0.004	bdl	bdl	bdl	bdl	bdl	bdl	bdl	bdl	bdl
R009	13.69	9.1	0.004	0.001	0.003	0.27	184	0.11		0.004	0.022	0.04	0.28	0.2	0.2	0.02	0.335	18.7
R010	13.67	9.05	0.042	0.018	0.011	bdl	bdl	bdl	bdl	bdl	bdl	bdl	bdl	bdl	bdl	bdl	bdl	bdl
Sp001	13.51	9.29	0.007	0.002	0.008	0.03	162	0.42	0.004	0.005	0.044	0.22	0.36	1.6	0.2	0.02	0.675	80.0
Rk	-	-	67366.7	666.7	146286.7	-	720.8	-	-	-	18.4	99.3	46.2	11.4	46.1	14.5	90.6	55.4

B = borehole, W = dug-well, R = river or lake, Rk = rock, Temp = Temperature, EC = electrical conductivity, n = number of samples, bdl = below detection limit, letter following R004 and R006 represent the sample station. Data for rocks (which are presented here only as average values) are from Ndjigui et al. (2014)

Table 1b cont`d:

Ref. code	Be (µg/l)	Ga (µg/l)	Hf (µg/l)	Mo (µg/l)	Nb (µg/l)	Rb (µg/l)	Sb (µg/l)	Sc (µg/l)	Sn (µg/l)	Sr (µg/l)	Ta (µg/l)	Te (µg/l)	Th (µg/l)	Ti (µg/l)	Tl (µg/l)	U (µg/l)	W (µg/l)	Y (µg/l)	Zr (µg/l)
B001	0.007	0.002	bdl	2.11	bdl	1.55		0.30	0.03	245	0.001	bdl	bdl	0.34	0.007	0.029	bdl	0.004	bdl
B002	bdl	bdl	bdl	1.61	bdl	0.79	0.037	0.59	0.02	422	bdl	bdl	bdl	0.17	0.008	0.426	bdl	0.007	bdl
B004	bdl	0.004	0.001	0.35	bdl	1.65	0.027	0.51	0.03	667	0.001	bdl	bdl	0.39	0.010	1.62	bdl	0.068	bdl
B005	bdl	0.012	0.001	0.25	bdl	0.99	0.019	0.10	0.04	89.9	0.001	0.01	bdl	0.32	0.008	0.013	bdl	0.013	bdl
B008	bdl	0.010	0.001	0.85	bdl	0.55	0.019	0.50	0.03	771	0.001	bdl	bdl	0.30	0.009	2.09	bdl	0.165	0.006
B009	bdl	bdl	bdl	0.15	bdl	12.9	0.006	0.42	bdl	718	bdl	bdl	bdl	0.42	0.014	1.07	bdl	0.022	bdl
B010	bdl	0.002	bdl	0.55	bdl	29.7	bdl	0.40	bdl	1897	0.001	0.03	bdl	0.10	0.015	21.0	bdl	0.043	bdl
B011	bdl	bdl	bdl	0.01	bdl	29.3	0.009	0.21	0.03	90.3	bdl	bdl	bdl	0.21	0.047	0.283	bdl	0.002	bdl
B014	0.109	bdl	bdl	0.04	bdl	31.0	bdl	0.29	0.04	80.9	bdl	bdl	bdl	0.25	0.126	0.097	bdl	0.018	bdl
B015	0.030	0.006	bdl	0.06	bdl	128	0.014	0.39	0.03	609	bdl	bdl	bdl	0.30	0.657	0.219	bdl	0.308	bdl
B016	0.024	0.002	bdl	0.15	bdl	49.1	0.006	0.44	0.02	344	bdl	0.02	bdl	0.24	0.056	0.236	0.08	0.022	bdl
B019	0.014	0.005	0.001	0.01	bdl	27.4	bdl	0.24	bdl	36.9	bdl	0.03	bdl	0.28	0.061	0.530	bdl	0.004	bdl
B022	0.013	0.002	bdl	0.04	bdl	12.7	bdl	0.25	0.04	60.5	bdl	bdl	bdl	0.34	0.011	0.093	bdl	0.005	bdl
B025	0.224	0.880	0.049	0.09	0.366	22.6	0.081	0.79	0.49	63.6	0.023	bdl	0.384	69.7	0.076	0.192	bdl	0.849	1.86
B026	0.019	0.005	bdl	1.15	bdl	13.1	bdl	0.53	0.03	383	bdl	bdl	bdl	0.28	0.006	3.13	bdl	0.020	bdl
B028	bdl	0.002	bdl	0.92	bdl	0.43	0.007	0.49	0.04	430	bdl	0.02	bdl	0.30	0.005	1.19	bdl	0.072	bdl
B029	bdl	0.010	0.001	1.67	bdl	0.39	0.006	0.65	bdl	333	0.001	bdl	bdl	0.39	0.004	1.20	bdl	0.241	bdl
B031	bdl	0.017	0.001	28.8	bdl	0.31	0.020	0.52	0.03	180	bdl	0.02	bdl	0.38	0.003	0.757	0.51	0.037	0.009
B032	bdl	0.008	0.001	9.73	bdl	0.47	0.008	0.54	0.04	173	bdl	0.02	bdl	0.51	0.005	0.918	bdl	0.015	bdl

Sample																			
B034	bdl	0.006	0.001	7.14	bdl	0.97	bdl	0.58	bdl	636	0.001	0.03	bdl	0.79	0.007	2.93	bdl	0.132	0.006
B035		0.017	0.003	10.7	0.021	5.92	0.328	0.42	bdl	1653	0.005	0.03	bdl	0.45	0.010	1.56	0.48	0.021	0.010
B036	0.008	0.008	bdl	23.3	bdl	6.19	0.007	0.36	0.01	1455	bdl	0.01	bdl	0.42	0.005	9.21	0.11	0.173	0.005
B037	0.300	1.15	0.075	0.13	0.407	7.08	0.007	0.78	0.15	39.8	0.034	bdl	0.543	60.2	0.034	0.334	bdl	2.63	1.65
B039	0.058	0.012	0.003	35.4	bdl	1.68	0.005	0.41	0.02	834	0.001	0.01	bdl	0.52	0.004	38.3	bdl	0.049	0.015
B040	0.028	0.005	bdl	0.22	bdl	0.98	0.054	0.75	0.04	221	bdl		bdl	0.58	0.004	0.451	bdl	0.006	bdl
B041	0.007	0.004	bdl	0.13	bdl	4.15	0.011	0.50	0.02	786	bdl	0.01	bdl	0.35	0.006	0.928	bdl	0.023	bdl
B042	0.023	0.006	bdl	0.07	bdl	1.62		0.40	0.02	636	bdl		bdl	0.37	0.004	0.111	bdl	0.009	bdl
B043	0.014	0.002	bdl	0.12	bdl	0.98	0.020	0.51	0.03	947	bdl	0.02	bdl	0.30	0.004	0.232	bdl	0.013	bdl
B044	bdl	0.006	bdl	0.22	bdl	5.34	0.014	0.51		1973	bdl	0.01	bdl	0.30	0.006	4.87	bdl	0.031	bdl
B046	0.289	0.005	0.001	0.01	bdl	19.0	0.051	0.33	0.03	103	bdl	0.02	bdl	0.37	0.080	0.059	bdl	0.016	bdl
B049	bdl	0.004	bdl	0.08	bdl	0.50	0.098	0.51	bdl	836	0.001	0.04	bdl	0.38	0.005	0.279	bdl	0.054	bdl
B051	bdl	bdl	bdl	0.14	bdl	0.85		0.66	0.03	336	0.001	0.01	bdl	0.40	0.003	0.074	bdl	0.011	bdl
B053	0.023	bdl	bdl	0.13	bdl	1.60	0.014	0.68	0.02	2989	0.001	0.04	bdl	0.23	0.013	1.52	bdl	0.088	bdl
B055	bdl	0.005	bdl	2.18	bdl	2.69	0.026	0.48	bdl	735	0.001	0.03	bdl	0.27	0.006	1.02	0.08	0.014	bdl
W005	bdl	0.005	bdl	1.45	bdl	1.29	0.016	0.47	0.04	840	0.001	0.02	bdl	0.52	0.006	4.26	bdl	0.028	bdl
W006	bdl	bdl	0.001	0.97	bdl	1.40	0.030	0.56	bdl	1771	0.001	0.01	bdl	0.18	0.006	1.86	0.07	0.038	bdl
W008	bdl	0.004	bdl	0.08	bdl	23.4	0.021	0.50	bdl	533	bdl	0.04	bdl	0.51	0.051	0.023	bdl	0.077	bdl
W009	0.016	bdl	bdl	0.08	bdl	25.2	0.048	0.57	bdl	1384	bdl	bdl	bdl	0.31	0.050	0.169	bdl	0.036	bdl
W012	bdl	0.018	bdl	1.44	bdl	41.3	0.069	0.40	0.04	333	bdl	0.01	bdl	0.26	0.045	0.059	bdl	0.088	0.006
W014	bdl	bdl	bdl	bdl	bdl	bdl	bdl	bdl	bdl	bdl	bdl	bdl	bdl	bdl	bdl	bdl	bdl	bdl	bdl
W015	0.021	0.001	bdl	0.02	bdl	18.8	0.014	0.11	0.03	152	bdl	0.06	bdl	0.20	0.020	0.004	bdl	0.020	bdl

ID																			
W016	bdl	bdl	bdl	3.93	bdl	88.4	0.425	0.38	0.02	532	0.001	bdl	bdl	0.18	0.133	0.532	0.10	0.034	bdl
W017	bdl	0.003	bdl	0.99	bdl	52.6	0.053	0.37	0.02	467	bdl	0.01	bdl	0.23	0.062	0.317	bdl	0.018	0.006
W020	0.009	0.001	bdl	0.01	bdl	21.5	0.004	0.27	bdl	24.4	bdl	bdl	bdl	0.21	0.016	0.026	bdl	0.002	bdl
W021	bdl	0.001	bdl	0.20	bdl	40.2	0.066	0.35	bdl	218	bdl		bdl	0.37	0.067	0.013	bdl	0.044	bdl
W022	bdl	0.003	bdl	1.79	bdl	67.4	0.048	0.32	bdl	298	bdl	0.02	bdl	0.26	0.128	0.287	bdl	0.015	bdl
W023	bdl	0.003	bdl	0.15	bdl	15.6	0.022	0.49	0.04	478	bdl	0.02	bdl	0.38	0.060	0.219	bdl	0.017	bdl
W024	bdl	0.013	bdl	0.19	bdl	35.5	0.022	0.16	bdl	212	bdl	bdl	bdl	0.31	0.117	0.018	bdl	0.177	bdl
W025	bdl	0.008	bdl	0.18	bdl	67.5	0.284	0.27	0.06	521	bdl	bdl	bdl	0.16	0.336	0.031	bdl	0.125	bdl
W028	0.307	0.056	bdl	0.23	bdl	43.5	0.047	0.46	0.03	352	bdl	0.03	bdl	0.65	0.297	0.238	bdl	1.22	0.011
W029	0.065	0.011	bdl	0.08	bdl	19.5	0.017	0.41	0.04	144	bdl	0.02	bdl	0.34	0.032	0.090	bdl	0.039	bdl
W033	bdl	0.007	bdl	0.19	bdl	0.15	0.008	0.27	bdl	123	bdl	bdl	bdl	0.19	bdl	0.154	bdl	0.013	bdl
W034	bdl	bdl	bdl	bdl	bdl	bdl	bdl	bdl	bdl	bdl	bdl	bdl	bdl	bdl	bdl	bdl	bdl	bdl	bdl
W036	bdl	0.002	0.001	6.35	0.005	1.17	0.186	0.62	0.03	2483	0.002	0.04	bdl	0.38	0.006	1.47	0.09	0.035	0.005
W038	bdl	0.003	bdl	0.44	bdl	0.72	0.013	0.84	0.02	2560	0.001	bdl	bdl	0.74	0.005	3.43	bdl	0.093	bdl
W041	0.012	0.005	0.001	1.91	bdl	1.58	0.012	0.66	0.03	1601	bdl	bdl	bdl	0.54	0.004	2.75	bdl	0.045	0.008
W049	bdl	0.002	bdl	1.24	bdl	0.52	0.020	0.60	bdl	349	0.002	0.03	bdl	0.26	0.003	0.157	bdl	0.011	bdl
W051	bdl	0.007	bdl	1.07	bdl	0.65	0.008	0.46	0.03	349	bdl	bdl	bdl	0.64		0.369	bdl	0.017	0.005
W052	0.008	0.002	0.001	7.77	bdl	0.65	0.007	0.66	0.03	564	bdl	0.03	bdl	0.54	0.005	5.06	bdl	0.020	0.008
W053	0.016	0.002	bdl	5.81	bdl	0.69	0.008	0.62	0.03	599	0.001	bdl	bdl	0.40	0.003	7.00	bdl	0.045	0.005
W054	bdl	0.003	0.001	0.98	bdl	0.75	0.013	0.62	0.02	662	0.001	bdl	bdl	0.39	0.006	0.470	bdl	0.026	0.006
W057	bdl	0.003	0.001	0.88	bdl	3.61	0.045	1.15	0.03	2588	0.001	0.04	bdl	0.35	0.008	2.73	bdl	0.064	0.006
W061	0.013	0.009	bdl	0.27	bdl	31.9	0.028	0.74	bdl	661	0.001	bdl	bdl	0.48	0.038	0.161	bdl	0.050	bdl

Sample																			
W062	bdl	0.002	bdl	0.56	bdl	6.93	0.010	0.63	0.02	690	0.001	0.02	bdl	0.70	0.010	0.556	bdl	0.046	bdl
W065	bdl	bdl	bdl	bdl	bdl	bdl	bdl	bdl	bdl	bdl	bdl	bdl	bdl	bdl	bdl	bdl	bdl	bdl	bdl
W067	0.008	0.005	bdl	0.16	bdl	12.8	0.013	1.08	bdl	643	0.001	bdl	bdl	0.99	0.014	0.047	bdl	0.018	bdl
W069	0.085	0.021	bdl	0.01	bdl	19.9	bdl	0.15	0.04	158	bdl	bdl		0.20	0.024	1.04	bdl	0.327	bdl
W071	0.020	0.006	bdl	0.01	bdl	38.5	bdl	0.27	0.03	510	0.001	bdl	bdl	0.29	0.043	0.013	bdl	0.054	bdl
W076	bdl	0.003	bdl	0.05	bdl	0.59	0.008	0.54	0.02	899	0.001	0.02	bdl	0.57	0.003	0.251	bdl	0.046	bdl
W077	bdl	bdl	0.007	2.84	0.017	1.10	0.036	0.82	0.27	1059	0.006	bdl	bdl	0.31	0.003	5.02	0.28	0.045	0.016
W081	bdl	bdl	0.001	0.71	bdl	0.72	0.009	1.13	bdl	2512	0.001	0.02	bdl	0.44	0.005	1.18	0.05	0.075	bdl
R001	bdl	bdl	bdl	bdl	bdl	bdl	bdl	bdl	bdl	bdl	bdl	bdl	bdl	bdl	bdl	bdl	bdl	bdl	bdl
R003	bdl	0.006	bdl	0.20	bdl	1.22	0.009	0.09	0.02	98.1	bdl	0.03	bdl	0.41	0.003	0.041	bdl	0.024	bdl
R004 A	bdl	0.023	bdl	0.56	bdl	0.65	0.023	0.09	bdl	156	0.001	bdl	bdl	0.37	bdl	0.142	bdl	0.038	0.006
R004 B	bdl	0.006	bdl	0.27	bdl	0.99	0.026	0.14	bdl	94.4	bdl	0.03	bdl	0.24	bdl	0.015	bdl	0.020	bdl
R004 C	bdl	0.006	bdl	0.29	bdl	1.05	0.012	0.08	0.02	99.1	bdl	0.02	bdl	0.32	bdl	0.014	bdl	0.014	bdl
R005	bdl	bdl	bdl	bdl	bdl	bdl	bdl	bdl	bdl	bdl	bdl	bdl	bdl	bdl	bdl	bdl	bdl	bdl	bdl
R006 A	bdl	bdl	bdl	bdl	bdl	bdl	bdl	bdl	bdl	bdl	bdl	bdl	bdl	bdl	bdl	bdl	bdl	bdl	bdl
R006 B	bdl	bdl	bdl	bdl	bdl	bdl	bdl	bdl	bdl	bdl	bdl	bdl	bdl	bdl	bdl	bdl	bdl	bdl	bdl
R007	bdl	bdl	bdl	bdl	bdl	bdl	bdl	bdl	bdl	bdl	bdl	bdl	bdl	bdl	bdl	bdl	bdl	bdl	bdl
R008	bdl	bdl	bdl	bdl	bdl	bdl	bdl	bdl	bdl	bdl	bdl	bdl	bdl	bdl	bdl	bdl	bdl	bdl	bdl
R012	bdl	bdl	bdl	bdl	bdl	bdl	bdl	bdl	bdl	bdl	bdl	bdl	bdl	bdl	bdl	bdl	bdl	bdl	bdl
R013	bdl	bdl	bdl	bdl	bdl	bdl	bdl	bdl	bdl	bdl	bdl	bdl	bdl	bdl	bdl	bdl	bdl	bdl	bdl
R009	bdl	0.007	bdl	0.25	bdl	1.20	0.015	0.13	0.03	102	bdl	0.03	bdl	0.10	bdl	0.012		0.006	bdl
R010	bdl	bdl	bdl	bdl	bdl	bdl	bdl	bdl	bdl	bdl	bdl	bdl	bdl	bdl	bdl	bdl	bdl	bdl	bdl

| Sp001 | 0.013 | 0.008 | 0.001 | 0.04 bdl | | 16.9 | 0.006 | 0.31 bdl | | 12.4 bdl | bdl | bdl | 0.27 | 0.009 | 0.005 bdl | | 0.017 bdl |
| Rk | 1.0 | 17.5 | 5.3 | 3.4 | 11.6 | 36.6 | - | 10.9 | 1.2 | 115.5 | 0.8 - | | 29.9 | 8100.0 | 0.3 | 2.2 | 0.4 | 18.4 | 542.6 |

B = borehole, W = dug-well, R = river or lake, Rk = rock, Temp = Temperature, EC = electrical conductivity, n = number of samples, bdl = below detection limit, letter following R004 and R006 represent the sample station. Data for rocks (which are presented here only as average values) are from Ndjigui et al. (2014)

Table 1d :

Ref. code	La	Ce	Pr	Nd	Sm	Eu	Gd	Tb	Dy	Ho	Er	Tm	Yb	Lu	ΣREE	LREE	HREE	MREE	LREE/HREE	(Er/Nd)$_N$	Eu/Eu*	Ce/Ce*	La/Yb	La/Sm	Gd/Dy
B001	0.002	0.002	0.001	-	0.003	0.050	0.002	-	-	-	0.001	-	-	-	0.061	0.005	0.001	0.055	5.000	-	96.119	0.326	-	0.667	-
B002	0.001	-	-	-	-	0.041	0.002	-	-	-	-	-	-	-	0.044	0.001	0.000	0.043	-	-	-	-	-	-	-
B004	0.014	0.010	0.002	0.012	0.007	0.086	0.007	0.001	0.003	0.001	0.002	-	0.002	0.001	0.148	0.038	0.009	0.101	4.222	1.982	57.852	0.436	7.000	2.000	2.333
B005	0.013	0.020	0.003	0.014	0.004	0.054	0.004	-	0.001	-	0.001	-	0.001	-	0.115	0.050	0.003	0.062	16.667	0.850	63.570	0.739	13.000	3.250	4.000
B008	0.047	0.051	0.008	0.045	0.007	0.074	0.010	0.002	0.014	0.004	0.007	0.001	0.004	-	0.274	0.151	0.030	0.093	5.033	1.850	41.648	0.607	11.750	6.714	0.714
B009	0.003	0.003	-	0.002	0.003	0.094	0.007		0.002	-	-	-	0.001	-	0.115	0.008	0.003	0.104	2.667	0.000	96.590	-	3.000	1.000	3.500
B010	0.010	0.028	0.002	0.008	0.010	0.156	0.008	0.001	0.003	-	0.001	-	0.001	-	0.228	0.048	0.005	0.175	9.600	1.487	82.129	1.445	10.000	1.000	2.667
B011	0.005	0.003	-	0.002	0.005	0.184	0.006	-	0.001	-	-	-	-	-	0.206	0.010	0.001	0.195	10.000	0.000	158.188	-	-	1.000	6.000
B014	0.007	0.004	0.001	0.002	0.005	0.081	0.006	-	0.001	-	0.001	-	-	-	0.108	0.014	0.002	0.092	7.000	5.947	69.637	0.349	-	1.400	6.000
B015	0.217	0.030	0.026	0.119	0.019	0.181	0.024	0.002	0.016	0.003	0.009	0.001	0.007	0.001	0.655	0.392	0.037	0.226	10.595	0.900	39.913	0.092	31.000	11.421	1.500
B016	0.007	0.006	0.001	0.005	0.005	0.067	0.007	-	0.001	0.001	0.002	-	0.006	0.001	0.109	0.019	0.011	0.079	1.727	4.758	53.328	0.523	1.167	1.400	7.000
B019	0.003	0.002	-	0.002	0.004	0.088	0.005	-	-	-	-	-	-	-	0.104	0.007	0.000	0.097	28.000	0.000	92.658	-	-	0.750	-
B022	0.008	0.009	0.002	0.009	0.003	0.081	0.002	-	-	-	0.001	-	-	-	0.115	0.028	0.001	0.086	17.145	1.322	155.710	0.519	-	2.667	-
B025	2.000	2.640	0.461	1.500	0.318	0.168	0.240	0.033	0.174	0.031	0.091	0.012	0.065	0.012	7.745	6.601	0.385	0.759	11.333	0.722	2.860	0.634	30.769	6.289	1.379
B026	0.009	0.013	0.002	0.010	0.008	0.153	0.009	-	0.002		0.001	-	-	-	0.207	0.034	0.003	0.170	4.000	1.189	84.910	0.707	-	1.125	4.500
B028	0.028	0.009	0.005	0.022	0.003	0.022	0.007	0.001	0.007	0.002	0.003	0.001	0.002	0.001	0.113	0.064	0.016	0.033	3.044	1.622	22.610	0.176	14.000	9.333	1.000
B029	0.041	0.014	0.015	0.067	0.013	0.049	0.014	0.003	0.018	0.004	0.013	0.001	0.008	0.001	0.261	0.137	0.045	0.079	28.000	2.308	17.100	0.130	5.125	3.154	0.778
B031	0.182	0.095	0.031	0.118	0.012	0.065	0.007	-	0.002	0.001	0.001	-	0.002	-	0.516	0.426	0.006	0.084	71.000	0.101	33.396	0.292	91.000	15.167	3.500
B032	0.036	0.038	0.006	0.021	0.003	0.057	0.003	-	0.001	-	0.001	-	0.001	0.001	0.168	0.101	0.004	0.063	25.250	0.566	89.468	0.597	36.000	12.000	3.000
B034	0.022	0.028	0.005	0.030	0.014	0.080	0.008	0.001	0.011	0.002	0.008	0.001	0.009	0.002	0.221	0.085	0.033	0.103	2.576	3.172	35.596	0.616	2.444	1.571	0.727
B035	0.003	-	-	-	-	0.045	-	-	0.001	-	-	-	-	0.001	0.050	0.003	0.002	0.045	1.500	-	-	-	-	-	0.000
B036	0.034	0.047	0.005	0.029	0.009	0.043	0.012	-	0.008	0.002	0.007	0.001	0.002	0.001	0.200	0.115	0.021	0.064	5.476	2.871	19.484	0.832	17.000	3.778	1.500
B037	3.300	4.960	0.870	3.310	0.674	0.146	0.600	0.084	0.474	0.078	0.225	0.039	0.219	0.037	15.016	12.44	1.072	1.504	11.604	0.809	1.081	0.675	15.068	4.896	1.266
B039	0.012	0.022	0.003	0.011	0.007	0.050	0.002	0.001	0.004	0.002	0.004	-	0.001	-	0.119	0.048	0.011	0.060	4.364	4.325	62.925	0.846	12.000	1.714	0.500
B040	0.005	0.008	0.001	0.005	0.007	0.059	0.003	-	0.001	-	-	-	0.001	-	0.090	0.019	0.002	0.069	9.500	0.000	60.626	0.825	5.000	0.714	3.000
B041	0.006	0.018	0.001	0.005	0.006	0.089	0.003	-	0.001	-	0.001	-	0.001	-	0.131	0.030	0.003	0.098	10.000	2.379	98.780	1.695	6.000	1.000	3.000
B042	0.004	0.005	-	0.003	0.006	0.083	0.004	-	-	-	-	-	0.001	-	0.106	0.012	0.001	0.093	12.000	-	79.779	-	4.000	0.667	-
B043	0.008	0.015	0.001	0.003	0.003	0.104	0.002	-	-	-	-	-	0.002	-	0.138	0.027	0.002	0.109	13.500	0.000	199.928	1.224	4.000	2.667	-
B044	0.007	0.012	-	0.003	0.004	0.224	0.010	-	-	-	0.002	-	0.001	-	0.263	0.022	0.003	0.238	7.333	7.930	166.776	-	7.000	1.750	-
B046	0.017	0.107	0.010	0.024	0.006	0.117	0.013	0.001	0.002	0.001	-	-	0.001	-	0.299	0.158	0.004	0.137	39.500	0.000	62.381	1.893	17.000	2.833	6.500
B049	0.032	0.032	0.007	0.021	0.005	0.112	0.007	-	0.002	0.001	0.004	-	0.002	-	0.225	0.092	0.009	0.124	10.222	2.266	89.146	0.493	16.000	6.400	3.500
B051	0.003	0.006	-	0.003	0.006	0.070	0.004	-	-	-	0.000	-	-	-	0.092	0.012	0.000	0.080	-	0.000	67.283	-	-	0.500	-
B053	0.024	0.026	0.005	0.011	0.019	0.400	0.019	0.001	0.003	0.001	0.002	-	0.005	0.001	0.517	0.066	0.012	0.439	5.500	2.163	99.134	0.548	4.800	1.263	6.333
B055	0.002	0.002	-		0.002	0.031	0.002	-	-	-	-	-	0.001	-	0.040	0.004	0.001	0.035	4.000	-	72.987	-	2.000	1.000	-
W005	0.014	0.026	0.002	0.008	0.000	0.063	0.002	0.001	0.002	0.001	0.001	-	-	0.001	0.121	0.050	0.005	0.066	10.000	1.487	-	1.134	-	-	1.000
W006	0.005	0.004	0.001	0.006	0.009	0.080	0.005	-	0.001	-	0.001	-	-	-	0.112	0.016	0.002	0.094	8.000	1.982	56.156	0.413	-	0.556	5.000
W008	0.047	0.014	0.012	0.075	0.014	0.177	0.015	0.001	0.006	0.001	0.004	0.001	0.002	-	0.369	0.148	0.014	0.207	10.571	0.634	57.515	0.136	23.500	3.357	2.500
W009	0.019	0.014	0.004	0.011	0.013	0.327	0.015		0.002		0.002	-	0.001	-	0.408	0.048	0.005	0.355	9.600	2.163	110.267	0.371	19.000	1.462	7.500
W012	0.070	0.048	0.020	0.092	0.011	0.089	0.016	0.002	0.013	0.003	0.014	0.002	0.016	0.003	0.399	0.230	0.051	0.118	4.510	1.810	31.590	0.296	4.375	6.364	1.231
W015	0.011	0.011	0.004	0.022	0.012	0.154	0.008	0.001	0.005	0.001	0.003	-	0.003	0.001	0.236	0.048	0.013	0.175	3.692	1.622	74.012	0.383	3.667	0.917	1.600
W016	0.004	-	-	-	0.006	0.054	0.002	-	0.003	0.001	0.006	0.002	0.024	0.006	0.108	0.004	0.042	0.062	0.095	-	73.404	-	0.167	0.667	0.667
W017	0.005	0.004	-	-	0.007	0.117	0.006	-	0.001	-	0.002	-	0.003	0.001	0.146	0.009	0.007	0.130	1.286	-	85.011	-	1.667	0.714	6.000
W020	0.006	0.005	0.001	0.002	0.008	0.099	0.003	-	-	-	-	-	-	-	0.124	0.014	0.000	0.110	-	0.000	95.158	0.471	-	0.750	-
W021	0.025	0.015	0.007	0.024	0.005	0.074	0.008	0.001	0.004	0.001	0.003	-	0.002	0.001	0.170	0.071	0.011	0.088	6.455	1.487	55.096	0.262	12.500	5.000	2.000
W022	0.009	0.017	0.003	0.003	0.006	0.062	0.008	-	0.001	-	-	-	0.001	-	0.110	0.032	0.002	0.076	16.000	0.000	42.139	0.755	9.000	1.500	8.000
W023	0.010	0.014	0.002	0.011	0.006	0.122	0.003	-	-	-	0.001	-	0.001	-	0.170	0.037	0.002	0.131	18.500	1.081	135.406	0.722	10.000	1.667	-
W024	0.076	0.073	0.023	0.103	0.035	0.174	0.030	0.005	0.021	0.005	0.019	0.002	0.017	0.004	0.587	0.275	0.068	0.244	4.044	2.194	25.285	0.403	4.471	2.171	1.429
W025	0.037	0.020	0.009	0.058	0.029	0.366	0.021	0.002	0.016	0.003	0.020	0.004	0.020	0.004	0.609	0.124	0.067	0.418	1.851	4.102	69.837	0.253	1.850	1.276	1.313
W028	0.109	0.411	0.085	0.505	0.131	0.195	0.164	0.025	0.164	0.037	0.125	0.020	0.126	0.022	2.119	1.110	0.494	0.515	2.247	2.944	6.265	0.985	0.865	0.832	1.000
W029	0.025	0.092	0.006	0.035	0.013	0.134	0.008	0.001	0.006	0.001	0.004	-	0.002	-	0.327	0.158	0.013	0.156	12.154	1.359	61.873	1.733	12.500	1.923	1.333
W033	0.007	0.018	0.001	0.003	0.002	0.020	0.002	-	0.002	0.001	0.002	-	0.001	-	0.059	0.029	0.006	0.024	4.833	7.930	47.089	1.570	7.000	3.500	1.000
W036	0.001	0.002	-	0.002	0.002	0.073	0.002	-	-	-	-	-	-	-	0.082	0.005	0.000	0.077	-	0.000	171.873	-	-	0.500	-
W038	0.046	0.022	0.005	0.021	0.025	0.591	0.027	0.002	0.007	0.001	0.002	-	0.001	0.002	0.752	0.094	0.013	0.645	7.231	1.133	107.115	0.335	46.000	1.840	3.857
W041	0.016	0.008	0.002	0.008	0.013	0.249	0.013	-	0.006	0.001	0.001	-	0.001	-	0.318	0.034	0.009	0.275	3.778	1.487	90.193	0.326	16.000	1.231	2.167
W049	0.003	-	-	0.001	0.004	0.036	0.003	-	0.001	-	0.001	-	0.001	-	0.050	0.004	0.003	0.043	1.333	11.895	48.936	-	3.000	0.750	3.000
W051	0.011	0.018	0.002	0.004	0.009	0.078	0.005	-	0.001	-	-	-	0.001	-	0.129	0.035	0.002	0.092	17.500	0.000	54.753	0.885	11.000	1.222	5.000
W052	0.010	0.010	0.001	0.007	0.002	0.059	0.003	-	0.001	0.001	0.002	-	0.001	-	0.097	0.028	0.005	0.064	5.600	3.398	113.421	0.730	10.000	5.000	3.000
W053	0.010	0.017	0.003	0.007	0.005	0.049	0.003	-	0.002	-	-	0.001	0.001	0.001	0.099	0.037	0.005	0.057	7.400	0.000	59.575	0.716	10.000	2.000	1.500
W054	0.014	0.069	0.005	0.017	0.012	0.099	0.009	-	0.001	-	0.002	-	-	-	0.228	0.105	0.003	0.120	35.000	1.399	44.858	1.903	-	1.167	9.000
W057	0.012	0.032	0.002	0.006	-	0.063	0.003	-	0.003	0.001	0.001	0.001	0.001	-	0.125	0.052	0.007	0.066	7.429	1.982	-	1.507	12.000	-	1.000
W061	0.024	0.015	0.004	0.023	0.006	0.218	0.014	0.001	0.007	0.001	0.004	-	0.003	0.001	0.320	0.066	0.015	0.239	4.400	2.069	112.004	0.353	8.000	4.000	2.000
W062	0.017	0.032	0.003	0.012	0.008	0.141	0.011	-	0.005	-	0.002	-	0.001	-	0.232	0.064	0.008	0.160	8.000	1.982	70.777	1.034	17.000	2.125	2.200
W067	0.014	0.026	0.004	0.006	0.017	0.270	0.012	-	0.004	-	0.001	-	-	-	0.354	0.050	0.005	0.299	10.000	1.982	89.015	0.802	-	0.824	3.000
W069	0.045	0.080	0.032	0.141	0.087	0.243	0.080	0.012	0.070	0.011	0.037	0.004	0.024	0.006	0.872	0.298	0.152	0.422	1.961	3.121	13.716	0.486	1.875	0.517	1.143
W071	0.028	0.023	0.009	0.029	0.019	0.229	0.017	0.001	0.004	0.001	0.004	0.001	0.004	0.001	0.370	0.089	0.015	0.266	5.933	1.641	60.000	0.334	7.000	1.474	4.250

W076	0.026	0.019	0.005	0.034	0.001	0.074	0.009	-	0.004	-	0.001	0.001	0.001	0.001	0.176	0.084	0.008	0.084	10.500	0.350	116.152	0.384	26.000	26.000	2.250
W077	0.010	0.002	0.001	0.011	0.010	0.134	0.007	0.001	0.003	-	0.003	0.001	0.001	0.001	0.185	0.024	0.009	0.152	2.667	3.244	75.417	0.146	10.000	1.000	2.333
W081	0.007	-	0.001	0.005	0.004	0.039	0.003	-	0.002	0.001	0.003	0.001	0.001	0.001	0.068	0.013	0.009	0.046	1.444	7.137	53.014	0.000	7.000	1.750	1.500
R003	0.032	0.071	0.006	0.025	0.008	0.076	0.008	0.001	0.003	-	0.002	-	0.001	-	0.233	0.134	0.006	0.093	22.333	0.952	44.734	1.182	32.000	4.000	2.667
R004 A	0.057	0.103	0.010	0.041	0.003	0.126	0.010	0.002	0.003	0.001	0.003	-	0.001	-	0.360	0.211	0.008	0.141	26.375	0.870	108.324	0.995	57.000	19.000	3.333
R004 B	0.012	0.024	0.004	0.012	0.004	0.065	0.004	-	0.002	-	0.002	-	0.002	0.001	0.132	0.052	0.007	0.073	7.429	1.982	76.519	0.799	6.000	3.000	2.000
R004 C	0.013	0.027	0.002	0.019	0.007	0.071	0.003	-	-	-	0.001	-	0.001	-	0.144	0.061	0.002	0.081	30.500	0.626	72.957	1.222	13.000	1.857	-
R009	0.008	0.014	0.001	-	0.002	0.056	0.003	-	0.001	-	0.001	-	-	-	0.086	0.023	0.002	0.061	11.500	-	107.653	1.142	-	4.000	3.000
Sp001	0.019	0.044	0.003	0.015	0.012	0.045	0.004	0.001	0.001	0.001	0.001	-	0.002	-	0.148	0.081	0.005	0.062	16.200	0.793	30.585	1.345	9.500	1.583	4.000
PAAS	38.2	79.6	8.83	33.9	5.55	1.08	4.66	0.77	4.68	0.990	2.85	0.41	2.82	0.43	184.770	160.530	12.180	12.060	13.180	1.000	1.000	1.000	13.546	6.883	0.996

Table 2

Table 2:

	mean_Rock	mean_trend	Average	B025	B037	B044	B053	W028	W038	W061	W069	R004A	Sp001
Al	146286.67	79.46	0	0.01	0.02	0	NA	0	0	0	0	0	0
Th	29.93	0.46	0.01	0.15	0.3	NA	NA	NA	NA	NA	NA	NA	
Fe	67366.67	181.7	0	0.02	0.25	0	NA	0	NA	NA	0	0	0.01
Pb	14.53	0.19	0.01	3.96	1	0.02	0	0	0	0	0.03	0.01	0.07
Cu	46.16	1.81	0.03	3.02	0.68	0.16	0.04	0.51	0	0.02	0.11	0.06	0.41
Co	18.37	1.06	0.04	0.51	0.39	0	0	3.09	0	0.01	1.49	0.01	0.13
Cr	99.33	0.27	0	0.35	0.23	0	0	0	0	0.01	0.06	0	0.12
Ni	46.1	1.81	0.03	0.65	0.57	0	0.01	1.45	0	0.03	0.44	0.04	0.23
V	90.61	5.44	0.04	0.25	0.37	0.09	0.01	0.01	0.02	0.03	0	0.06	0.39
Mn	666.67	61.3	0.06	0.29	1.11	0	0	1.71	0	0.01	0.27	0.01	0.18
Zn	55.4	134.57	1.6	87.55	9.29	1.19	1.19	6.67	0.26	2.07	7.11	0.44	76.33
Ba	720.78	421.1	0.38	6.68	2.64	1.24	0.7	1.38	0.38	1.09	3.05	1.49	11.82
Sr	115.47	670.3	3.82	6.61	5.71	17.42	8.77	5.19	2.92	6.51	4.15	3.54	5.65
Li	11.38	7.19	0.42	4.43	3.35	1.26	0.29	5.88	0.08	0.13	0.91	0.07	7.39
Ca	8926.67	40312	2.98	5.04	5.68	0.4	4.9	2.88	2.17	6.59	1.74	3.82	5.77
Rb	36.58	15.28	0.28	7.42	3.2	0.15	0.01	2.02	0	0.99	1.65	0.05	24.3
K	16673.33	8024	0.32	8.35	1.89	0.23	0.26	2.35	0.04	1.79	0.96	0.52	26.81
Na	9606.67	31459	2.16	32.24	14.99	6.29	1.09	5.46	0.76	2.72	14.83	17.74	6.02
U	2.23	1.85	0.55	1.03	2.48	2.22	0.23	0.18	0.2	0.08	1.41	0.17	0.12
Mo	3.36	2.34	0.46	0.32	0.64	0.07	0.01	0.12	0.02	0.09	0.01	0.44	0.63
Mg	9520	14449	1	1	1	1	1	1	1	1	1	1	1

NA= not analysed. B0 = borehole. W0 = Hand dug wells. Sp = Spring. R = River. Rk= rocks (the average values for elements in rocks were calculated from the data of Ndjigui et al. 2014)